

DISSERTATION

A New Era of Leptogenesis

by

STEVE BLANCHET

Technische Universität München
Physik Department
Institut für Theoretische Physik T30e
Univ.-Prof. Dr. Michael Ratz



angefertigt am
Max-Planck-Institut für Physik, München
(Werner-Heisenberg-Institut)
unter Betreuung von
Dr. Pasquale Di Bari und Dr. habil. Georg G. Raffelt



MAX-PLANCK-GESELLSCHAFT

Technische Universität München
Physik Department
Institut für Theoretische Physik T30e
Univ.-Prof. Dr. Michael Ratz

A New Era of Leptogenesis

STEVE BLANCHET

Vollständiger Abdruck der von der Fakultät für Physik der Technischen Universität München zur Erlangung des akademischen Grades eines

Doktors der Naturwissenschaften (Dr. rer. nat.)

genehmigten Dissertation.

Vorsitzender:	Univ.-Prof. Dr. L. Oberauer
Prüfer der Dissertation:	1. Univ.-Prof. Dr. M. Ratz
	2. Hon.-Prof. Dr. W. F. L. Hollik

Die Dissertation wurde am 10.04.2008 bei der Technischen Universität München eingereicht und durch die Fakultät für Physik am 09.05.2008 angenommen.

Summary

The present thesis, which is mainly based on my research papers I–IV listed overleaf, is devoted to some forefront issues in the field of leptogenesis. As well as nicely explaining the origin of the matter-antimatter asymmetry of the Universe, this mechanism is intimately related to the nature of neutrino masses in that it is the cosmological consequence of the see-saw mechanism. This connection makes possible to relate parameters measured or to be measured in neutrino experiments to a cosmological parameter, the baryon-to-photon ratio, $\eta_B \simeq 6 \times 10^{-10}$.

According to the mass M of the heavy neutrino that decays, the generation of asymmetry has to be described by different sets of classical Boltzmann equations: in the unflavored regime, when $M \gtrsim 10^{12}$ GeV, the lepton flavors are summed over, and the asymmetry is estimated from two equations, one of which tracks N_{B-L} , the total $B-L$ number, where B and L denote baryon and lepton numbers, respectively. In the fully flavored regime, when $M \lesssim 10^{12}$ GeV, the lepton flavor asymmetries $B/3 - L_\alpha$, $\alpha = e + \mu$ or τ , must be tracked instead. The fact that two descriptions coexist is due to the τ -lepton Yukawa interactions, which become important roughly when the temperature in the primordial plasma drops below 10^{12} GeV. As we pointed out in paper III, the transition between the two regimes requires a quantum kinetic treatment, where correlations in flavor space and partial losses of coherence are properly accounted for.

In the unflavored regime, when the heavy neutrino masses are hierarchical, one typically obtains a scenario where only the contribution from the lightest right-handed neutrino, N_1 , matters. A lower bound on M_1 of about 10^9 GeV for successful leptogenesis can then be derived. The associated lower bound on the reheat temperature T_{reh} of the Universe after inflation being of the same order, a tension arises between leptogenesis and supergravity theories because of a possible overproduction of gravitinos. Furthermore, it is interesting that one finds a stringent upper bound on the absolute neutrino mass scale, $m_1 \lesssim 0.1$ eV. Finally, it should be noted that, in the unflavored regime, the final asymmetry does not depend on the lepton mixing matrix,

which contains the potentially measurable Dirac and Majorana CP -violating phases. The necessary source of CP violation is instead provided by unmeasurable phases in the high-energy sector.

In the fully flavored regime, the lowest bounds on M_1 and on the reheat temperature do not change, as we stressed in paper II. On the other hand, the parameters accessible in neutrino experiments, notably the angle θ_{13} and the Dirac and Majorana CP -violating phases, acquire importance. According to the value they take, the predictions from leptogenesis can differ by orders of magnitude, as we showed in paper II. Moreover, as investigated in detail in paper IV, the source of CP violation required for leptogenesis may be exclusively provided by the Dirac phase, which is the low-energy phase with the best prospects of being measured in the near future.

There are different ways to go beyond the “vanilla” picture where the asymmetry is produced by the lightest right-handed neutrino and the lower bounds introduced above hold. Following paper I, three possibilities are discussed. First, a quasi-degenerate mass spectrum for the heavy neutrinos is considered, implying that two or three heavy neutrinos contribute to the generation of asymmetry. It is then possible to relax the bounds on M_1 and T_{reh} to the TeV scale, and the upper bound on m_1 can be evaded. Second, specific situations can be found where the asymmetry is produced by the next-to-lightest right-handed neutrino, N_2 . The lower bound on M_1 is then replaced by a lower bound on M_2 , still implying a lower bound on T_{reh} similar to the vanilla case. Finally, even within the N_1 -dominated scenario, a special choice of high-energy parameters, which requires large cancellations, can be chosen in order to relax the lower bounds on M_1 and T_{reh} .

Leptogenesis has recently entered a new era in that some of what has been discussed above has only been realized in the last couple of years. Notably, let me mention the importance of flavor effects, the possible relevance of quantum effects, as well as the role played by the next-to-lightest right-handed neutrino.

In the future, the case for leptogenesis will be weakened or strengthened depending on the outcome of the next-generation neutrinoless double-beta decay searches, the planned long-baseline neutrino experiments, as well as the LHC.

The content of this thesis is mainly based on the following works:

- I S. Blanchet and P. Di Bari,
Leptogenesis beyond the limit of hierarchical heavy neutrino masses,
JCAP **0606** (2006) 023 [arXiv:hep-ph/0603107].
- II S. Blanchet and P. Di Bari,
Flavor effects on leptogenesis predictions,
JCAP **0703** (2007) 018 [arXiv:hep-ph/0607330].
- III S. Blanchet, P. Di Bari and G. G. Raffelt,
Quantum Zeno effect and the impact of flavor in leptogenesis,
JCAP **0703** (2007) 012 [arXiv:hep-ph/0611337].
- IV A. Anisimov, S. Blanchet and P. Di Bari,
Viability of Dirac phase leptogenesis,
JCAP **0804** (2008) 033 [arXiv:0707.3024].

Acknowledgments

It is a very difficult task, if not impossible, to list all people who contributed directly or indirectly to the achievement of my Ph.D. studies. Therefore, I shall undertake the more modest task of underlining the major contributions.

I would like first to express my gratitude to the Max-Planck-Institut für Physik (MPI) for providing funding and optimal research possibilities through the newly born International Max Planck Research School for Elementary Particle Physics. Thanks also to the Technische Universität München (TUM), in particular to Prof. Michael Ratz, for providing the academic framework to my Ph.D. studies.

Next, I would like to thank my supervisor within the institute, Georg Raffelt, for his kindness, support, availability, and the many useful advice he gave me both at the scientific and non-scientific levels.

For the research presented in this thesis, I am mostly indebted to Pasquale Di Bari. I benefited a lot from his expertise in the fields of leptogenesis and cosmology in general. Moreover, I enjoyed the long discussions about our work and beyond.

Then, my thanks go to all members of the “astroparticle” theory group who overlapped with me since October 2005 at the MPI for a nice, relaxed and inspiring atmosphere. Special thanks to Yvonne Wong for suggestions about English issues and to Pasquale Serpico for useful information about the process of terminating a Ph.D. at the MPI and TUM. Thanks also to my office mate Stefano Pozzorini for the enjoyable “Swiss” atmosphere inside the office. Finally, thanks to the other IMPRS students, especially Florian Hahn-Wörnle, Edoardo Mirabella, and Joseph Pradler.

Last but not least, I am grateful to my parents for the irreplaceable role they played from the very beginning until the present achievement of my studies.

Contents

Summary	i
Acknowledgments	v
1 Introduction	1
1.1 The matter-antimatter puzzle	1
1.2 The puzzle of neutrino masses	7
1.2.1 Theory of neutrino oscillations	7
1.2.2 Experimental evidence for neutrino oscillations	8
1.2.3 Absolute neutrino mass scale	11
1.3 The see-saw mechanism and leptogenesis	12
2 Vanilla leptogenesis	17
2.1 General scenarios of unflavored leptogenesis	17
2.2 The N_1 -dominated scenario	24
2.3 Leptogenesis and supersymmetry	35
3 Adding flavor to vanilla leptogenesis	39
3.1 When does flavor matter and why?	39
3.2 Flavored Boltzmann equations and spectator processes	41
3.3 In practice, what changes?	44
3.4 Dependence on the initial conditions and lower bounds	48
3.4.1 Alignment	49
3.4.2 Democratic and semi-democratic cases	51
3.4.3 One-flavor dominance	52
3.5 Study of a specific example	54
4 From classical to quantum kinetic equations	61
4.1 Validity of the different pictures	62
4.1.1 When are flavor effects important?	62
4.1.2 Maximum flavor effects	65

4.2	Neutrino mass bound	67
4.3	Limitations of a simple rate comparison	70
4.4	Density matrix equation	71
5	Going beyond vanilla leptogenesis	79
5.1	Degenerate limit for the heavy neutrinos	80
5.2	N_2 -dominated scenario	83
5.3	Effects of $ \Omega_{22} $	85
6	Leptogenesis from low-energy CP-violating phases	87
6.1	CP violation in neutrino physics	88
6.1.1	Neutrino oscillations and the Dirac phase	88
6.1.2	Neutrinoless double-beta decay and the Majorana phases	89
6.2	Dirac phase leptogenesis	90
6.2.1	The hierarchical limit	90
6.2.2	The degenerate limit	101
6.3	Leptogenesis from the Majorana phases	110
6.4	Discussion	111
7	Conclusion	115
A	Neutrino mixing parameters	121
B	The see-saw mechanism with three RH neutrinos	123

Chapter 1

Introduction

1.1 The matter-antimatter puzzle

One can surely say that our understanding of the Universe has made a huge leap forward in the last few years. This is partly because the amount of data has dramatically increased, so that an epoch of “precision cosmology” has started. But this is also due to an accumulation of evidence for concepts that were still considered exotic not so long ago, such as dark matter and dark energy. Even though their nature is still unknown, at least there seems to be a consensus about their existence.

Nowadays, one speaks about a “Standard Cosmological Model”, in analogy with its very successful counterpart of particle physics. The Standard Cosmological Model tells us that the Universe is in a phase of accelerated expansion and that the total energy in the Universe is shared among at least four components (see Fig. 1.1) which sum to $\Omega_{\text{tot}} \simeq 1$, meaning that the Universe is flat to a good precision. The dominant component (about 73%) is called dark energy, dark matter makes about 23%, ordinary matter (both luminous and dark) only 4% and neutrinos 0.2–2%, the uncertainty here stemming from the unknown absolute neutrino mass scale, as we shall see in Section 1.2.3.

It is well known that the nature of dark matter is still mysterious. The particle interpretation seems to be widely supported, and the candidates are numerous: axion, lightest supersymmetric particle (neutralino, gravitino), sterile neutrino, and many others.

Dark energy is probably a much bigger issue still than dark matter. It is supposed to drive the accelerated expansion, but its nature is very unclear. It also raises a fundamental question about how to treat the vacuum energy in quantum field theory.

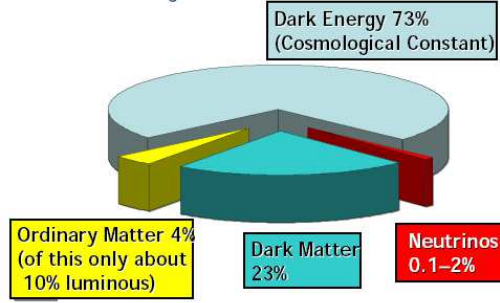


Figure 1.1: The mass-energy budget of the Universe.

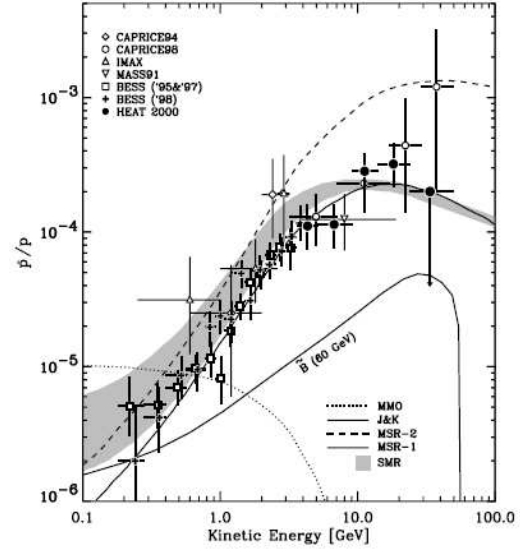


Figure 1.2: The antiproton-to-proton ratio at the top of the atmosphere, as observed (points) and predicted from the models (lines) [1].

Ordinary matter, which constitutes our bodies as well as the Earth and the stars, does not seem at first to introduce any challenge to our understanding. However, this naive perception is wrong because two very puzzling questions remain:

- 1) Why is antimatter essentially absent in the observable Universe?
- 2) Why is the number density of baryons so small compared to photons or neutrinos?

These two questions are puzzling because, according to the Standard Big-Bang Theory, matter and antimatter evolved in the same way in the early Universe. On the other hand, today the observable Universe is composed almost exclusively of matter. Antimatter is only seen in particle physics accelerators and in cosmic rays. Moreover, the rates observed in cosmic rays are consistent with the secondary emission of antiprotons, $n_{\bar{p}}/n_p \sim 10^{-4}$ (see Fig. 1.2).

Ordinary matter is composed of baryons (protons, neutrons) and leptons (electrons). One can assign an experimentally conserved number to baryons and leptons. Baryons and leptons carry one unit of these numbers, whereas

antibaryons and antileptons carry one negative unit. In this way one can say that the predominance of matter over antimatter is equivalent to the existence of a net baryon number.

Following the Standard Big-Bang Theory and relying on the Standard Model (SM) of particle physics, the relic density of baryons, i.e. nucleons here, can be easily estimated. One has the usual Boltzmann equation for the number density of baryons n_B (or antibaryons)

$$\frac{dn_B}{dz} + 3Hn_B = -\langle\sigma_A|v|\rangle \left[n_B^2 - (n_B^{\text{eq}})^2 \right], \quad (1.1)$$

where $z = M_B/T$, M_B is the baryon mass, H the Hubble expansion rate, n_B^{eq} the equilibrium number density of baryons, and T the cosmic temperature. The collision term on the right-hand side is given in terms of an thermally-averaged annihilation cross-section $\langle\sigma_A|v|\rangle$, whose definition can be found in [2] for example. Eq. (1.1) can be conveniently rewritten in terms of the variable n_B/n_γ , where n_γ is the number density of photons, allowing one to factor out the effects of the expansion of the Universe. One obtains

$$\frac{d(n_B/n_\gamma)}{dz} = -\frac{n_\gamma z}{H(M_B)} \langle\sigma_A|v|\rangle \left[\left(\frac{n_B}{n_\gamma} \right)^2 - \left(\frac{n_B^{\text{eq}}}{n_\gamma} \right)^2 \right]. \quad (1.2)$$

In our case, the important annihilation channel is into pions (e.g. $p + \bar{p} \rightarrow \pi^+ + \pi^-$). Taking the averaged cross-section to be $\langle\sigma|v|\rangle = C_1 M_\pi^{-2}$, with $M_\pi \simeq 135$ MeV and where C_1 is a numerical factor of order unity, the freeze-out occurs at $T \sim 22$ MeV. Neglecting the entropy production in e^+e^- -annihilations, one finds for today's abundance (subscript '0') [2]

$$\left. \frac{n_B}{n_\gamma} \right|_0 = \left. \frac{n_{\bar{B}}}{n_\gamma} \right|_0 \simeq 7 \times 10^{-20} C_1^{-1}. \quad (1.3)$$

Note that the ratio of baryon number density to photon number density today is usually referred to as the *baryon-to-photon ratio*,

$$\eta_B \equiv \left. \frac{n_B}{n_\gamma} \right|_0. \quad (1.4)$$

The result of our simple computation, Eq. (1.3), is clearly a small number, which would perhaps explain the question 2) above. But one notices immediately a first problem, namely because the abundances of baryons and antibaryons are predicted in this way to be the same. Baryons and antibaryons do not evolve in distinctive ways so that one expects today the same amount of each of them. So, the argument we have just described leaves open the

question 1) above. But let us for the moment ignore this point and try to see if the abundance of baryons matches observation.

The photon density follows directly from the measurement of the Cosmic Microwave Background (CMB) temperature and from Bose-Einstein statistics: $n_\gamma \sim T^3$. Determining the baryon content of the Universe is more difficult. Direct measurements are not accurate, because only a small fraction of baryons formed stars and other luminous objects (see Fig. 1.1). However, we can rely on two different indirect probes.

The first probe is Big-Bang Nucleosynthesis (BBN). The abundances of light elements such as ^4He , D , ^3He and ^7Li predicted by the standard theory of BBN crucially depend on η_B . Comparing predictions with observations, as shown in Fig. 1.3, the following baryon-to-photon ratio is inferred [3]:

$$\eta_B \simeq (5.5 \pm 1.0) \times 10^{-10}. \quad (1.5)$$

The CMB temperature anisotropies, very well measured by the WMAP satellite, offer the second probe. These anisotropies reflect the acoustic oscillations of the baryon-photon fluid which happened around photon decoupling. A precise computation can be done evolving Boltzmann equations for anisotropies, assuming that they are generated by quantum fluctuations during inflation. Fig. 1.4 illustrates how the amount of anisotropies with angular scale $\sim 1/\ell$ depends on η_B . The baryon-to-photon ratio obtained from 3 years of WMAP data is [4]

$$\eta_B \simeq (6.1 \pm 0.2) \times 10^{-10}. \quad (1.6)$$

The synthesis of light elements occurred during the first 3 minutes in the history of the Universe, whereas the photon decoupling occurred when the Universe was 400 thousand years old. The fact that these two completely different probes of the baryon content of the Universe give compatible results is one of the great successes of modern cosmology.¹

It should now be clear that the result from the “classical” computation of the baryon density given in Eq. (1.3) is at odds with the observed value, Eq. (1.6). In order to avoid the “baryon annihilation catastrophe” leading to the value in Eq. (1.3), one has to generate a primordial asymmetry between baryons and antibaryons. This small asymmetry, *at the level of one part in one billion*, would imply that after the annihilation process has occurred at full strength, one remains with the small excess of baryons over antibaryons. The problem of generating this small excess of baryons over antibaryons is often called the *baryogenesis problem*.

¹Throughout the thesis, we shall exclusively use the value of η_B obtained from CMB temperature anisotropies, Eq. (1.6), which has much smaller errors.

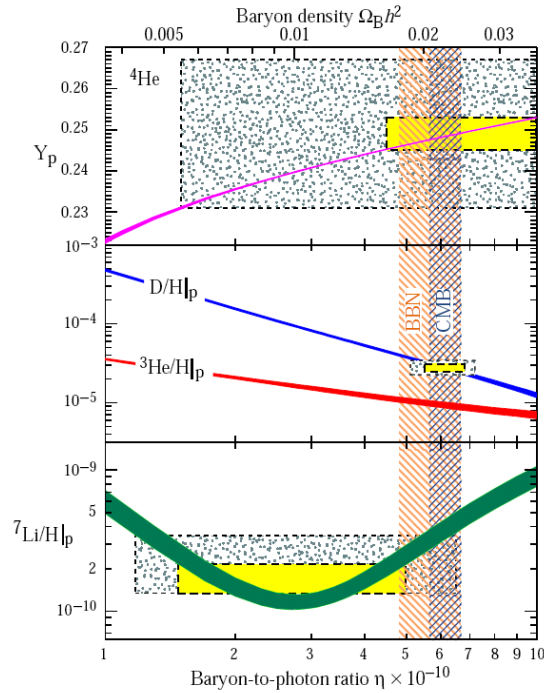


Figure 1.3: The observed abundances of light elements compared to the standard BBN predictions [5]. The smaller boxes indicate 2σ statistical errors, the larger ones $\pm 2\sigma$ statistical and systematic errors.

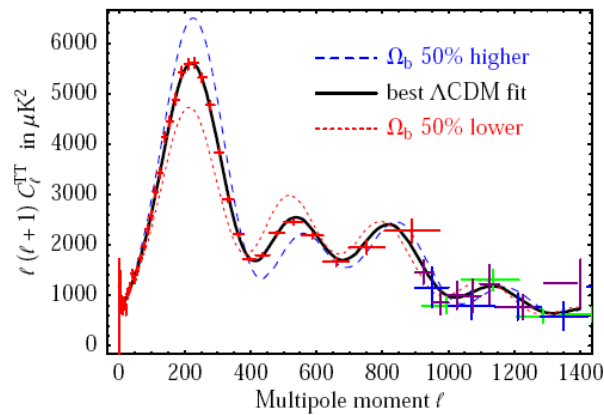


Figure 1.4: The dependence of CMB temperature anisotropies on the baryon abundance Ω_b (or η_B), compared with data [6].

The solution to the baryogenesis problem requires the generation of a small baryon asymmetry primordially. Sakharov, in 1967, enunciated the three necessary conditions for such a process to be possible at some stage in the history of the Universe [7]:

1. Baryon number violation.
2. C and CP violation.
3. Departure from thermal equilibrium.

In principle, the SM contains all these ingredients. Indeed,

1. Due to the chiral nature of weak interactions, B and L are not conserved [8]. At zero temperature, this has no observable effect due to the smallness of the weak coupling. However, as the temperature reaches the critical temperature T_{EW} of the electroweak phase transition, B and L violating processes come into thermal equilibrium [9, 10]. The rate of these processes is related to the free energy of the sphaleron-type field configurations which carry topological charge [11]. In the SM they lead to an effective interaction operator of all left-handed fermions, $O_{B+L} = \prod_i Q_{Li} Q_{Li} Q_{Li} \ell_{Li}$, which violates baryon and lepton number by three units. On the other hand, $B - L$ remains conserved.
2. The weak interactions of the SM violate C maximally and violate CP via the Kobayashi-Maskawa mechanism [12]. The latter originates from the quark mixing matrix, often called the Cabibbo-Kobayashi-Maskawa (CKM) matrix, which contains one CP -violating phase. This phase is known to be non-zero since CP violation has been observed in the K and B mesons systems (see e.g. the review on CP violation in [5]).
3. A strongly first-order electroweak phase transition in the early Universe could provide the out-of-equilibrium condition. A first-order phase transition proceeds via nucleation and growth of bubbles [13].

This scenario is called *electroweak baryogenesis in the Standard Model*. However, it fails for two reasons. First, it turns out that, for the electroweak phase transition to be strongly first order, the mass of the Higgs particle should be smaller than about 45 GeV [14] (see also [15]). However, LEP II gives the well-known bound $M_h > 114$ GeV [5]. Second, the source of CP violation in the quark sector is far too small, due to the smallness of some of the quark masses [16].

In conclusion, successful baryogenesis requires physics beyond the SM, just as the dark matter and dark energy problems! One intriguing solution to the problem of baryogenesis is deeply connected with the neutrino sector and in particular with neutrino masses. This is the topic of the next section.

1.2 The puzzle of neutrino masses

1.2.1 Theory of neutrino oscillations

Even with tiny masses, massive neutrinos can behave very differently from massless ones. In particular, massive neutrinos naturally lead to neutrino mixing and to neutrino oscillations, which have been recently observed, as we shall see below. Let us sketch how this happens.

Consider a neutrino beam created in a charged current interaction along with the antilepton α^+ , $\alpha = e, \mu, \tau$. By definition the neutrino created is called ν_α . In general, this is not a physical particle, but rather a superposition of physical fields ν_i with different masses m_i :

$$|\nu_\alpha\rangle = \sum_i U_{\alpha i}^* |\nu_i\rangle, \quad (1.7)$$

where U is the lepton mixing matrix, also known as the Pontecorvo-Maki-Nakagawa-Sakata (PMNS) matrix [17–19]. By analogy with the CKM matrix in the quark sector, the lepton mixing matrix can be conveniently parametrized as

$$U = V \times \text{diag}(e^{i\frac{\Phi_1}{2}}, e^{i\frac{\Phi_2}{2}}, 1), \quad (1.8)$$

$$V = \begin{pmatrix} 1 & 0 & 0 \\ 0 & c_{23} & s_{23} \\ 0 & -s_{23} & c_{23} \end{pmatrix} \begin{pmatrix} c_{13} & 0 & s_{13} e^{-i\delta} \\ 0 & 1 & 0 \\ -s_{13} e^{i\delta} & 0 & c_{13} \end{pmatrix} \begin{pmatrix} c_{12} & s_{12} & 0 \\ -s_{12} & c_{12} & 0 \\ 0 & 0 & 1 \end{pmatrix},$$

where $s_{ij} \equiv \sin \theta_{ij}$, $c_{ij} \equiv \cos \theta_{ij}$, δ and $\Phi_{1,2}$ are the Dirac and Majorana CP -violating phases, respectively. The Majorana phases, which are not present in the quark sector, are related to the possible Majorana nature of neutrinos (see Section 1.3).

For a simple-minded approach to the propagation of the state $|\nu_\alpha\rangle$, we assume that the 3-momentum \mathbf{p} of the different components in the beam are the same. However, since their masses are different, the energies of all these components cannot be equal. Rather, for the component ν_i , the energy is given by the relativistic energy-momentum relation $E_i = \sqrt{\mathbf{p}^2 + m_i^2}$. After a time t , the evolution of the initial beam, Eq. (1.7), assuming that neutrinos

are stable particles, gives

$$|\nu_\alpha(t)\rangle = \sum_i e^{-iE_i t} U_{\alpha i}^* |\nu_i\rangle. \quad (1.9)$$

Since all E_i 's are not equal if the masses are not, Eq. (1.9) represents a different superposition of the physical eigenstates ν_i compared to Eq. (1.7). In general, the state in Eq. (1.9) can therefore show properties of other flavor states. The amplitude of finding a $\nu_{\alpha'}$ in the original ν_α beam is

$$\langle \nu_{\alpha'} | \nu_\alpha(t) \rangle = \sum_i e^{-iE_i t} U_{\alpha i}^* U_{\alpha' i}, \quad (1.10)$$

using the fact that $\langle \nu_i | \nu_j \rangle = \delta_{ij}$. The probability of finding a $\nu_{\alpha'}$ in the original ν_α beam at any time t is then the modulus squared of the amplitude, $P_{\nu_\alpha \rightarrow \nu_{\alpha'}}(t) = |\langle \nu_{\alpha'} | \nu_\alpha(t) \rangle|^2$. In all practical situations, neutrinos are extremely relativistic, so that one can approximate the energy-momentum relation as $E_i \simeq |\mathbf{p}| + m_i^2/(2|\mathbf{p}|)$ and replace t by the distance x traveled by the beam. After a few manipulations one can finally write the vacuum oscillation probability as

$$\begin{aligned} P_{\nu_\alpha \rightarrow \nu_{\alpha'}}(x) &= \delta_{\alpha\alpha'} - 4 \sum_{i>j} \text{Re} (U_{\alpha i}^* U_{\alpha' i} U_{\alpha j} U_{\alpha' j}^*) \sin^2 \left(\frac{\Delta m_{ij}^2}{4E} x \right) \\ &\quad + 2 \sum_{i>j} \text{Im} (U_{\alpha i}^* U_{\alpha' i} U_{\alpha j} U_{\alpha' j}^*) \sin \left(\frac{\Delta m_{ij}^2}{4E} x \right), \end{aligned} \quad (1.11)$$

where $E \simeq |\mathbf{p}|$ and $\Delta m_{ij}^2 \equiv m_i^2 - m_j^2$. From this formula it is apparent that neutrino oscillations require non-zero neutrino masses and mixings.

1.2.2 Experimental evidence for neutrino oscillations

The last 10 years have been extremely successful for the field of neutrino physics. In 1998, the Super-Kamiokande experiment in Japan reported the first compelling evidence for neutrino oscillations as a way to explain the anomaly in atmospheric neutrinos. Super-Kamiokande not only confirmed the previously found deficit in ν_μ -type events but also measured a zenith angle dependent ν_μ -deficit which was inconsistent with expectations based on calculations of the atmospheric neutrino flux. The neutrino oscillation explanation $\nu_\mu \rightarrow \nu_\tau$ with a quasi-maximal mixing angle [20] appeared therefore as the most convincing one.

Two dedicated laboratory experiments have been conceived in order to check this picture. The experiment K2K in Japan, which collected data until

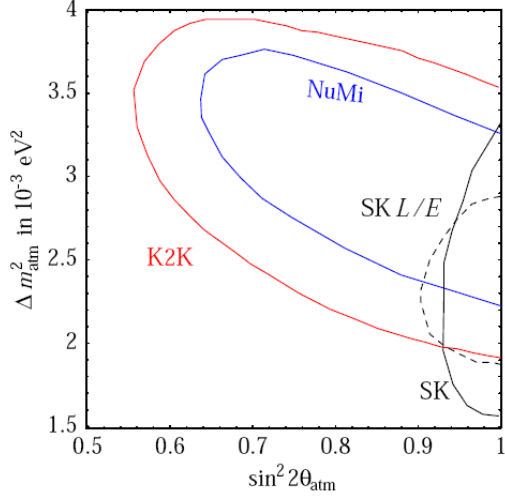


Figure 1.5: Best fit regions at 90% C.L. for atmospheric and accelerator neutrinos [23].

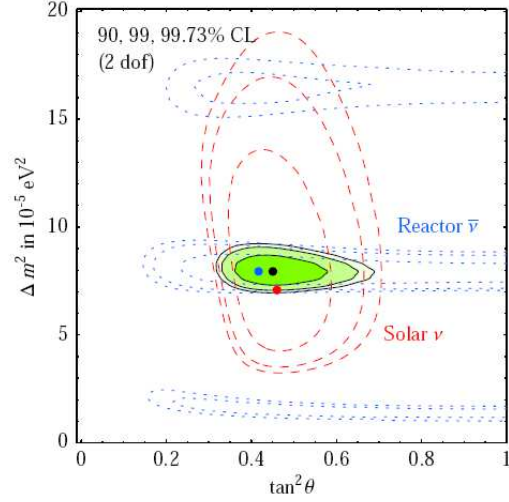


Figure 1.6: Best fit regions at 90, 99 and 99.73% C.L. for solar and reactor neutrinos [23].

November 2004, used a pulsed beam of muon-neutrinos produced at KEK and detected at Super-Kamiokande (distance of 250 km). The currently running MINOS experiment uses a pulsed beam of muon-neutrinos produced at NuMI (Fermilab), and the far detector is located at a distance of 735 km in the Soudan mine, Minnesota. Both experiments point to a neutrino oscillation interpretation of their data, with mixing parameters compatible with those explaining the atmospheric anomaly [21, 22]. A summarizing plot for “atmospheric” neutrinos can be found in Fig. 1.5. The best-fit parameters are [23]:

$$|\Delta m_{32}^2| \equiv \Delta m_{\text{atm}}^2 = (2.5 \pm 0.2) \times 10^{-3} \text{eV}^2, \quad (1.12)$$

$$\sin^2 2\theta_{23} = 1.02 \pm 0.04, \quad (1.13)$$

where the ranges indicated are at 1σ .

Neutrinos from the Sun were first studied by Ray Davis in the Homestake mine in South Dakota in the 1960’s [24]. This pioneering work made use of the radiochemical technique, $\nu_e + {}^{37}\text{Cl} \rightarrow e^- + {}^{37}\text{Ar}$. He quickly found that the observed flux was smaller than the one predicted by Bahcall and collaborators from the Standard Solar Model [25]. The *solar neutrino puzzle* was born. Later, other experiments were conceived to check this deficit in solar neutrinos: Kamiokande [26] and later Super-Kamiokande [27], which used the water Cherenkov technique, also found a deficit, as well as SAGE [28] and

GALLEX/GNO [29, 30], which used the radiochemical method with Gallium.

It should be noted that the deficits found in the different experiments were different, highlighting the energy dependence, as well as the fact that the experiments were based on different techniques. The radiochemical method allows only for the measurement of charged-current (CC) events, which is exclusively sensitive to electron neutrinos. Experiments relying on water Cherenkov detection register only elastic scattering (ES) events, $\nu + e \rightarrow \nu + e$. This technique can measure in principle all neutrino flavors, but the efficiency in the μ and τ channels is much lower, due to the lower cross-sections.

Only the SNO experiment in Sudbury, Canada, used a heavy water detection which allowed for the detection via three channels simultaneously: CC, ES as well as neutral current (NC) thanks to the reaction $\nu + d \rightarrow \nu + n + p$, where d denotes deuteron. This made possible a reliable measurement of the total flux of neutrinos from the Sun. Hence, in addition to confirming the deficit in solar neutrinos in the CC and ES detection channels [31], this experiment allowed for the first direct test of the Standard Solar Model. In 2002, the data were found to be actually consistent with the prediction [32], finally resolving the longstanding solar neutrino puzzle. This can be seen as a huge success in the history of neutrino physics. The Borexino experiment, located in the Gran Sasso laboratory, has recently added another milestone to the understanding of neutrinos from the Sun by detecting in real time a flux of ${}^7\text{Be}$ neutrinos consistent with the Standard Solar Model prediction [33].

The neutrino oscillation explanation $\nu_e \rightarrow \nu_{\mu,\tau}$ to the deficits in neutrinos from the Sun in different experiments was popular from the beginning, because it appeared as the simplest and most elegant solution. But the first experiment which really left neutrino oscillations as the only possible explanation for the solar neutrino puzzle is KamLAND, rejecting, for instance *spin flavor oscillations* [34, 35], which were still allowed after SNO. KamLAND is a scintillation detector located in Japan which observed the $\bar{\nu}_e$ from neighboring nuclear reactors thanks to the process $\bar{\nu}_e + p \rightarrow n + e^+$. This experiment saw a 6σ evidence for the disappearance of $\bar{\nu}_e$ [36, 37]. A summarizing plot of the solar neutrino and KamLAND data can be found in Fig. 1.6. The best-fit parameters are [23]:

$$|\Delta m_{21}^2| \equiv \Delta m_{\text{sol}}^2 = (8.0 \pm 0.3) \times 10^{-5} \text{eV}^2, \quad (1.14)$$

$$\tan^2 \theta_{12} = 0.45 \pm 0.05, \quad (1.15)$$

where the ranges indicated are at 1σ .

For completeness, we should add that a short-baseline reactor neutrino experiment named CHOOZ, in France, was performed to get a handle on the third mixing angle, θ_{13} [38]. They report no signal, which, together with

atmospheric and K2K data, yields the 1σ upper bound [23]

$$\sin^2 2\theta_{13} < 0.05. \quad (1.16)$$

1.2.3 Absolute neutrino mass scale

The oscillation formula Eq. (1.11) shows that neutrino oscillation experiments are only able to provide information on neutrino mass-squared *differences*. They are insensitive to the absolute neutrino mass scale. Fortunately, there are other ways to probe it.

First, the so-called “direct” measurement makes use of the very precise determination of the upper end of the spectral distribution of the electron in the tritium β -decay, ${}^3\text{H} \rightarrow {}^3\text{He} + \bar{\nu}_e + e^-$. The Mainz experiment obtained the bound $m_{\nu_e} < 2.2$ eV [39] and the Troitsk experiment $m_{\nu_e} < 2.5$ eV [40], both at 95% C.L., where

$$m_{\nu_e} \equiv \sqrt{\sum_{i=1}^3 |U_{ei}|^2 m_i^2}, \quad (1.17)$$

with U denoting the lepton mixing matrix we introduced in Section 1.2.1 [cf. Eq. (1.8)]. The upcoming KATRIN experiment [41], which is under construction at the moment, is expected to have a discovery potential down to $m_{\nu_e} \simeq 0.35$ eV.

Second, if neutrinos are Majorana particles (see next section), then it might be possible to observe neutrinoless double-beta ($0\nu\beta\beta$) decay for nuclei like ${}^{76}\text{Ge}$. Double- β decay, $(A, Z) \rightarrow (A, Z+2) + 2e^- + 2\bar{\nu}_e$, has been already observed, even though the rate is of second order in the Fermi coupling constant G_F , implying for instance a lifetime of about 10^{21} years for ${}^{76}\text{Ge}$. The $0\nu\beta\beta$ -decay rate is even more suppressed, and depends on yet another combination of the neutrino masses as in Eq. (1.17) [42],

$$|\langle m \rangle| \equiv \left| \sum_{i=1}^3 U_{ei}^2 m_i \right|. \quad (1.18)$$

Up to now, no compelling signal² for $0\nu\beta\beta$ -decay has been observed, and the currently running CUORICINO experiment, which uses ${}^{130}\text{Te}$, obtains now a bound [45]

$$|\langle m \rangle| < 0.19\text{--}0.68 \text{ eV} \quad (90\% \text{ C.L.}) \quad (1.19)$$

²Part of the Heidelberg-Moscow collaboration claims an evidence for $0\nu\beta\beta$ -decay, leading to the measurement $|\langle m \rangle| = 0.2\text{--}0.6$ eV (90% C.L.) [43, 44], where the uncertainty is due to the poorly known nuclear matrix elements.

which is slightly stronger than the one obtained in the previous Heidelberg-Moscow [46] and IGEX experiments [47, 48], where ^{76}Ge was used. Note that the range shown in Eq. (1.19) stems from the uncertainty in the nuclear matrix elements. Future planned experiments such as GERDA [49], MAJORANA [50] or CUORE [51] aim at a sensitivity in the 50 meV range.

There is a third probe of the absolute neutrino mass scale, and this is cosmology. More precisely, the CMB data and the data from the large scale structure (LSS) have a sensitivity to the sum of the neutrino masses $\sum_i m_i$. Looking at the literature in the last 3 years that dealt with this issue, it is clear that the bound on the sum of the neutrino masses depends on which data sets are included. We simply show here the result from a somewhat conservative calculation in [52]:

$$\sum_{i=1}^3 m_i < 0.6 \text{ eV} \quad (95\% \text{ C.L.}). \quad (1.20)$$

The three probes we have presented involve different combinations of the neutrino masses, where even cancellations are possible in the case of $0\nu\beta\beta$ -decay [cf. Eq. (1.18)]. But the bottom line here is that all three probes tend to the same conclusion: *the neutrino mass scale has to be in the sub-eV range*. In this sense, this makes neutrinos a very peculiar particle in the SM, with a mass that is six orders of magnitude smaller than the electron! Fig. 1.7 illustrates nicely this gap between neutrinos and the other SM particles. Clearly, such a gap must be explained on theoretical grounds, and this is the topic of the next section.

1.3 An elegant solution: the see-saw mechanism and leptogenesis

As we have just seen, neutrinos are very special particles due to their extreme lightness. This might suggest that neutrinos have a unique mass generation mechanism that leads to small masses in a natural way. One of the first attempts in the late 1970's and early 1980's was the use of the see-saw mechanism [53–58], which we shortly describe now.

Let us imagine that we would like to write down the most simple and general extension of the Standard Model that accomodates neutrino masses. For simplicity we consider here only one generation of neutrinos. In the SM, in order to generate massive fermions, one introduces a right-handed (RH) component for each particle. So let us introduce one RH neutrino N_R in a usual Dirac-type term $m_D \bar{\nu}_L N_R + h.c.$ Contrary to the other SM particles,

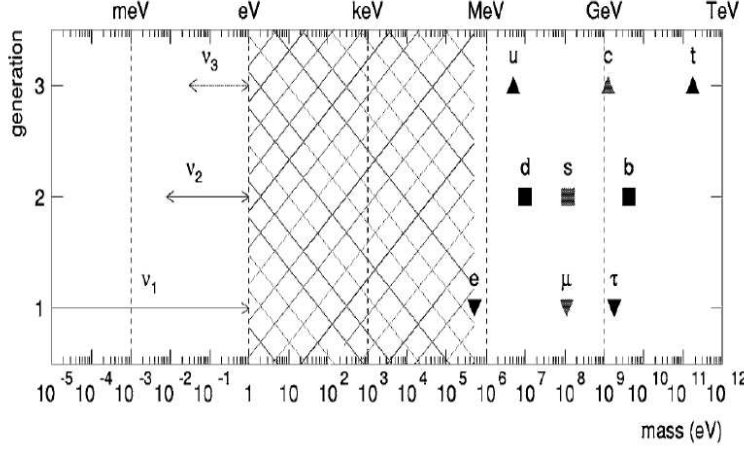


Figure 1.7: Mass spectrum of fermions.

this is not the only term allowed for neutrinos. Since neutrinos are neutral particles, the RH component can only be a singlet of all SM gauge interactions, including hypercharge. This unique property of neutrinos implies that the Majorana mass term $\frac{1}{2}M_M(\overline{N_R})^c N_R + h.c.$ is allowed, where the superscript c denotes charge conjugation. Actually, in general there is no reason why this term should be absent. The mass term for neutrinos can then be conveniently written in a matrix form as

$$\mathcal{L}_{\text{mass}} = -\frac{1}{2} \begin{pmatrix} \overline{\nu_L} & \overline{(N_R)^c} \end{pmatrix} \begin{pmatrix} 0 & m_D \\ m_D & M_M \end{pmatrix} \begin{pmatrix} (\nu_L)^c \\ N_R \end{pmatrix} + h.c. \quad (1.21)$$

Note that upper left component of the mass matrix is zero because it is not possible to write down a Majorana mass term for left-handed fields without breaking gauge invariance.

The see-saw mechanism then assumes that the Majorana mass is much larger than the Dirac mass, i.e. $M_M \gg m_D$. Diagonalizing the mass matrix with this assumption yields the two mass eigenvalues

$$m \simeq \frac{m_D^2}{M_M}, \quad M \simeq M_M, \quad (1.22)$$

where the first eigenvalue corresponds to the mass of a light Majorana neutrino, and the second eigenvalue corresponds to the mass of a heavy Majorana neutrino. It is interesting to notice that plugging a Dirac mass at the electroweak scale, $m_D = 100 \text{ GeV}$, with a heavy neutrino mass of $M_M = 10^{14} \text{ GeV}$

maybe related to the underlying Grand Unified Theory (GUT), one obtains a light neutrino mass $m = 0.1$ eV. This can be seen as a strong support for this model. For the generalization of the previous discussion to three massive neutrinos and more details, see Appendix B.

The version of the see-saw mechanism we have just described, with the addition of RH neutrinos to the SM, is nowadays referred to as the type-I see-saw mechanism. For completeness, let us mention that other see-saw mechanisms were proposed to explain the smallness of neutrino masses: the addition of $SU(2)$ triplet Higgses to the SM leads to the type-II mechanism [58–60], and the addition of $SU(2)$ triplet fermions leads to the type-III mechanism [61, 62]. Throughout the thesis, we shall exclusively deal with the type-I mechanism.

As we have just shown, the see-saw mechanism elegantly solves the problem of generating small neutrino masses in a natural way. But this is not the only virtue of the model: its cosmological consequence is indeed that it can also solve the puzzle of the matter-antimatter asymmetry of the Universe through *thermal leptogenesis*, as first proposed by Fukugita and Yanagida 20 years ago [63]. We saw in Section 1.1 that one needs to satisfy all three Sakharov’s conditions in order to solve the baryogenesis problem. Let us see how they are satisfied in the case of thermal leptogenesis.

1. Lepton number is violated in the decays of the heavy neutrinos into lepton doublets and Higgs doublets. Additionally, B and L are violated by the non-perturbative sphaleron processes, which however conserve $B - L$. This is thus the same source of B violation as the one described in the case of electroweak baryogenesis (see Section 1.1). The difference is that the sphaleron transitions are here transferring L number produced in the decays of the heavy neutrinos into the required B number. These transitions should be in equilibrium for temperatures [64–66]

$$T_{\text{EW}} \sim 100 \text{ GeV} < T \lesssim 10^{12} \text{ GeV}. \quad (1.23)$$

2. CP violation occurs in the decays of the heavy neutrinos. The relevant quantity to evaluate is the CP asymmetry parameter, defined as

$$\varepsilon_i \equiv -\frac{\Gamma_i - \bar{\Gamma}_i}{\Gamma_i + \bar{\Gamma}_i}, \quad (1.24)$$

where $\Gamma_i = \sum_{\alpha} \Gamma(N_i \rightarrow \ell_{\alpha} \Phi^{\dagger})$ and $\bar{\Gamma}_i = \sum_{\alpha} \Gamma(N_i \rightarrow \bar{\ell}_{\alpha} \Phi)$. As shown in Fig. 1.8, one can calculate such an asymmetry by computing the interference between the tree-level diagram and the two relevant one-loop diagrams, namely the self-energy diagram and the vertex correction.

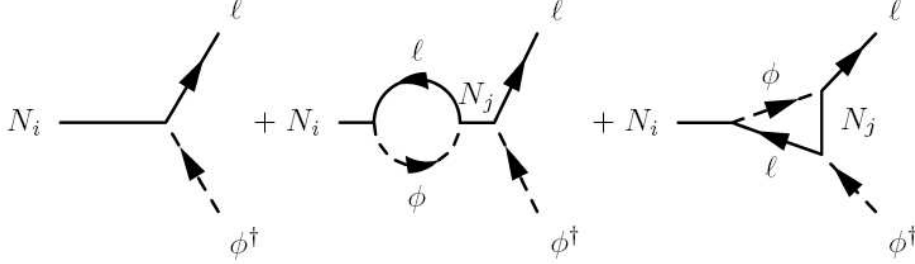


Figure 1.8: The diagrams necessary to compute the CP asymmetry in leptogenesis.

We will show the result of such a calculation in the next chapter. This source of CP violation is typically sufficient to explain the matter-antimatter problem.

3. The out-of-equilibrium condition will be satisfied thanks to the expansion of the Universe. Convenient quantities to describe when the decays of the heavy neutrinos freeze out are the decay parameters, K_i , defined as the ratio of the total decay width of the heavy neutrino N_i to the expansion rate at $T = M_i$,

$$K_i \equiv \frac{\Gamma_{D,i}(T=0)}{H(T=M_i)}, \quad (1.25)$$

where $\Gamma_{D,i} \equiv \Gamma_i + \bar{\Gamma}_i$. This is the key quantity for the thermodynamical description of the decays of heavy particles in the early Universe [2]. In leptogenesis it can be conveniently expressed in terms of the *effective neutrino mass* [67]

$$\tilde{m}_i \equiv \frac{(m_D^\dagger m_D)_{ii}}{M_i} = K_i m_\star, \quad (1.26)$$

where m_\star is the *equilibrium neutrino mass*, given by

$$m_\star \simeq 1.08 \times 10^{-3} \text{ eV}. \quad (1.27)$$

In this thesis, when referring to “leptogenesis” we will exclusively mean the production of a lepton asymmetry by the decays of heavy singlet neutrinos. Other “leptogenesis” scenarios, such as the Affleck-Dine mechanism in

supersymmetric theories [68–70] or leptogenesis via neutrino oscillations [71, 72] will not be discussed here.

After the clear evidence for non-zero neutrino masses appeared in 1998, the see-saw mechanism, and hence leptogenesis, became very attractive, solving simultaneously two important puzzles of modern physics within a simple and minimal extension of the SM. Another nice feature of the model is that the heavy fermionic singlets (RH neutrinos) necessary for the (type-I) see-saw mechanism have a natural connection with grand unification; e.g. $SO(10)$ [73] predicts the existence of such fermionic singlets. It is therefore not a surprise if a huge activity was registered in this field since 1998, with an ever growing precision in the computations.

We present in Chapter 2 the picture of leptogenesis that emerges when the flavor content of the leptons coming from the decays of the heavy neutrinos is ignored. This is what we call the “unflavored” treatment. In Chapter 3 we discuss why flavor effects are important in a considerable part of the parameter space, and what their main implications are. This will allow us to build up a “flavored” picture of leptogenesis. In Chapter 4 the validity of the classical computation of the final baryon asymmetry in the case of flavored leptogenesis is analyzed. We shall argue that the use of a more complicated density matrix equation might be relevant in some region of the parameter space. Then, in Chapter 5, an overview of different ways to go beyond the conventional picture of leptogenesis, where only the lightest RH neutrino is taken into account and the mass spectrum of the heavy neutrinos is very hierarchical, is given. In Chapter 6 we consider a by-product of flavor effects, namely the fact that the low-energy phases in the PMNS matrix have a more important role than previously thought. In particular, the role played by the Dirac phase, source of CP violation in neutrino oscillation experiments, will be thoroughly studied. Finally, we conclude with a summary of the main results and a discussion about what one can expect from the experimental side in the next few years regarding a possible test of leptogenesis.

Chapter 2

Vanilla leptogenesis

In this chapter, following a purely unflavored¹ treatment, we first introduce the most general Boltzmann equations which need to be solved in order to estimate the baryon asymmetry of the Universe produced through leptogenesis. This will allow us to introduce very useful quantities and definitions which will be used in the remainder of the thesis. Then, we describe how the general picture simplifies considerably under natural assumptions, such as a hierarchical mass spectrum for the heavy neutrinos. This will enable us to arrive at a “vanilla” leptogenesis, i.e. a typical scenario of leptogenesis, where the lightest RH neutrino, N_1 , provides the main contribution. We will then derive two important constraints on the parameters of the model: a lower bound on the mass of the lightest RH neutrino, M_1 , and an upper bound on the absolute neutrino mass scale, m_1 . Finally, we shortly comment on leptogenesis within a supersymmetric framework and discuss the so-called *gravitino problem*.

2.1 General scenarios of unflavored leptogenesis

We would like here to describe how to calculate the baryon asymmetry produced through leptogenesis in full generality, i.e. for an arbitrary RH neutrino mass spectrum and no restrictions on the parameters of the model.

The Lagrangian in Eq. (B.1) contains all the terms relevant for leptogenesis. Since we are concerned here with a purely unflavored analysis, it will

¹In the literature the expressions “flavor-independent” or “one-flavor” are often used to describe the same concept.

prove useful to define the states

$$|\ell_i\rangle \equiv \frac{1}{\sqrt{(h^\dagger h)_{ii}}} \sum_{\alpha} h_{\alpha i} |\ell_{\alpha}\rangle \quad (2.1)$$

and

$$|\bar{\ell}'_i\rangle \equiv \frac{1}{\sqrt{(h^\dagger h)_{ii}}} \sum_{\alpha} h_{\alpha i}^* |\bar{\ell}_{\alpha}\rangle, \quad (2.2)$$

which can be thought of as the states produced in decays and inverse decays (and $\Delta L = 1$ scattering processes, see below) in the process of leptogenesis. So, to each heavy neutrino N_i corresponds one lepton state $|\ell_i\rangle$ and one anti-lepton state $|\bar{\ell}'_i\rangle$. Note that $|\bar{\ell}'_i\rangle$ is not the CP conjugate of $|\ell_i\rangle$, although $|\bar{\ell}_{\alpha}\rangle$ is the CP conjugate of $|\ell_{\alpha}\rangle$. We shall discuss this point in more detail in the next chapter and see which important consequences follow.

Let us list now the processes that are relevant for the computation of the baryon asymmetry through leptogenesis [67, 74–76]:

- Decays and inverse-decays: $N_i \leftrightarrow \ell_i \Phi^\dagger$ and the conjugate processes $N_i \leftrightarrow \bar{\ell}'_i \Phi$.
- $\Delta L = 1$ Higgs-mediated scattering processes, such as the s -channel $\ell_i N_i \leftrightarrow Q_3 \bar{t}$ and the t -channels $\ell_i Q_3 \leftrightarrow N_i \bar{t}$, and $\ell_i t \leftrightarrow N_i Q_3$, where Q_3 and t are the third generation quark doublet and the top $SU(2)$ singlet, respectively, as well as those involving gauge bosons, such as $\ell_i N_i \rightarrow \Phi^\dagger A$ (with $A = W^{3,\pm}$ or B).
- The s -channel $\Delta L = 2$ scattering processes $\ell_i \Phi \leftrightarrow \bar{\ell}'_i \Phi^\dagger$ with on-shell N_i are already accounted for by decays and inverse decays. However, the off-shell s -channel contribution, as well as the u -channel and t -channel scatterings ($\ell\ell \leftrightarrow \Phi^\dagger \Phi$), must be included.

For simplicity, we shall neglect in the following the so-called *spectator processes* [77, 78], which are processes that are not directly related to the generation of the asymmetry but that are fast and could affect it indirectly. For example, the sphaleron transitions belong to spectator processes, since they are supposed to be in equilibrium during the leptogenesis process and since they are responsible for transmitting the L asymmetry produced in the decays into a $B-L$ asymmetry in a non-trivial way. For the time being, we neglect spectator processes, and simply assume that the asymmetry is directly produced in $B-L$ instead of L . In any case, spectator processes altogether are not expected to induce corrections larger than 30% [78]. We shall discuss in detail spectator processes in the next chapter (Section 3.2).

Thermal corrections will also be neglected. They may lead to relevant corrections, though with big theoretical uncertainties, in the weak washout regime ($K_i \lesssim 5$), but negligible corrections are expected in the more relevant strong washout regime ($K_i \gtrsim 5$) [75].

Following an unflavored treatment, the set of Boltzmann equations can be worked out in the form [67, 74, 79]

$$\frac{dN_{N_i}}{dz} = -(D_i + S_i) (N_{N_i} - N_{N_i}^{\text{eq}}), \quad i = 1, 2, 3 \quad (2.3)$$

$$\frac{dN_{B-L}}{dz} = \sum_{i=1}^3 \varepsilon_i (D_i + S_i) (N_{N_i} - N_{N_i}^{\text{eq}}) - N_{B-L} W, \quad (2.4)$$

where $z \equiv M_1/T$. With N_X we denote the abundance of X per RH neutrino in ultra-relativistic thermal equilibrium. Defining $x_i \equiv M_i^2/M_1^2$ and $z_i \equiv z\sqrt{x_i}$, the decay factors are given by

$$D_i \equiv \frac{\Gamma_{D,i}}{H z} = K_i x_i z \left\langle \frac{1}{\gamma_i} \right\rangle, \quad (2.5)$$

where H is the expansion rate and the decay parameters K_i were introduced in Eq. (1.25). The total decay rates, $\Gamma_{D,i} \equiv \Gamma_i + \bar{\Gamma}_i$, are the product of the decay widths times the thermally averaged dilation factors $\langle 1/\gamma_i \rangle$, given by the ratio $\mathcal{K}_1(z_i)/\mathcal{K}_2(z_i)$ of the modified Bessel functions.

As we have seen, the $\Delta L = 1$ scatterings S_i and the related washout contribution $W_i^{\Delta L=1}$ arise from two different classes of Higgs- and lepton-mediated inelastic scatterings involving the top quark (Q_3) and gauge bosons (A). Their main effect is to enhance the heavy neutrino production and thus the efficiency factor in the weak washout regime, and, since they also contribute to the washout, they lead to a correction of the efficiency factor in the strong washout regime as well. Top quark and gauge boson scattering terms are expected to be of similar size. However, the reactions densities for the gauge boson processes are presently controversial [75, 76]. Therefore, we will not discuss these processes here. A simple analytic approximation for the sum $D_1 + S_1$ was obtained in [80],

$$D_1 + S_1 \simeq 0.1 K_1 \left[1 + \ln \left(\frac{M_1}{M_h} \right) z^2 \ln \left(1 + \frac{a}{z} \right) \right], \quad (2.6)$$

where

$$a \simeq \frac{10}{\ln(M_1/M_h)}. \quad (2.7)$$

The Higgs mass M_h was introduced to cut off the infrared divergence of the t -channel process. It turns out that $D_1 + S_1 \simeq D_1$ in the strong washout regime. The generalization of Eq. (2.6) for $i \neq 1$ can be derived from [76].

The equilibrium abundances of the heavy neutrinos and their rates are also expressed through the modified Bessel functions,

$$N_{N_i}^{\text{eq}}(z_i) = \frac{1}{2} z_i^2 \mathcal{K}_2(z_i) \quad , \quad \frac{dN_{N_i}^{\text{eq}}}{dz_i} = -\frac{1}{2} z_i^2 \mathcal{K}_1(z_i) \quad . \quad (2.8)$$

The RH neutrinos can be produced by inverse decays and $\Delta L = 1$ scatterings. Nevertheless, in the relevant strong washout regime, inverse decays alone are sufficient to make the RH neutrino abundance reach its thermal equilibrium value prior to the decays which produce the asymmetry. The asymmetry generated together with the RH neutrino production will then be efficiently washed out, so that the details of the RH neutrino production will not affect the final asymmetry, thus greatly reducing theoretical uncertainties. This is one of the nice features of the strong washout regime on which we shall focus. For this reason, the $\Delta L = 1$ scattering terms S_i will play a subdominant role.

The washout factor W in Eq. (2.4) can be written as the sum of two contributions [81],

$$W = \sum_i W_i(K_i) + \Delta W \quad . \quad (2.9)$$

The first term is the sum of the contributions from inverse decays and $\Delta L = 1$ scatterings,

$$W_i = W_i^{\text{ID}} + W_i^{\Delta L=1} \quad . \quad (2.10)$$

For the lightest RH neutrino, N_1 , it was shown in [80] that W_1 can be conveniently rewritten as $W_1(z) = j(z)W_1^{\text{ID}}(z)$, where

$$j(z) = 0.1 \left(1 + \frac{15}{8z} \right) \left[z \ln \left(\frac{M_1}{M_h} \right) \ln \left(1 + \frac{a}{z} \right) + \frac{\mu}{z} \right] \quad , \quad (2.11)$$

where $\mu = 1$ (2/3) in the strong (weak) washout regime. The corresponding results for $i \neq 1$ can again be obtained from [76].

In the strong washout regime, inverse decays, where the resonant $\Delta L = 2$ contribution has to be properly subtracted [75, 82], dominate $\Delta L = 1$ scatterings [75, 80], so that

$$W_i(z) \simeq W_i^{\text{ID}}(z) = \frac{1}{4} K_i \sqrt{x_i} \mathcal{K}_1(z_i) z_i^3 \quad . \quad (2.12)$$

The second term in Eq. (2.9) arises from the non-resonant $\Delta L = 2$ processes and gives typically a non-negligible contribution only in the non-relativistic limit, for $z \gg 1$ [74, 80, 81]. For hierarchical light neutrinos, it can be safely neglected for reasonable values $M_1 \ll 10^{14}$ GeV. We shall come back to this contribution when discussing the upper bound on the absolute neutrino mass scale at the end of Section 2.2.

The effects of production and washout are simultaneously accounted for by the efficiency factors κ_i associated with each N_i . Let us indicate with N_{B-L}^{in} a possible pre-existing asymmetry at the initial temperature of leptogenesis T_{in} . The final $B-L$ asymmetry can then be written as [2, 80],

$$N_{B-L}^{\text{f}} = N_{B-L}^{\text{in}} \exp \left(- \sum_i \int dz' W_i(z') \right) + \sum_i \varepsilon_i \kappa_i^{\text{f}}, \quad (2.13)$$

with the final efficiency factors $\kappa_i^{\text{f}} \equiv \kappa_i(z \rightarrow \infty)$ given by

$$\kappa_i^{\text{f}} = - \int_{z_{\text{in}}}^{\infty} dz' \frac{dN_{N_i}}{dz'} \exp \left(- \sum_i \int_{z'}^z dz'' W_i(z'') \right), \quad (2.14)$$

where we defined $z_{\text{in}} \equiv M_1/T_{\text{in}}$. Notice that each efficiency factor depends in general on all decay parameters, i.e. $\kappa_i^{\text{f}} = \kappa_i^{\text{f}}(K_1, K_2, K_3)$.

The baryon-to-photon ratio at recombination can then be calculated as

$$\eta_B = a_{\text{sph}} \frac{N_{B-L}^{\text{f}}}{N_{\gamma}^{\text{rec}}} \simeq 0.96 \times 10^{-2} N_{B-L}^{\text{f}}, \quad (2.15)$$

where $N_{\gamma}^{\text{rec}} \simeq 37$, and $a_{\text{sph}} = n_B/n_{B-L}$ accounts for the sphaleron conversion of a $B-L$ asymmetry into a B asymmetry. If the electroweak sphalerons go out of equilibrium before the electroweak phase transition, one has $a_{\text{sph}} = 28/79$ [83]. If, instead, electroweak sphalerons remain in equilibrium until slightly after the electroweak phase transition (as would be the case if, as presently believed, the electroweak phase transition was not strongly first order), this factor would be $a_{\text{sph}} = 12/37$ [84]. Both coefficients are of order 1/3 and, for definiteness, we shall use $a_{\text{sph}} = 28/79$ throughout the thesis.

If the mass differences satisfy the condition for the applicability of perturbation theory, $|M_j - M_i|/M_i \gg \max[(h^\dagger h)_{ij}]/(16\pi^2)$ with $j \neq i$ [85], then a perturbative calculation from the interference of tree-level with one-loop self-energy and vertex diagrams (see Fig. 1.8) gives [86, 87]

$$\varepsilon_i = \frac{3}{16\pi} \sum_{j \neq i} \frac{\text{Im} [(h^\dagger h)_{ij}^2]}{(h^\dagger h)_{ii}} \frac{\xi(x_j/x_i)}{\sqrt{x_j/x_i}}, \quad (2.16)$$

where the function $\xi(x)$, shown in Fig. 2.1, is defined as [88]

$$\xi(x) = \frac{2}{3} x \left[(1+x) \ln \left(\frac{1+x}{x} \right) - \frac{2-x}{1-x} \right]. \quad (2.17)$$

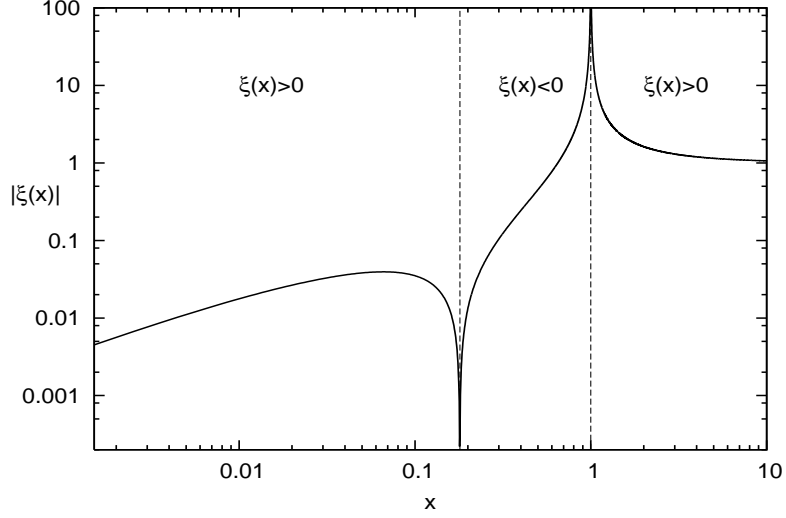


Figure 2.1: The function $\xi(x)$ defined in Eq. (2.17).

A particularly useful parametrization of the Yukawa coupling matrix in the context of leptogenesis involves the orthogonal matrix Ω [89]²,

$$h = U \sqrt{D_m} \Omega \sqrt{D_M}/v, \quad (2.18)$$

where we defined $D_M \equiv \text{diag}(M_1, M_2, M_3)$ and $D_m \equiv \text{diag}(m_1, m_2, m_3)$. The matrix U diagonalizes the light neutrino mass matrix m_ν given in Eq. (B.5), i.e. $U^\dagger m_\nu U^* \equiv D_m$, and it can be identified with the lepton mixing matrix in a basis where the charged lepton mass matrix is diagonal (see Appendix A). Moreover, neglecting the effect of the running of neutrino parameters from high energy to low energy [90, 91], one can assume the U matrix to be identified with the PMNS matrix, partially measured in neutrino oscillation experiments. In the following, we shall refer to the parametrization Eq. (2.18) as the “orthogonal” or the “Casas-Ibarra” parametrization.

The Ω matrix can be conveniently parametrized as

$$\Omega(\omega_{21}, \omega_{31}, \omega_{32}) = R_{12}(\omega_{21}) R_{13}(\omega_{31}) R_{23}(\omega_{32}), \quad (2.19)$$

where

$$R_{12} = \begin{pmatrix} \sqrt{1 - \omega_{21}^2} & -\omega_{21} & 0 \\ \omega_{21} & \sqrt{1 - \omega_{21}^2} & 0 \\ 0 & 0 & 1 \end{pmatrix}, \quad (2.20)$$

²Compared to the R matrix in [89], one has the simple relation $\Omega = R^\dagger$.

$$R_{13} = \begin{pmatrix} \sqrt{1 - \omega_{31}^2} & 0 & -\omega_{31} \\ 0 & 1 & 0 \\ \omega_{31} & 0 & \sqrt{1 - \omega_{31}^2} \end{pmatrix}, \quad (2.21)$$

$$R_{23} = \begin{pmatrix} 1 & 0 & 0 \\ 0 & \sqrt{1 - \omega_{32}^2} & -\omega_{32} \\ 0 & \omega_{32} & \sqrt{1 - \omega_{32}^2} \end{pmatrix}. \quad (2.22)$$

This parametrization for an orthogonal complex matrix corresponds to the transposed form of the CKM matrix in the quark sector or of the PMNS matrix in neutrino mixing [cf. Eq. (1.8)], with the difference that here one has complex rotations instead of real ones.

Notice that, using the orthogonal parametrization, Eq. (2.18), the decay parameters K_i can be expressed as linear combinations of the neutrino masses [80, 92],

$$K_i = \sum_j \frac{m_j}{m_\star} |\Omega_{ji}^2|. \quad (2.23)$$

The parametrization Eq. (2.19) is especially useful to understand the general structure of different scenarios of leptogenesis.

- For $\Omega = R_{13}$, one has $\varepsilon_2 = 0$, while ε_1 is maximal if [93]

$$m_3 \operatorname{Re}(\omega_{31}^2)/|\omega_{31}^2| = m_1 [1 - \operatorname{Re}(\omega_{31}^2)]/|1 - \omega_{31}^2|. \quad (2.24)$$

In the hierarchical limit for the heavy neutrinos (HL), i.e. $M_1 \ll M_2 \ll M_3$, one obtains the N_1 -dominated scenario (N_1 DS), where the final asymmetry is the result of only N_1 -related processes.

- For $\Omega = R_{23}$, one has $\varepsilon_1 = 0$, while ε_2 is maximal if

$$m_2 \operatorname{Re}(\omega_{32}^2)/|\omega_{32}^2| = m_3 [1 - \operatorname{Re}(\omega_{32}^2)]/|1 - \omega_{32}^2|. \quad (2.25)$$

At the same time, one has $\tilde{m}_1 = m_1$, so that the washout from N_1 can be neglected if m_1 is small enough. Therefore, in the HL and for hierarchical light neutrinos, one obtains the N_2 -dominated scenario (N_2 DS) [93], which will be the topic of Section 5.2.

- If $\Omega = R_{12}$, then ε_1 undergoes a phase suppression compared to its maximal value but $|\varepsilon_2| \propto (M_1/M_2) |\varepsilon_1|$. This implies that in the HL one again recovers the N_1 DS [93]. On the other hand, if $M_1 \simeq M_2$, both N_1 and N_2 should be taken into account since both CP asymmetries are expected to be of the same order.

Before ending this section, we would like to make two remarks. First, using the Casas-Ibarra parametrization, Eq. (2.18), it can be easily seen that the PMNS matrix U cancels out in combinations like $(h^\dagger h)_{ij}$ (or $(m_D^\dagger m_D)_{ij}$). This implies that both the CP asymmetry, Eq. (2.16), and the decay parameters or effective neutrino masses, Eq. (1.26), do not depend on U . Hence, the final asymmetry is completely independent of the PMNS matrix. In particular, if the CP asymmetry is insensitive to the CP -violating phases in U , then the source of CP violation necessary for leptogenesis must come from the “high-energy” sector, i.e. the Ω matrix, which is not probed in neutrino experiments. We shall see in the next chapter that the situation is completely different when flavor effects are taken into account.

Second, the border between the N_1 DS and the N_2 DS will also be affected by flavor effects. Furthermore, contrary to the unflavored case, where ε_3 is always suppressed by factors $M_1/M_{2,3}$, the flavored CP asymmetries $\varepsilon_{3\alpha}$ are not suppressed, opening the way to a potential N_3 -dominated scenario. We shall nonetheless see, for instance in Section 6.2.1, that, even though the CP asymmetry may not be suppressed, the washout from the other two heavy neutrinos is difficult to avoid.

2.2 The N_1 -dominated scenario

Let us now discuss the N_1 DS, where the asymmetry is dominantly generated by the lightest RH neutrino, N_1 . This typically (but not necessarily) occurs when a hierarchical heavy neutrino spectrum is considered, $3 M_1 \lesssim M_2$ [94].

The general expression for the final asymmetry, Eq. (2.15), reduces to

$$\eta_B \simeq 10^{-2} \varepsilon_1 \kappa_1^f, \quad (2.26)$$

where κ_1^f can be calculated solving a system of just two kinetic equations [2, 75, 81],

$$\frac{dN_{N_1}}{dz} = -(D_1 + S_1) (N_{N_1} - N_{N_1}^{\text{eq}}), \quad (2.27)$$

$$\frac{dN_{B-L}}{dz} = \varepsilon_1 (D_1 + S_1) (N_{N_1} - N_{N_1}^{\text{eq}}) - W_1 N_{B-L}. \quad (2.28)$$

These equations are obtained from the general set, Eqs. (2.3) and (2.4), neglecting the asymmetry generation and the washout terms from the two heavier RH neutrinos.

For $M_1 \ll 10^{14} \text{ GeV}$ ($m_{\text{atm}}^2 / \sum m_i^2$), the term $\Delta W(z)$ in the washout term [cf. Eq. (2.9)] is negligible and the solutions depend just on K_1 , since this is the only parameter in the equations. The $B-L$ asymmetry can be worked

out in an integral form [2], and one obtains a special case of the more general Eq. (2.13),

$$N_{B-L}(z; \bar{z}) = \bar{N}_{B-L} \exp \left(- \int_{\bar{z}}^z dz' W_1(z') \right) + \varepsilon_1 \kappa_1(z; \bar{z}), \quad (2.29)$$

where now a possible asymmetry produced by the two heavier RH neutrinos and frozen at $\bar{z} \geq z_{\text{in}}$ is included in \bar{N}_{B-L} . The efficiency factor $\kappa_1(z; \bar{z})$ can be expressed through a Laplace integral,

$$\begin{aligned} \kappa_1(z; \bar{z}) &= - \int_{\bar{z}}^z dz' \frac{dN_{N_1}}{dz'} \exp \left(- \int_{z'}^{\infty} dz'' W_1(z'') \right) \\ &= \int_{\bar{z}}^z dz' \exp [-\psi(z', z)]. \end{aligned} \quad (2.30)$$

In the strong washout regime we are interested in, for $K_1 \gtrsim 5$, one can safely use the approximations $dN_{N_1}/dz' \simeq dN_{N_1}^{\text{eq}}/dz'$, $D_1 + S_1 \simeq D_1$, $W_1(z') \simeq W_1^{\text{ID}}(z')$ [cf. Eq. (2.12)], and one finds that the final value for the efficiency factor, when $z \rightarrow \infty$, is given by [80]

$$\kappa_1^f(K_1) \simeq \kappa(K_1) \equiv \frac{2}{K_1 z_B(K_1)} \left[1 - \exp \left(-\frac{1}{2} K_1 z_B(K_1) \right) \right], \quad (2.31)$$

if $\bar{z} \lesssim z_B - 2$. The value $z' = z_B(K_1)$ is where the quantity $\psi(z', \infty)$ has a minimum and the integral in Eq. (2.30) receives a dominant contribution from a restricted z' -interval centered around it. In the strong washout regime, it can be calculated as a solution of

$$W_1^{\text{ID}}(z_B) = \frac{d^2 N_{N_1}^{\text{eq}}/dz^2}{|dN_{N_1}^{\text{eq}}/dz|} \Big|_{z=z_B} = \left\langle \frac{1}{\gamma} \right\rangle^{-1} (z_B) - \frac{3}{z_B}. \quad (2.32)$$

For very large K_1 , the right-hand side of this equation tends to unity and $z_B \simeq z_{\text{off}}$, the value of z when the washout from inverse decays switches off, i.e. $W_{\text{ID}}(z > z_{\text{off}}) < 1$. Fig. 2.2 shows (dashed lines) that Eq. (2.31), with $z_B(K_1)$ given by Eq. (2.32), reproduces the numerical result (solid line) within 10% for $K_1 \gtrsim 3$ [80].

Even though the approximation $dN_{N_1}/dz' \simeq dN_{N_1}^{\text{eq}}/dz'$ works rigorously only in the strong washout regime, Eq. (2.31) describes also the correct weak washout regime for a thermal initial N_1 -abundance ($N_{N_1}^{\text{in}} = 1$), because κ_1^f depends only on the value of the initial abundance and not on the decay rate. However, in the intermediate regime ($K_1 \simeq 1$) the error is about 30%. For $K_1 \lesssim 1$, the approximation $dN_{N_1}/dz' \simeq dN_{N_1}^{\text{eq}}/dz'$ does not work well and $z_B(K_1)$, evaluated with Eq. (2.32), incorrectly saturates to a constant value

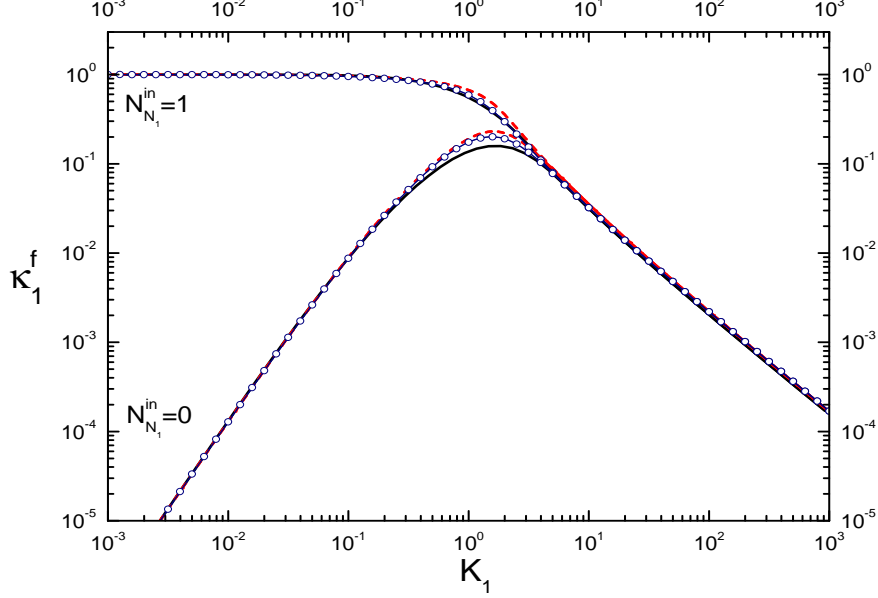


Figure 2.2: Efficiency factor in the N_1 DS. The solid lines are the numerical solutions of Eqs. (2.27) and (2.28) with $\Delta W = 0$. The analytical expression (2.31) yields the dashed line if $z_B(K_1)$ is given by Eq. (2.32) and the circled line if it is given by Eq. (2.34).

$z_{\max}^{\text{eq}} \simeq 1.33$ in the limit $K_1 \rightarrow 0$, corresponding to the maximum of $dN_{N_1}^{\text{eq}}/dz$ (see upper panel of Fig. 2.4). As a matter of fact, in the weak washout regime the maximum of the asymmetry production does not occur at z_{\max}^{eq} but at higher values

$$z_{\max}^{\text{weak}}(K_1) \simeq 1/\sqrt{K_1} + 15/8, \quad (2.33)$$

roughly when the age of the Universe is equal to the RH neutrino lifetime. Indeed, in the weak washout regime, the N_1 's decay far from equilibrium, when inverse decays can be neglected. In this case one has approximately $N_{N_1}(z) \simeq N_{N_1}^{\text{weak}}(z)$, where [80]

$$\begin{aligned} N_{N_1}^{\text{weak}}(z) &\simeq N_{N_1}^{\text{in}} \exp \left[- \int_{z_i}^z dz' D_1(z') \right] \\ &\simeq N_{N_1}^{\text{in}} \exp \left\{ -K_1 \left[\frac{z^2}{2} - \frac{15z}{8} + \left(\frac{15}{8} \right)^2 \ln \left(1 + \frac{8}{15}z \right) \right] \right\}, \end{aligned}$$

with $N_{N_1}^{\text{in}} = 1$ for a thermal initial N_1 -abundance. The maximum of $dN_{N_1}^{\text{weak}}/dz$ gives the value of z where the production of the asymmetry is maximum in the weak washout regime, and one can easily find that this value

is given approximately by $z_{\max}^{\text{weak}}(K_1)$ [cf. Eq. (2.33)]. An example is shown in the upper panel of Fig. 2.3 for $K_1 = 0.01$. An improvement of the analytical expression in Eq. (2.31) is obtained replacing $z_B(K_1)$ from Eq. (2.32) with an expression that coincides with it at large K_1 and with $z_{\max} \simeq 2$ at $K_1 \simeq 1$, such as

$$z_B(K_1) \simeq 2 + 4 K_1^{0.13} \exp\left(-\frac{2.5}{K_1}\right). \quad (2.34)$$

Fig. 2.2 shows (circles) that this expression, plugged into Eq. (2.31), reproduces the numerical solution (solid line) with a precision always better than 10%.

Notice that, in the particularly relevant range $5 \lesssim K_1 \lesssim 100$, Eq. (2.31) is well approximated by a power law [95],

$$\kappa_1^f(K_1) \simeq \frac{0.5}{K_1^{1.2}}. \quad (2.35)$$

In the case of a vanishing initial N_1 -abundance ($N_{N_1}^{\text{in}} = 0$), one has to take into account two different contributions, a negative and a positive one,

$$\kappa_1^f(K_1) = \kappa_-^f(K_1) + \kappa_+^f(K_1). \quad (2.36)$$

Defining z_{eq} by the condition $N_{N_1}(z_{\text{eq}}) = N_{N_1}^{\text{eq}}(z_{\text{eq}})$, the negative contribution arises from a first stage when $N_{N_1} \leq N_{N_1}^{\text{eq}}$, for $z \leq z_{\text{eq}}$, and is given approximately by [80]

$$\kappa_-^f(K_1) \simeq -2 \exp\left(-\frac{3\pi K_1}{8}\right) \left[\exp\left(\frac{1}{2} N_{N_1}(z_{\text{eq}})\right) - 1 \right]. \quad (2.37)$$

The N_1 -abundance at z_{eq} is well approximated by

$$N_{N_1}(z_{\text{eq}}) \simeq \overline{N}(K_1) \equiv \frac{N(K_1)}{\left(1 + \sqrt{N(K_1)}\right)^2}, \quad (2.38)$$

interpolating between the limit $K_1 \gg 1$, where $z_{\text{eq}} \ll 1$ and $N_{N_1}(z_{\text{eq}}) = 1$, and the limit $K_1 \ll 1$, where $z_{\text{eq}} \gg 1$ and $N_{N_1}(z_{\text{eq}}) = N(K_1) \equiv 3\pi K_1/4$. The positive contribution arises from a second stage when $N_{N_1} \geq N_{N_1}^{\text{eq}}$, for $z \geq z_{\text{eq}}$, and is approximately given by [80]

$$\kappa_+^f(K_1) \simeq \frac{2}{z_B(K_1) K_1} \left[1 - \exp\left(-\frac{1}{2} K_1 z_B(K_1) N_{N_1}(z_{\text{eq}})\right) \right]. \quad (2.39)$$

As can be seen in Fig. 2.2, the use of Eq. (2.34) yields an improvement also for a vanishing initial N_1 -abundance.

Figures 2.3 and 2.4 show, for a thermal initial N_1 -abundance, the dynamics of the asymmetry generation, comparing one example of weak washout with one example of strong washout [94]. In the top panels we show the function $d\kappa_1/dz' \equiv \exp[-\psi(z', z)]$, defined for $z' \leq z$, for different values of z . The difference between the two cases is striking. In the weak washout regime, each decay contributes to the final asymmetry for any value of z' at which the asymmetry is produced. In the strong washout regime, all the asymmetry produced at $z' \lesssim z_B - 2$ is efficiently washed out by inverse decays, so that only decays occurring at $z' \sim z_B$ give a contribution to the final asymmetry.

After having thoroughly studied the efficiency factor, we would like to turn now to the other important piece in the calculation of the baryon asymmetry Eq. (2.26), namely the CP asymmetry ε_1 . The general expression (2.16) for ε_1 can be re-cast through the Ω matrix as [93]

$$\varepsilon_1 = \xi(x_2) \varepsilon_1^{\text{HL}}(m_1, M_1, \Omega_{21}, \Omega_{31}) + [\xi(x_3) - \xi(x_2)] \Delta\varepsilon_1(m_1, M_1, \Omega_{21}, \Omega_{31}, \Omega_{22}). \quad (2.40)$$

In the hierarchical limit (HL), for $x_3, x_2 \gg 1$, one has $\xi(x_2) \simeq \xi(x_3) \simeq 1$, yielding $\varepsilon_1 \simeq \varepsilon_1^{\text{HL}}(m_1, M_1, \Omega_{21}, \Omega_{31})$. Therefore, the dependence on four of the see-saw parameters, namely M_2, M_3 and Ω_{22} , disappears in the HL, and one is left with only six parameters. Notice moreover that $\kappa_1^f = \kappa_1^f(m_1, M_1, K_1)$, where $K_1 = K_1(m_1, \Omega_{21}, \Omega_{31})$, and thus the final asymmetry depends on the same six parameters. In particular, let us emphasize once more that the final asymmetry is independent of the PMNS matrix, which contains three mixing angles and three phases [cf. Eq. (A.5)].

Let us define

$$\bar{\varepsilon}(M_1) \equiv \frac{3}{16\pi} \frac{M_1 m_{\text{atm}}}{v^2} \simeq 10^{-6} \left(\frac{M_1}{10^{10} \text{ GeV}} \right) \left(\frac{m_{\text{atm}}}{0.05 \text{ eV}} \right), \quad (2.41)$$

and

$$\beta(m_1, \Omega_{21}, \Omega_{31}) \equiv \frac{\sum_j m_j^2 \text{Im}[\Omega_{j1}^2]}{m_{\text{atm}} \sum_j m_j |\Omega_{j1}|^2}. \quad (2.42)$$

The HL for ε_1 can then be written as [96]

$$\varepsilon_1^{\text{HL}}(m_1, M_1, \Omega_{21}, \Omega_{31}) \equiv \bar{\varepsilon}(M_1) \beta(m_1, \Omega_{21}, \Omega_{31}). \quad (2.43)$$

It is interesting that $\beta(m_1, \Omega_{21}, \Omega_{31}) \leq 1$, so that in the HL one has the upper bound $|\varepsilon_1^{\text{HL}}| \leq \bar{\varepsilon}(M_1)$ [97]. A more precise bound, which is known as the Davidson-Ibarra bound, was later derived [96],

$$|\varepsilon_1^{\text{HL}}| \leq \bar{\varepsilon}(M_1) \frac{m_{\text{atm}}}{m_1 + m_3}, \quad (2.44)$$

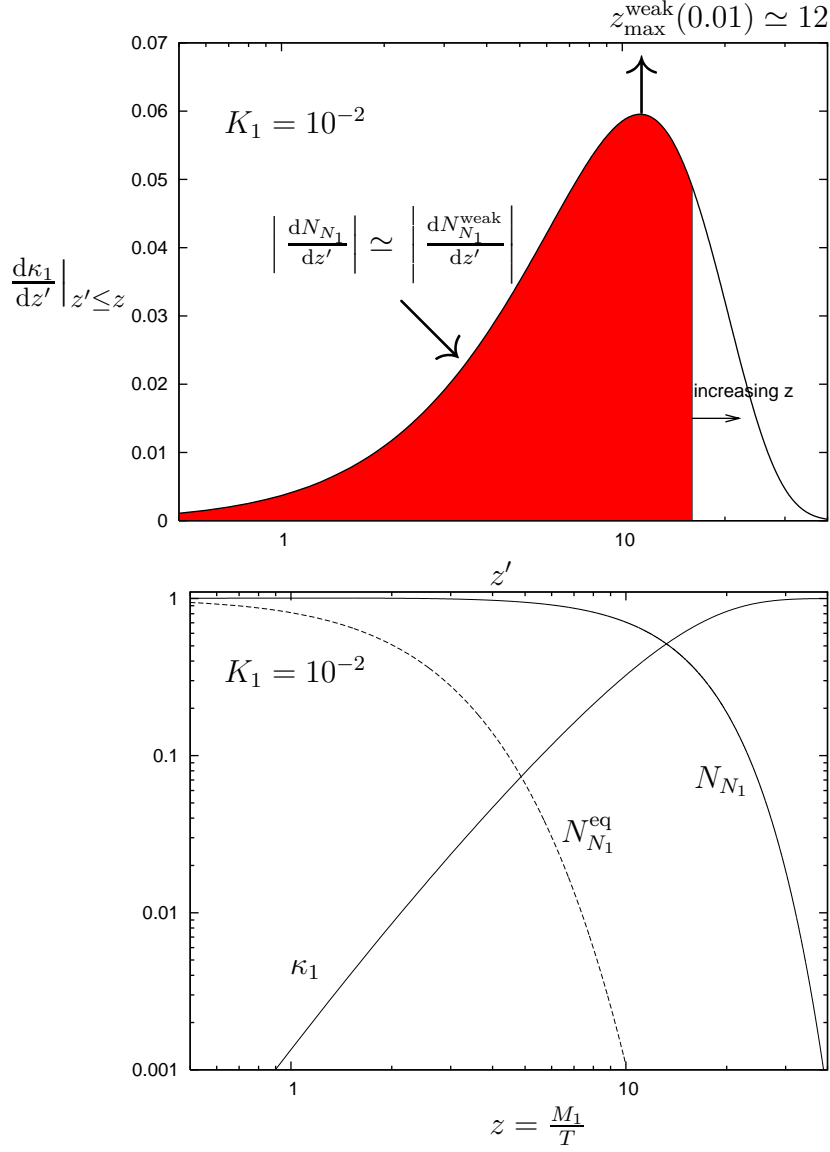


Figure 2.3: Dynamics in the weak washout regime for a thermal initial N_1 -abundance ($N_{N_1}^{\text{in}} = 1$). Top panel: rates. Bottom panel: efficiency factor κ_1 and N_1 -abundance. The maximum of the asymmetry production rate occurs at $z' \simeq z_{\max}^{\text{weak}}(K_1 = 0.01) \simeq 12$ [cf. Eq. (2.33)].

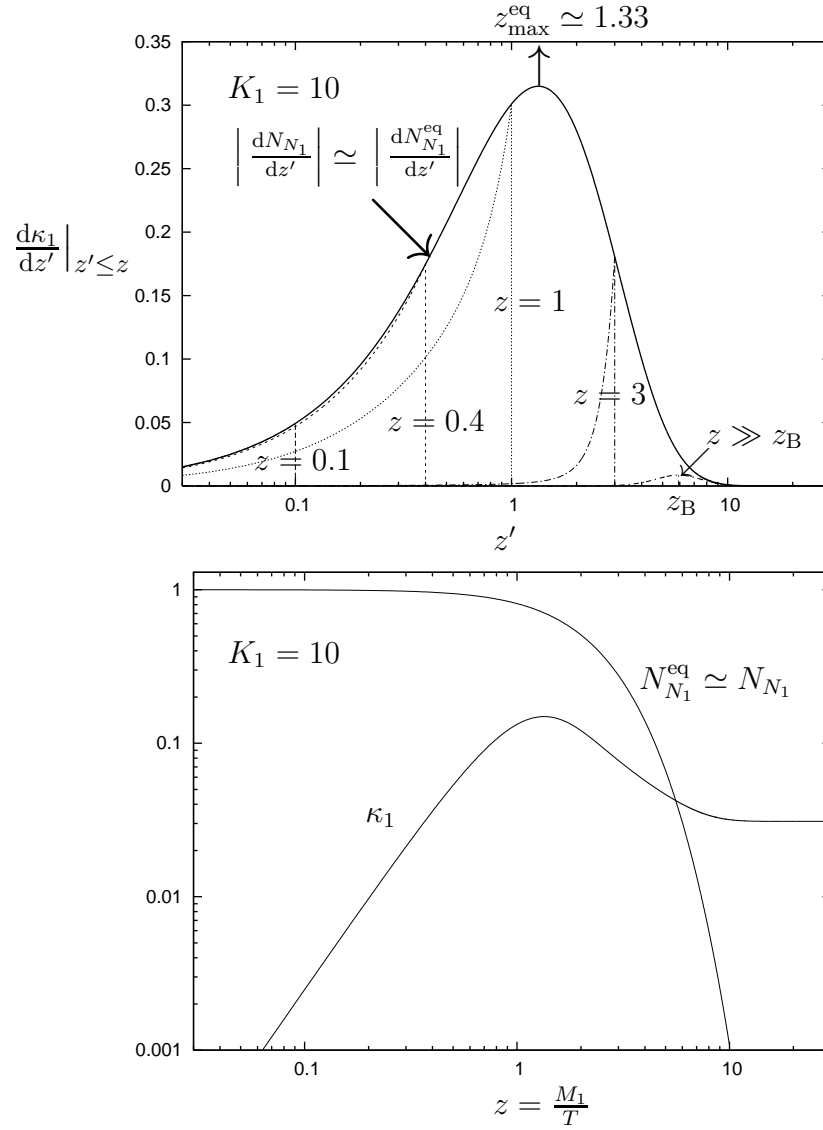


Figure 2.4: Dynamics in the strong washout regime. Top panel: rates. Bottom panel: efficiency factor κ_1 and N_1 -abundance. The maximum of the final asymmetry production rate occurs at $z' \simeq z_B$.

where we used the fact that $(m_3 - m_1)/m_{\text{atm}} = m_{\text{atm}}/(m_1 + m_3)$. Further refinements were added, leading to the even more accurate \tilde{m}_1 -dependent bound,

$$|\varepsilon_1^{\text{HL}}| \leq \bar{\varepsilon}(M_1) \frac{m_{\text{atm}}}{m_1 + m_3} f(m_1, \tilde{m}_1), \quad (2.45)$$

where [88, 98]

$$f(m_1, \tilde{m}_1) \simeq \begin{cases} 1 - m_1/\tilde{m}_1 & \text{if } m_1 \ll m_3, \\ \sqrt{1 - (m_1/\tilde{m}_1)^2} & \text{if } m_1 \simeq m_3, \end{cases} \quad (2.46)$$

obtained by maximizing over the Ω -parameters at fixed \tilde{m}_1 . From this bound one gets that $f(m_1, \tilde{m}_1)$ and hence the CP asymmetry are maximal in the limit $m_1 \rightarrow 0$. One notices as well that the CP asymmetry vanishes when $\tilde{m}_1 = m_1$.

The presence of the bound on the CP asymmetry Eq. (2.45) motivates the introduction of the so-called “effective leptogenesis phase” δ_L as

$$\beta(m_1, \Omega_{21}, \Omega_{31}) = \beta_{\text{max}}(m_1, \tilde{m}_1) \sin \delta_L(m_1, \Omega_{21}, \Omega_{31}), \quad (2.47)$$

where

$$\beta_{\text{max}}(m_1, \tilde{m}_1) = \frac{m_{\text{atm}}}{m_1 + m_3} f(m_1, \tilde{m}_1), \quad (2.48)$$

such that the upper bound in Eq. (2.45) corresponds to $\sin \delta_L = 1$.

It is also useful to express the function $f(m_1, \tilde{m}_1)$ as [93]

$$f(m_1, \tilde{m}_1) = \frac{m_1 + m_3}{\tilde{m}_1} Y_{\text{max}}(m_1, \tilde{m}_1), \quad (2.49)$$

where $Y_{\text{max}}(m_1, \tilde{m}_1)$ represents the configuration of Ω parameters which maximizes the CP asymmetry at fixed \tilde{m}_1 . It turns out that such a configuration always occurs for $\Omega_{21} = 0$ [93], and hence Y_{max} is the maximum of $\text{Im}[\Omega_{31}^2]$ at fixed \tilde{m}_1 . In other words, for $\Omega_{21} = 0$ and $Y_{\text{max}}(m_1, \tilde{m}_1) = \text{Im}[\Omega_{31}^2]$, the phase δ_L is maximal, while for a generic choice of Ω , the CP asymmetry undergoes a phase suppression

$$\begin{aligned} \sin \delta_L(m_1, \Omega_{21}, \Omega_{31}) &= \frac{m_1 + m_3}{\tilde{m}_1 f(m_1, \tilde{m}_1)} (\text{Im}[\Omega_{31}^2] + \sigma^2 \text{Im}[\Omega_{21}^2]) \\ &= \frac{\text{Im}[\Omega_{31}^2] + \sigma^2 \text{Im}[\Omega_{21}^2]}{Y_{\text{max}}(m_1, \tilde{m}_1)}, \end{aligned} \quad (2.50)$$

where $\sigma \equiv \sqrt{m_2^2 - m_1^2}/m_{\text{atm}}$. It can be readily seen that $\sin \delta_L = 1$ for $\text{Im}[\Omega_{21}^2] = 0$ and $\text{Im}[\Omega_{31}^2] = Y_{\text{max}}$.

It is instructive to calculate $\sin \delta_L$ for each of the three elementary complex rotations that can be used to parametrize Ω [cf. Eq. (2.19)]:

- For $\Omega = R_{13}$, one has $\sin \delta_L = \text{Im}[\Omega_{31}^2]/Y_{\max}$ and the phase is maximal if $\text{Im}[\Omega_{31}^2] = Y_{\max} = \tilde{m}_1/m_{\text{atm}}$; notice that there is no difference between normal and inverted hierarchy.
- For $\Omega = R_{12}$, one has $\sin \delta_L = \sigma^2 \text{Im}[\Omega_{21}^2]/Y_{\max} \leq \sigma$, larger for inverted hierarchy than for normal; however, for fully hierarchical light neutrinos ($m_1 \ll m_{\text{sol}}$), one has that $K_1 = K_{\text{sol}} |\Omega_{21}^2|$ for normal hierarchy and $K_1 \simeq K_{\text{atm}} |\Omega_{21}^2|$ for inverted hierarchy, and since $\kappa_1^f \propto K_1^{-1.2}$ [cf. Eq. (2.35)], the final asymmetry is slightly higher for normal hierarchy compared to inverted at fixed $|\Omega_{21}^2|$ [93].
- For $\Omega = R_{23}$, one has $\sin \delta_L = \varepsilon_1 = 0$; one can check that $\varepsilon_1 = 0$ applies independently of M_2 and M_3 and therefore not only in the HL. Notice that the conclusions in the previous two cases are still valid if one multiplies R_{13} or R_{12} with R_{23} respectively, since it does not affect $\sin \delta_L$.

Interesting constraints follow if one imposes that the asymmetry produced from leptogenesis explains the value of the baryon-to-photon ratio inferred from CMB observations, Eq. (1.6), [4, 81]

$$\eta_B(m_1, M_1, \Omega_{21}, \Omega_{31}) = \eta_B^{\text{CMB}} = (6.1 \pm 0.2) \times 10^{-10}. \quad (2.51)$$

If $M_1 \ll 10^{14} \text{ GeV}$ ($m_{\text{atm}}^2/\sum_i m_i^2$), then

$$\begin{aligned} M_1 &= \frac{\overline{M}_1}{\kappa(K_1) \beta_{\max}(m_1, K_1) \sin \delta_L(\Omega_{21}, \Omega_{31})} \\ &\geq M_1^{\min}(K_1) \equiv \frac{\overline{M}_1}{\kappa(K_1) \beta_{\max}(m_1, K_1)}, \end{aligned} \quad (2.52)$$

where we introduced the quantity

$$\overline{M}_1 \equiv \frac{16\pi}{3} \frac{N_{\gamma}^{\text{rec}} v^2}{a_{\text{sph}}} \frac{\eta_B^{\text{CMB}}}{m_{\text{atm}}} = (6.25 \pm 0.4) \times 10^8 \text{ GeV} \gtrsim 5 \times 10^8 \text{ GeV}. \quad (2.53)$$

The last inequality gives the 3σ value that we used to obtain all the results shown in the figures.³ Eq. (2.52) is quite general and shows the effect of the phase suppression [93] and of a higher absolute neutrino mass scale [95] in making M_1 higher. In Fig. 2.5 we show M_1^{\min} (thick solid line) for fully hierarchical light neutrinos ($m_1 = 0$) and maximal phase ($\sin \delta_L = 1$). It

³Notice that \overline{M}_1 gives the lower bound on M_1 for a thermal initial N_1 -abundance in the limit $K_1 \rightarrow 0$.

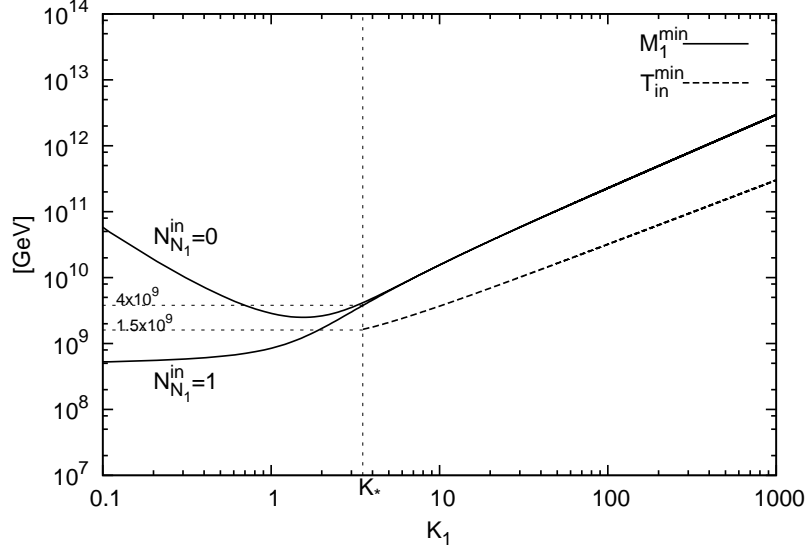


Figure 2.5: Lower bounds on M_1 and T_{in} vs. K_1 [cf. Eqs. (2.52) and (2.55)] in the case of maximal phase ($\sin \delta_L = 1$) and for $m_1 = 0$.

is convenient to introduce a value K_* such that, for $K_1 \geq K_*$, the final asymmetry calculated for a thermal initial N_1 -abundance ($N_{N_1}^{\text{in}} = 1$) differs from the one calculated for a vanishing initial N_1 -abundance ($N_{N_1}^{\text{in}} = 0$) by less than some quantity δ . When $\delta = 10\%$, $K_* \simeq 3.5$ and one obtains the lowest value [93],

$$M_1 \gtrsim 4 \times 10^9 \text{ GeV}. \quad (2.54)$$

The lower bound on M_1 also translates into a lower bound on T_{in} , the initial temperature of leptogenesis,

$$T_{\text{in}} \geq (T_{\text{in}}^{\text{min}})_{\text{HL}} \simeq \frac{(M_1^{\text{min}})_{\text{HL}}}{z_{\text{B}}(K_1) - 2} \gtrsim 1.5 \times 10^9 \text{ GeV} \quad (K_1 \gtrsim 3.5). \quad (2.55)$$

A plot of this lower bound is shown in Fig. 2.5 (thick dashed line). The relation between M_1^{min} and $T_{\text{in}}^{\text{min}}$ can be understood from the top panel of Fig. 2.4, which shows that the final asymmetry is the result of the decays occurring just around z_{B} , when inverse decays switch off, whereas all the asymmetry produced before is efficiently washed out.

Assuming a period of inflation at early stages, the minimal initial temperature $T_{\text{in}}^{\text{min}}$ that allows for successful leptogenesis can be identified with the minimal reheat temperature $T_{\text{reh}}^{\text{min}}$ after inflation. In locally supersymmetric theories, the high temperature required poses a problem known as the *gravitino problem*, as we shall see in the next section.

For increasing values of the absolute neutrino mass scale, m_1 , there is a joint effect of the suppression of the CP asymmetry, more specifically of $\beta_{\max}(m_1, \tilde{m}_1)$ [cf. Eq. (2.48)], plus the extra washout from $\Delta L = 2$ processes mediated by off-shell RH neutrinos, which can be conveniently factored out of the efficiency factor in the following way [80]:

$$\bar{\kappa}^f(\tilde{m}_1, M_1 \overline{m}^2) = \kappa^f(\tilde{m}_1) \exp \left\{ -\frac{\omega}{z_B} \left(\frac{M_1}{10^{10} \text{ GeV}} \right) \left(\frac{\overline{m}}{\text{eV}} \right)^2 \right\}, \quad (2.56)$$

where $\omega \simeq 0.186$ and $\overline{m}^2 \equiv m_1^2 + m_2^2 + m_3^2$. This suppression leads to a stringent upper bound on the lightest neutrino mass,

$$m_1 \leq 0.12 \text{ eV}, \quad (2.57)$$

as derived analytically in [80] and numerically in [75, 88, 99]. The upper bound can be seen in the upper part of Fig. 4.3, corresponding to the unflavored regime. It is obtained for high values $M_1 \sim 10^{13} \text{ GeV}$.

There have been earlier attempts to get a bound on the absolute neutrino mass scale simply from the fact that $m_1 \leq \tilde{m}_1$ and then imposing an upper limit $\tilde{m}_1 \lesssim 10^{-3} \text{ eV}$, justified as a generic ‘out-of-equilibrium’ condition. However, it turns out that such a restrictive upper limit on \tilde{m}_1 does not hold for reasons that are clear from Fig. 2.4: the ‘out-of-equilibrium’ condition is realized also in the strong washout regime when $z \gtrsim z_{\text{off}} \simeq z_B$. Therefore, within the N_1 DS, it is not a problem to have \tilde{m}_1 as large as 1 eV. Incidentally, the upper bound can only be understood when the washout from $\Delta L = 2$ processes and the upper bound on the CP asymmetry are jointly taken into account [99].

We would like now to summarize the results of this section. As we have seen, in the limit where the heavy neutrino mass spectrum is hierarchical (HL), $M_1 \ll M_2 \ll M_3$, the picture of leptogenesis in the unflavored case simplifies considerably. A typical scenario of leptogenesis, which we call “vanilla leptogenesis”, emerges and it turns out that one has to study only the production of asymmetry by the lightest RH neutrino, N_1 , reducing the number of parameters from 10 to 6. This is possible because the theoretically favored range for K_1 lies between $K_{\text{sol}} \equiv m_{\text{sol}}/m_\star = 8.2$, given by the solar scale, and $K_{\text{atm}} \equiv m_{\text{atm}}/m_\star = 48$, given by the atmospheric scale. In this range, the washout from the lightest RH neutrino is strong enough to make the contributions from the heavier two RH neutrinos negligible, and the final result is independent of the initial number of N_1 [80, 88, 93]. This is an extremely nice feature of the strong washout regime. Note that the N_1 DS can actually be ensured by setting $R_{23} = 1$, which excludes a large contribution from N_2 [93].

Within vanilla leptogenesis, it is possible to derive from successful leptogenesis a lower bound on M_1 and on the initial temperature T_{in} , as shown in Eqs. (2.54) and (2.55). Moreover, there is a stringent upper bound on the absolute neutrino mass scale, as shown in Eq. (2.57).

We shall discuss the implications of going beyond the assumptions leading to vanilla leptogenesis in Chapter 5.

2.3 Leptogenesis and supersymmetry

In the Minimal Supersymmetric Standard Model (MSSM) complemented with three RH neutrinos and the corresponding superpartners, the picture of leptogenesis is qualitatively quite different from the non-supersymmetric case, but it turns out that, quantitatively, they are very similar.

The interactions of the heavy (s)neutrino field can be derived from the leptonic superpotential

$$W = \frac{1}{2} M_i N_i N_i + h_{\alpha i} L_\alpha H_u N_i + f'_\alpha L_\alpha H_d E_\alpha, \quad (2.58)$$

where L_α and E_α are the $SU(2)$ lepton doublets and singlets chiral superfields, respectively, and H_u and H_d are the Higgs chiral superfields. The scalar components of both Higgs bosons, which we denote $\Phi_{u,d}$, have vacuum expectation values: $\langle \Phi_u \rangle \equiv v_u = v \sin \beta$ and $\langle \Phi_d \rangle \equiv v_d = v \cos \beta$, where $v = 174$ GeV. Their ratio is then given by

$$\tan \beta \equiv \frac{v_u}{v_d}. \quad (2.59)$$

When flavor effects (see next chapter) are included in supersymmetric leptogenesis, the value of $\tan \beta$ is relevant because $f_\alpha'^2 = (1 + \tan^2 \beta) f_\alpha^2$, where f_α is the SM Yukawa coupling.

Typically, supersymmetry breaking terms are of no relevance for the mechanism of lepton number generation, and we are left with the following trilinear couplings in the Lagrangian, written in terms of four-component spinors,

$$-h_{\alpha i} \left[M_i \tilde{L}_\alpha^\dagger \tilde{N}_i \Phi_u + \bar{\ell}_\alpha P_R N_i \Phi_u + \bar{\ell}_\alpha P_R \tilde{\phi}^c \tilde{N}_i + \tilde{L}_\alpha^\dagger P_R \tilde{\phi}^c N_i \right] + h.c., \quad (2.60)$$

where \tilde{L} , ϕ and \tilde{N} denote sleptons, higgsinos and singlet sneutrinos, respectively.

From these couplings one obtains the tree-level relations

$$\Gamma_{N_i \ell} + \Gamma_{N_i \bar{\ell}} = \Gamma_{N_i \tilde{L}} + \Gamma_{N_i \tilde{L}^\dagger} = \Gamma_{\tilde{N}_i^* \ell} = \Gamma_{\tilde{N}_i \tilde{L}} = \frac{(h^\dagger h)_{ii}}{8\pi} M_i. \quad (2.61)$$

There are now new diagrams contributing to the CP asymmetry. On top of the usual contributions shown in Fig. 1.8, there are three additional sources coming from the decay of the heavy neutrinos into sleptons, from the decay of RH sneutrinos into leptons and from the decay of RH sneutrinos into sleptons. One can then define a CP asymmetry for the decay of RH neutrinos into leptons and sleptons, and another one for the decay of RH sneutrinos into leptons and sleptons, as follows:

$$\tilde{\varepsilon}_N \equiv -\frac{(\Gamma_{N\bar{L}} + \Gamma_{N\ell}) - (\Gamma_{N\bar{L}^\dagger} + \Gamma_{N\bar{\ell}})}{\Gamma_N}, \quad (2.62)$$

$$\tilde{\varepsilon}_{\tilde{N}} \equiv -\frac{(\Gamma_{\tilde{N}^*\ell} + \Gamma_{\tilde{N}\bar{L}}) - (\Gamma_{\tilde{N}\bar{\ell}} + \Gamma_{\tilde{N}^*\bar{L}^\dagger})}{\Gamma_{\tilde{N}}}, \quad (2.63)$$

where Γ_N and $\Gamma_{\tilde{N}}$ denote the total decay rate of RH neutrinos and RH sneutrinos, respectively.

These CP asymmetries were computed in [87] to be

$$\tilde{\varepsilon}_N = \tilde{\varepsilon}_{\tilde{N}} = \frac{1}{8\pi} \frac{1}{(h^\dagger h)_{11}} \sum_{j \neq 1} \text{Im} \left[(h^\dagger h)_{1j}^2 \right] g(x_j), \quad (2.64)$$

where we recall that $x_j = M_j^2/M_1^2$, and

$$g(x) = \sqrt{x} \left[\frac{2}{x-1} + \ln \left(\frac{1+x}{x} \right) \right] \xrightarrow{x \gg 1} \frac{3}{\sqrt{x}}. \quad (2.65)$$

In the HL ($x_j \gg 1$), the CP asymmetry in the MSSM is therefore twice as large as the one in the SM.

Then, since in the MSSM there are two Higgses, the coefficient a_{sph} is slightly different from its value in the SM, and one obtains for the baryon-to-photon ratio

$$\eta_B \simeq 1.03 \times 10^{-2} \tilde{\varepsilon}_N \kappa_1^f. \quad (2.66)$$

As we have seen, there are new decay channels in the MSSM, which yield an enhancement of the CP asymmetry by a factor 2. On the other hand, there is also an enhancement of the washout by a factor of 2, which implies that the constraints on M_1 , T_{in} and m_1 derived in the last section remain essentially unchanged [75].

Assuming a period of inflation and reheating before leptogenesis occurs, the lower bound on the initial temperature of leptogenesis T_{in} can be identified with a lower bound on the reheat temperature T_{reh} of the Universe after inflation. Within locally supersymmetric theories, it is well known that gravitinos are produced during the reheating phase. The point is actually

that they may be overproduced, i.e. their abundance may overclose the Universe, leading to the so-called *gravitino problem* (for early discussions, see [100–103]). There are two situations to be distinguished: stable gravitinos and unstable ones.

If the gravitino is the lightest supersymmetric particle, it is stable and therefore represents a good dark matter candidate. In order for gravitinos not to exceed the dark matter abundance, the reheat temperature has to satisfy [104–107]

$$T_{\text{reh}} \lesssim 10^7\text{--}10^9 \text{ GeV}. \quad (2.67)$$

On the other hand, if gravitinos are unstable, they may lead to a large entropy production when they decay during or after big-bang nucleosynthesis, spoiling the nice agreement between theory and observations (see Fig. 1.3). This leads to the bound (see [108] and references therein)

$$T_{\text{reh}} \lesssim 10^6 \text{ GeV}, \quad (2.68)$$

unless the gravitino mass is larger than about 20 TeV.

Consequently, whatever specific scenario of supergravity one considers, there is a clear tension with the lower bound from leptogenesis given in Eq. (2.55). Different ways to relax this tension have been proposed in the literature. Let us give three well-known examples.

One possibility is to produce RH neutrinos non-thermally in the decays of the inflaton [75, 109–113]. A recent study [114] shows that the lower bound on T_{reh} from leptogenesis can be relaxed in this way by two orders of magnitude.

Another possibility is provided by “soft leptogenesis” [115, 116], which is a supersymmetric scenario which requires only one heavy RH neutrino. The interference between the CP -odd and CP -even states of the heavy scalar neutrino resembles very much the neutral kaon system. The mass splitting as well as the required CP violation in the heavy sneutrino system comes from the soft supersymmetry breaking A and B terms, associated with the Yukawa coupling and mass term of N_1 , respectively. The lower bound on the reheat temperature in this scenario can go as low as 10^6 GeV [75].

Finally, it is also possible to use the enhancement of the CP asymmetry for quasi-degenerate heavy neutrinos $M_1 \simeq M_2 \simeq M_3$ [87] (see Fig. 2.1) in order to relax the lower bound on the reheat temperature. This inspired the scenario of “resonant leptogenesis” [76, 117, 118], in which case the scale can be lowered to TeV. We shall come back to quasi-degenerate heavy neutrinos in Section 5.1.

Chapter 3

Adding flavor to vanilla leptogenesis

We described in the last chapter a picture of leptogenesis where the flavor content of the lepton doublets produced in the decays of the heavy neutrinos is neglected. This is done by summing over the flavor in the CP asymmetry parameter [cf. Eq. (1.24)], in the decay, inverse-decay and scattering rates, and the properly normalized number density in the Boltzmann equation (2.28) is $N_{B-L} = \sum_{\alpha} N_{B/3-L_{\alpha}}$. Summing over the flavor implies that all quantities in unflavored leptogenesis depend on some combination of $(h^{\dagger}h)_{ij}$, where the sum over α was explicitly carried out. Thus, even though the Yukawa coupling in the Lagrangian has a flavor index α [cf. Eq. (B.1)], the latter never shows up in the calculation.

This picture of leptogenesis was thought to be the correct one, or at least a good approximation of it, until the beginning of 2006, when two groups published independently results that showed the importance of flavor effects in leptogenesis [119, 120]. In this chapter we would like to explain in detail why flavor effects may be important, when they are expected to matter and how they modify in practice the results presented in the previous chapter.

3.1 When does flavor matter and why?

The SM Lagrangian contains a term that gives rise to the masses of the charged leptons. Before spontaneous symmetry breaking, this term can be written as $f_{\alpha} \bar{\ell}_{L\alpha} e_{R\alpha} \Phi + h.c.$, where $e_{R\alpha}$ denote the right-handed lepton fields, which are singlets under $SU(2)$, but with hypercharge -2. Note that we chose a lepton basis such that this term is flavor diagonal.

In the early Universe the Yukawa coupling f_{α} can be strong enough to

maintain processes like $\ell_\alpha \bar{e}_\alpha \leftrightarrow \Phi^\dagger$ or $\ell_\alpha \bar{e}_\alpha \leftrightarrow \Phi^\dagger A$, where $A = W^{3,\pm}$, B are the $SU(2) \times U(1)$ gauge bosons, in equilibrium, i.e. $\Gamma_\alpha \gtrsim H$. With a vacuum Higgs mass of 120 GeV, the interaction rate was estimated in [121] to be

$$\Gamma_\alpha \simeq 5 \times 10^{-3} f_\alpha^2 T. \quad (3.1)$$

Obviously, when the temperature drops due to the expansion of the Universe, the first interactions that will enter equilibrium are the ones involving the τ -lepton, simply because its Yukawa coupling is larger. It turns out that the temperature at which the τ -lepton Yukawa interactions enter equilibrium is $\sim 10^{12}$ GeV. For the muon, this will happen at $T \sim 10^9$ GeV, and for the electron, at still much lower temperature.¹

If the charged-lepton Yukawa interactions are in equilibrium ($\Gamma_\alpha > H$) and faster than inverse decays (see Section 4.1.2),

$$\Gamma_\alpha \gtrsim \sum_i \Gamma_{\text{ID}}^i, \quad (3.2)$$

during the relevant period of the asymmetry generation, then the lepton quantum states $|\ell_i\rangle$ [cf. Eq.(2.1)] lose coherence between the production at decay and the subsequent absorption in inverse processes. When the loss of coherence is complete, the Higgs bosons will interact with incoherent lepton flavor eigenstates instead of the coherent superposition $|\ell_i\rangle$ produced in the decays. In the limit where the quantum state becomes completely incoherent and is fully projected onto one of the flavor eigenstates, each lepton flavor can be treated as a statistically independent particle species. This is what we call the “fully flavored regime”. One has to distinguish a two-flavor regime, for $10^9 \text{ GeV} \lesssim M_1 \lesssim 10^{12} \text{ GeV}$, such that the condition Eq. (3.2) is satisfied only for $\alpha = \tau$, and a three-flavor regime, for $M_1 \lesssim 10^9 \text{ GeV}$, where the condition Eq. (3.2) applies also to $\alpha = \mu$.

In the fully flavored regime, there are two new effects compared to the unflavored regime [119]. These can be understood introducing the projectors and writing them as the sum of two terms,

$$P_{i\alpha} \equiv |\langle \ell_i | \ell_\alpha \rangle|^2 = P_{i\alpha}^0 + \frac{\Delta P_{i\alpha}^0}{2} \quad (3.3)$$

$$\bar{P}_{i\alpha} \equiv |\langle \bar{\ell}_i | \bar{\ell}_\alpha \rangle|^2 = P_{i\alpha}^0 - \frac{\Delta P_{i\alpha}^0}{2}. \quad (3.4)$$

The first effect is a reduction of the washout compared to the unflavored regime and is described by the tree-level contribution $P_{i\alpha}^0 = (P_{i\alpha} + \bar{P}_{i\alpha})/2$,

¹In supersymmetric leptogenesis, the rate in Eq. (3.1) is multiplied by $(1 + \tan \beta)^2$ (see Section 2.3), so that flavor effects can start to matter at higher temperatures [122].

which sets the fraction of the total asymmetry produced in N_i -decays that goes into each single flavor α . In the fully flavored regime, the Higgs will make inverse decays on flavor eigenstates $|\ell_\alpha\rangle$, instead of the linear superposition $|\ell_i\rangle$, and hence the washout rate is reduced by the projector $P_{i\alpha}^0$.

The second effect is an additional CP -violating contribution due to a different flavor composition between $|\ell_i\rangle$ and $CP|\bar{\ell}'_i\rangle$. This can be described in terms of the projector differences $\Delta P_{i\alpha} \equiv P_{i\alpha} - \bar{P}_{i\alpha}$, such that $\sum_\alpha \Delta P_{i\alpha} = 0$. Indeed, defining the flavored CP asymmetries,

$$\varepsilon_{i\alpha} \equiv -\frac{\Gamma_{i\alpha} - \bar{\Gamma}_{i\alpha}}{\Gamma_i + \bar{\Gamma}_i}, \quad (3.5)$$

where $\Gamma_{i\alpha} \equiv P_{i\alpha}\Gamma_i$ and $\bar{\Gamma}_{i\alpha} \equiv \bar{P}_{i\alpha}\bar{\Gamma}_i$ and the total decay rates Γ_i and $\bar{\Gamma}_i$ were introduced after Eq. (1.24), these can be now expressed as

$$\varepsilon_{i\alpha} = \varepsilon_i P_{i\alpha}^0 + \frac{\Delta P_{i\alpha}}{2}, \quad (3.6)$$

showing that the first term is the usual contribution due to a different decay rate into leptons and antileptons, and the second is the additional contribution due to a possible different flavor composition between $|\ell_i\rangle$ and $CP|\bar{\ell}'_i\rangle$. Note that when the flavored CP asymmetries are summed over the flavor, one recovers the total CP asymmetry used in the unflavored regime, i.e. $\sum_\alpha \varepsilon_{i\alpha} = \varepsilon_i$.

It is interesting to notice at this point that one can imagine a scenario where the total CP asymmetry ε_i is 0, i.e. no asymmetry would have been produced in the unflavored regime, but, thanks to the ΔP contribution, the flavored CP asymmetries $\varepsilon_{i\alpha}$ do not vanish. More specifically, one can imagine that the only source of CP violation comes from low-energy phases in the PMNS matrix. Since the total CP asymmetry is insensitive to the PMNS matrix, $\varepsilon_i = 0$ in this case. However, $\Delta P_{i\alpha}$ and $\varepsilon_{i\alpha}$ do explicitly depend on the PMNS matrix [see for instance Eq. (3.28)], so that they can be non-zero only thanks to the low-energy phases. In great contrast to the unflavored picture, fully flavored leptogenesis can then be successful solely thanks to the CP violation coming from low-energy phases. This represents a very nice possibility which will be the subject of Chapter 6.

3.2 Flavored Boltzmann equations and spectator processes

We follow here the approach presented in [78, 119]. Heavy neutrino decays produce lepton flavor asymmetries, N_{L_α} , that are computed using Boltz-

mann equations similar to Eqs. (2.27) and (2.28). Rigorously, one should include the effect of electroweak sphalerons, which constitute an additional source of lepton flavor violation. This can be symbolically done by adding a washout term $dN_{L_\alpha}^{\text{EW}}/dz$. Then, for consistency, we also need to add the equation $dN_B/dz = dN_B^{\text{EW}}/dz$ to account for baryon number violation by the sphaleron processes. Given that the sphaleron interactions preserve the three charges $\Delta_\alpha \equiv B/3 - L_\alpha$ associated to anomaly-free currents, it follows that $N_B^{\text{EW}}/3 = N_{L_\alpha}^{\text{EW}}$. By subtracting the equations for the lepton flavor densities from the equation for baryon number weighted by a suitable factor $1/3$, one obtains the following network of flavored Boltzmann equations [119]:

$$\frac{dN_{N_1}}{dz} = -D_1 (N_{N_1} - N_{N_1}^{\text{eq}}) \quad (3.7)$$

$$\frac{dN_{\Delta_\alpha}}{dz} = \varepsilon_{1\alpha} D_1 (N_{N_1} - N_{N_1}^{\text{eq}}) - P_{1\alpha}^0 W_1^{\text{ID}} (N_{\ell_\alpha} + N_\Phi), \quad (3.8)$$

where, $\alpha = e, \mu, \tau$ and, for simplicity, we included only decays and inverse decays with proper subtraction of the resonant contribution from $\Delta L = 2$ and $\Delta L = 0$ processes, and only focused on the lightest RH neutrino N_1 . Notice that N_{Δ_α} is the Δ_α number density, properly normalized, and $N_{L_\alpha} = N_{\ell_\alpha} + N_{e_\alpha}$, where e_α denote the RH lepton fields.

We are neglecting non-resonant $\Delta L = 2$ and $\Delta L = 0$ processes, a good approximation for $M_1 \ll 10^{14}$ GeV, as we will always consider. We are also neglecting $\Delta L = 1$ scatterings, which give a correction to a level less than $\sim 10\%$ in the most interesting strong washout regime [123], and thermal corrections.

The number density asymmetries for the particles X entering in Eq. (3.8) are related to the corresponding chemical potentials through

$$n_X - n_{\bar{X}} = \frac{g_X T^3}{6} \begin{cases} \mu_X/T & \text{fermions,} \\ 2\mu_X/T & \text{bosons,} \end{cases} \quad (3.9)$$

where g_X is the number of degrees of freedom of X . For any given temperature regime, the specific set of reactions that are in chemical equilibrium enforce algebraic relations between different chemical potentials [83]. In the entire range of temperatures relevant for leptogenesis, the interactions mediated by the top-quark Yukawa coupling h_t , and by the gauge interactions, are always in equilibrium. Moreover, at the intermediate-low temperatures where flavor effects can be important, strong QCD sphalerons [124] are also in equilibrium. This situation has the following consequences:

- Equilibration of the chemical potentials for the different quark colors is guaranteed because the chemical potentials of the gluons vanish, $\mu_g = 0$.

- Equilibration of the chemical potentials for the two members of a $SU(2)$ doublet is guaranteed by the fact that $\mu_{W^+} = -\mu_{W^-} = 0$ above the electroweak phase transition. This condition was implicitly implemented in Eq. (3.8), where we used $\mu_\ell \equiv \mu_{e_L} = \mu_{\nu_L}$ and $\mu_\Phi \equiv \mu_{\phi^+} = \mu_{\phi^0}$ to write the particle number asymmetries directly in terms of the number densities of the $SU(2)$ doublets.
- Hypercharge neutrality implies

$$\sum_i (\mu_{Q_i} + 2\mu_{u_i} - \mu_{d_i} - \mu_{\ell_i} - \mu_{e_i}) + 2\mu_\Phi = 0, \quad (3.10)$$

where u_i , d_i and e_i denote the $SU(2)$ singlet fermions of the i -th generation.

- The equilibration condition for the Yukawa interactions of the top quark $\mu_t = \mu_{Q_3} + \mu_\Phi$.
- Because of their larger rates, QCD sphalerons equilibration occurs at higher temperatures than for the corresponding electroweak processes, presumably around $T_s \sim 10^{13}$ GeV [125, 126], and in any case long before equilibrium is reached for the τ -Yukawa processes. This implies the additional constraint

$$\sum_i (2\mu_{Q_i} - \mu_{u_i} - \mu_{d_i}) = 0. \quad (3.11)$$

To express the asymmetries N_{ℓ_α} and N_Φ in terms of the N_{Δ_α} , we define two matrices, C^ℓ and C^Φ , through the relations [119, 127]:

$$N_{\ell_\alpha} = - \sum_\beta C_{\alpha\beta}^\ell N_{\Delta_\beta}, \quad N_\Phi = - \sum_\beta C_\beta^\Phi N_{\Delta_\beta}, \quad (3.12)$$

so that Eq. (3.8) can be now rewritten as follows:

$$\frac{dN_{\Delta_\alpha}}{dz} = \varepsilon_{1\alpha} D_1 (N_{N_1} - N_{N_1}^{\text{eq}}) - P_{1\alpha}^0 W_1^{\text{ID}} \sum_\beta (C_{\alpha\beta}^\ell + C_\beta^\Phi) N_{\Delta_\beta}. \quad (3.13)$$

The numerical values of the entries in C^ℓ and C^Φ are determined by the constraints among the various chemical potentials enforced by the fast reactions that are in equilibrium in the temperature range ($T \sim M_1$) where the Δ_α asymmetries are produced.

In the temperature range 10^9 GeV $\lesssim T \lesssim 10^{12}$ GeV, we consider the bottom-, tau- and charm-Yukawa interactions to be in equilibrium, implying

that the asymmetries in the $SU(2)$ singlets b , e_τ and c degrees of freedom are populated. The corresponding chemical potentials obey the equilibrium constraints $\mu_b = \mu_{Q_3} - \mu_\Phi$, $\mu_c = \mu_{Q_2} + \mu_\Phi$ and $\mu_\tau = \mu_{\ell_\tau} - \mu_\Phi$. Moreover, the electroweak sphaleron processes are also in equilibrium, implying

$$\sum_i (3\mu_{Q_i} + \mu_{\ell_i}) = 0. \quad (3.14)$$

As concerns lepton number, each electroweak sphaleron transition creates all the doublets of the three generations, implying that individual lepton flavor numbers are no longer conserved. An asymmetry will then be generated along the ℓ_τ and $\ell_{e+\mu}$ directions in flavor space. Even though the electroweak sphalerons induce $L_\perp \neq 0$, where by the subscript \perp we mean the direction in flavor space perpendicular to ℓ_τ and $\ell_{e+\mu}$, the condition $\Delta_\perp = 0$ is not violated, and hence Eq. (3.13) consists of just two equations for N_{Δ_τ} and $N_{\Delta_{e+\mu}}$. This is what we call the *two-flavor regime*. As concerns baryon number, electroweak sphalerons are the only source of B violation, implying that baryon number is equally distributed among the three quark generations, i.e. $B/3$ in each generation. This modifies the detailed equilibrium conditions for the quark chemical potentials. Solving the corresponding set of linear equations for the chemical potentials, one obtains [128]

$$C^\Phi = \frac{1}{158}(41, 56), \quad C^\ell = \frac{1}{316} \begin{pmatrix} 270 & -32 \\ -17 & 208 \end{pmatrix}. \quad (3.15)$$

In the temperature range $T \lesssim 10^9$ GeV, one has to include the equilibration constraints from the strange-quark Yukawa interactions and, more importantly, from the muon-Yukawa interactions. Given that the electron remains the only lepton with a negligible Yukawa coupling, the Yukawa interactions completely define the flavor basis for the leptons as well as for the antileptons (that are now the CP -conjugate states of the leptons). Correspondingly, the lepton asymmetries are also completely defined in the flavor basis. In this regime the coefficients $C_{\alpha\beta}^\ell$ and C_β^Φ are given by [119, 129]

$$C^\Phi = \frac{1}{179}(37, 52, 52), \quad C^\ell = \frac{1}{1074} \begin{pmatrix} 906 & -120 & -120 \\ -75 & 688 & -28 \\ -75 & -28 & 688 \end{pmatrix}. \quad (3.16)$$

3.3 In practice, what changes?

We have seen in the last section that, if the relevant temperature for leptogenesis is below roughly 10^{12} GeV, a rigorous description of the asymme-

try evolution has to be performed in terms of the individual flavor asymmetries $\Delta_\alpha \equiv B/3 - L_\alpha$ rather than in terms of the total asymmetry $N_{B-L} = \sum_\alpha N_{\Delta_\alpha}$, as usually done in the unflavored treatment.

We would like to make two remarks:

- From Eq. (3.13) it can be seen that the two diagonal entries of C^ℓ sum up with the entries in C^Φ . Actually, this sum turns out to be close to 1 both using Eq. (3.15) and Eq. (3.16); moreover, the addition of the coefficients in C^Φ tends to equalize the flavored diagonal elements [128].
- It was shown in [130] that the off-diagonal elements in the matrix C^ℓ have an effect smaller than 40% on the final asymmetry. Taking into account the matrix C^Φ , this effect is even reduced.

Therefore, for simplicity, we shall use in the following $C^\ell + C^\Phi = \mathbb{1}$, which takes into account spectator processes in an approximate way. The generalization of the flavored Eqs. (3.7) and (3.8) to three RH neutrinos ($i = 1, 2, 3$) is then given by [119, 120, 131, 132]

$$\frac{dN_{N_i}}{dz} = -D_i (N_{N_i} - N_{N_i}^{\text{eq}}) \quad (3.17)$$

$$\frac{dN_{\Delta_\alpha}}{dz} = \sum_i \varepsilon_{i\alpha} D_i (N_{N_i} - N_{N_i}^{\text{eq}}) - \sum_i P_{i\alpha}^0 W_i^{\text{ID}} N_{\Delta_\alpha}. \quad (3.18)$$

Notice that, in the two-flavor regime, $\Delta_\alpha = B/2 - L_\alpha$, where $\alpha = e + \mu$ or τ , and the two equations for the individual electron and muon asymmetries are replaced by one kinetic equation for the sum $N_{\Delta_{e+\mu}}$, where the individual flavored CP asymmetries and projectors have to be replaced by their sum, namely $\varepsilon_{1e+\mu} \equiv \varepsilon_{1\mu} + \varepsilon_{1e}$ and $P_{1e+\mu}^0 \equiv P_{1\mu}^0 + P_{1e}^0$ [129]. The total asymmetry is then given by $N_{B-L} = N_{\Delta_{e+\mu}} + N_{\Delta_\tau}$. The calculation is therefore intermediate between the unflavored case and the three-flavor regime, though the results are very similar to the three-flavor regime [123].

The evolution of the N_{Δ_α} 's can be worked out in an integral form,

$$N_{\Delta_\alpha}(z) = N_{\Delta_\alpha}^{\text{in}} \exp \left(- \sum_i P_{i\alpha}^0 \int_{z_{\text{in}}}^z dz' W_i^{\text{ID}}(z') \right) + \sum_i \varepsilon_{i\alpha} \kappa_{i\alpha}(z), \quad (3.19)$$

with the 6, in the two-flavor case, or 9, in the three-flavor case, efficiency factors given by

$$\kappa_{i\alpha}(z; K_i, P_{i\alpha}^0) = - \int_{z_{\text{in}}}^z dz' \frac{dN_{N_i}}{dz'} \exp \left(- \sum_i P_{i\alpha}^0 \int_{z'}^z dz'' W_i^{\text{ID}}(z'') \right). \quad (3.20)$$

The final $B-L$ asymmetry is then given by

$$N_{B-L}^f = \sum_{\alpha} N_{\Delta\alpha}^f, \quad (3.21)$$

from which one obtains the baryon-to-photon ratio η_B using Eq. (2.15).

Using the convenient Casas-Ibarra parametrization, Eq. (2.18), the tree-level projectors can be written as

$$P_{i\alpha}^0 = \frac{|\sum_j \sqrt{m_j} U_{\alpha j} \Omega_{ji}|^2}{\sum_j m_j |\Omega_{ji}^2|}. \quad (3.22)$$

It will also prove useful to introduce the flavored decay parameters,

$$K_{i\alpha} \equiv P_{i\alpha}^0 K_i = \left| \sum_j \sqrt{\frac{m_j}{m_{\star}}} U_{\alpha j} \Omega_{ji} \right|^2, \quad (3.23)$$

obtained using Eqs. (3.22) and (2.23).

The flavored CP asymmetries are given by the following expression [87]:

$$\begin{aligned} \varepsilon_{i\alpha} = & \frac{3}{16\pi(h^\dagger h)_{ii}} \sum_{j \neq i} \left\{ \text{Im} [h_{\alpha i}^* h_{\alpha j} (h^\dagger h)_{ij}] \frac{\xi(x_j/x_i)}{\sqrt{x_j/x_i}} \right. \\ & \left. + \frac{2}{3(x_j/x_i - 1)} \text{Im} [h_{\alpha i}^* h_{\alpha j} (h^\dagger h)_{ji}] \right\}, \quad (3.24) \end{aligned}$$

where $\xi(x)$ was defined in Eq. (2.17), and we recall that $x_i \equiv M_i^2/M_1^2$.

In general, the final asymmetry will depend on all 18 see-saw parameters. As explained in the introduction (Section 1.2.2), until now we have only measured two mass-squared differences and two mixing angles in neutrino oscillation experiments. This is essentially the only information on the 18 see-saw parameters we have. Thus, we can write that $\eta_B = \eta_B(m_1, U, M_i, \omega_{21}, \omega_{31}, \omega_{32})$. It is interesting that including flavor effects there is a potential dependence of the final asymmetry also on the unknown parameters contained in the PMNS mixing matrix U [119, 131], namely the mixing angle θ_{13} and the CP -violating phases δ and $\Phi_{1,2}$ [cf. Eq. (A.5)].

Let us assume that the mass spectrum of the heavy neutrinos is hierarchical, $M_1 \ll M_2 \ll M_3$. In this case the general expression Eq. (3.24) for the CP asymmetries $\varepsilon_{i\alpha}$ reduces to

$$\varepsilon_{1\alpha} \simeq \frac{3}{16\pi(h^\dagger h)_{11}} \sum_{j \neq 1} \frac{M_1}{M_j} \text{Im} [h_{\alpha 1}^* h_{\alpha j} (h^\dagger h)_{1j}], \quad (3.25)$$

$$\varepsilon_{2\alpha} \simeq \frac{3}{16\pi(h^\dagger h)_{22}} \left\{ \frac{M_2}{M_3} \text{Im} [h_{\alpha 2}^* h_{\alpha 3} (h^\dagger h)_{23}] - \frac{2}{3} \text{Im} [h_{\alpha 2}^* h_{\alpha 1} (h^\dagger h)_{12}] \right\}, \quad (3.26)$$

$$\varepsilon_{3\alpha} \simeq -\frac{1}{8\pi(h^\dagger h)_{33}} \sum_{j \neq 3} \text{Im} [h_{\alpha 3}^* h_{\alpha j} (h^\dagger h)_{j3}]. \quad (3.27)$$

Expressing the flavored CP asymmetries $\varepsilon_{1\alpha}$ in terms of the orthogonal parametrization, one obtains [129]

$$\varepsilon_{1\alpha} = -\frac{3M_1}{16\pi v^2} \sum_{h,l} \frac{m_l \sqrt{m_l m_h}}{\tilde{m}_1} \text{Im}[U_{\alpha h} U_{\alpha l}^* \Omega_{h1} \Omega_{l1}], \quad (3.28)$$

where the explicit dependence on the PMNS matrix can be seen. Similar expressions can be found for $\varepsilon_{2\alpha}$ and $\varepsilon_{3\alpha}$, but as they are slightly more complicated, we do not show them here.

In the following, we shall assume no rotation in the plane 23, i.e. $R_{23} = \mathbb{1}$ [cf. Eq. (2.22)]. Under these conditions, both total CP asymmetries ε_2 and ε_3 are suppressed like $\sim M_1/M_{2,3}$. On the other hand, it is interesting to notice that the $\varepsilon_{2\alpha}$'s and the $\varepsilon_{3\alpha}$'s are not necessarily suppressed. This can potentially lead to a scenario where the final asymmetry is produced by the decays of the two heavier RH neutrinos, provided $M_{2,3} \lesssim 10^{12} \text{ GeV}$ in order for the flavored regime to apply. Here we do not pursue this possibility (see, however, Sections 5.2 and 6.2) and focus on a typical N_1 -dominated scenario where the dominant contribution to the final asymmetry comes from the decays of the lightest RH neutrino, so that

$$N_{B-L}^f \simeq N_{B-L}^f|_{N_1} \equiv \sum_{\alpha} \varepsilon_{1\alpha} \kappa_{1\alpha}. \quad (3.29)$$

It will prove important for our discussion that both the total CP asymmetry ε_1 and the flavored ones $\varepsilon_{1\alpha}$ cannot be arbitrarily large. The total CP asymmetry is indeed upper bounded by Eq. (2.45), and each flavored CP asymmetry $\varepsilon_{1\alpha}$ is bounded by [129]

$$|\varepsilon_{1\alpha}| < \bar{\varepsilon}(M_1) \sqrt{P_{1\alpha}^0} \frac{m_3}{m_{\text{atm}}} \max_j [|U_{\alpha j}|], \quad (3.30)$$

where we recall that $\bar{\varepsilon}(M_1) \equiv 3 M_1 m_{\text{atm}}/(16\pi v^2)$. Therefore, while the total CP asymmetry is suppressed when m_1 increases, the single-flavor CP asymmetries can be enhanced. The existence of an upper bound on the quantity

$$r_{1\alpha} \equiv \varepsilon_{1\alpha}/\bar{\varepsilon}(M_1) \quad (3.31)$$

independent of M_1 , implies, as in the unflavored analysis, Eq. (2.52), the existence of a lower bound on M_1 given by

$$M_1 \geq M_1^{\min}(K_1) = \frac{\overline{M}_1}{\kappa_1^f(K_1) \xi_1^{\max}(K_1)}, \quad (3.32)$$

where we will always use the 3σ lower value for \overline{M}_1 [cf. Eq. (2.53)], and we indicated with $\kappa_1^f(K_1)$ the efficiency factor in the unflavored case, corresponding to $\kappa_{1\alpha}^f$ with $P_{1\alpha}^0 = 1$. We also defined

$$\xi_1 \equiv \sum_{\alpha} \xi_{1\alpha}, \quad \text{with} \quad \xi_{1\alpha} \equiv \frac{r_{1\alpha} \kappa_{1\alpha}^f(K_{1\alpha})}{\kappa_1^f(K_1)}. \quad (3.33)$$

This quantity represents the deviation introduced by flavor effects compared to the unflavored treatment in the hierarchical light neutrino case. We could then use $r_{1\alpha} \leq \sqrt{P_{1\alpha}^0} m_3/m_{\text{atm}}$ to maximize ξ_1 . Notice however that, first, the $r_{1\alpha}$'s cannot be simultaneously equal to $\sqrt{P_{1\alpha}^0}$ because of the bound on the total asymmetry, and, second, there are sign cancellations in ξ_1 . Therefore, the bound (3.32) is more restrictive than this possible estimation, and we prefer to keep it in this form, maximizing ξ_1 in each particular situation.

As usual, the lower bound on M_1 implies an associated lower bound on the initial temperature T_{in} of leptogenesis and hence on the reheat temperature T_{reh} .

3.4 Dependence on the initial conditions and lower bounds

From Eq. (3.20), extending an analytic procedure derived within the unflavored treatment [80], one can obtain simple expressions for the flavored efficiency factors $\kappa_{1\alpha}^f$. In the case of a thermal initial N_1 -abundance ($N_{N_1}^{\text{in}} = 1$), one has

$$\kappa_{1\alpha}^f \simeq \kappa(K_{1\alpha}), \quad (3.34)$$

where the function $\kappa(x)$ was given in Eq. (2.31). Notice that, in the particularly relevant range $5 \lesssim K_{1\alpha} \lesssim 100$, this expression is well approximated by Eq. (2.35) replacing $K_1 \rightarrow K_{1\alpha}$.

In the case of vanishing initial N_1 -abundance ($N_{N_1}^{\text{in}} = 0$), one has to take into account two different contributions, a negative and a positive one,

$$\kappa_{1\alpha}^f = \kappa_-^f(K_1, P_{1\alpha}^0) + \kappa_+^f(K_1, P_{1\alpha}^0). \quad (3.35)$$

The negative contribution arises from a first stage when $N_{N_1} \leq N_{N_1}^{\text{eq}}$, for $z \leq z_{\text{eq}}$, and is given approximately by

$$\kappa_-^f(K_1, P_{1\alpha}^0) \simeq -\frac{2}{P_{1\alpha}^0} \exp\left(-\frac{3\pi K_{1\alpha}}{8}\right) \left[\exp\left(\frac{P_{1\alpha}^0}{2} N_{N_1}(z_{\text{eq}})\right) - 1 \right], \quad (3.36)$$

where $N_{N_1}(z_{\text{eq}})$ was defined in Eq. (2.38).

The positive contribution arises from a second stage when $N_{N_1} \geq N_{N_1}^{\text{eq}}$, for $z \geq z_{\text{eq}}$, and is approximately given by

$$\kappa_+^f(K_1, P_{1\alpha}^0) \simeq \frac{2}{z_B(K_{1\alpha}) K_{1\alpha}} \left[1 - \exp\left(-\frac{1}{2} K_{1\alpha} z_B(K_{1\alpha}) N_{N_1}(z_{\text{eq}})\right) \right]. \quad (3.37)$$

It is interesting to notice that $N_{N_1}(z_{\text{eq}})$ is still regulated by K_1 [cf. Eq. (2.38)], since the RH neutrino production is not affected by flavor effects, contrarily to the washout, which is reduced because regulated by $K_{1\alpha}$.

These analytic expressions make transparent the two conditions to have independence from the initial conditions. The first is the thermalization of the N_1 -abundance, such that, for an arbitrary initial N_1 -abundance, one has $N_{N_1}(z_{\text{eq}}) = 1$. The second is that the asymmetry produced during the non-thermal stage, for $z \leq z_{\text{eq}}$, has to be efficiently washed out, leading to $|\kappa_-^f| \ll \kappa_+^f$. They are both realized for large values $K_1 \gg 1$. More quantitatively, we introduced in Section 2.2 the quantity K_* such that, for $K_1 \geq K_*$, the final asymmetry calculated for a thermal initial N_1 -abundance differs from the one calculated for a vanishing initial abundance by less than some quantity δ . This can be used as a precise definition of the strong washout regime. Let us consider some particular cases, showing how flavor effects tend to enlarge the domain of the weak washout at the expense of the strong washout regime.

3.4.1 Alignment

The simplest situation is the alignment case, realized when the N_1 -decays are just into one flavor α , so that $P_{1\alpha} = \overline{P}_{1\alpha} = 1$ and $P_{1\beta \neq \alpha} = \overline{P}_{1\beta \neq \alpha} = 0$, implying $\varepsilon_{1\alpha} = \varepsilon_1$. Notice that we do not have to worry about the fact that the lightest RH neutrino inverse decays might not be able to wash out the asymmetry generated from the decays of the two heavier neutrinos, since we are assuming negligible $\varepsilon_{2\beta}$ and $\varepsilon_{3\beta}$ anyway. In this case the general set of kinetic equations (3.17) and (3.18) reduces to the usual unflavored equations and all results coincide with those in the unflavored analysis [119]. In particular one has $N_{B-L}^f = \varepsilon_1 \kappa_{1\alpha}^f$.

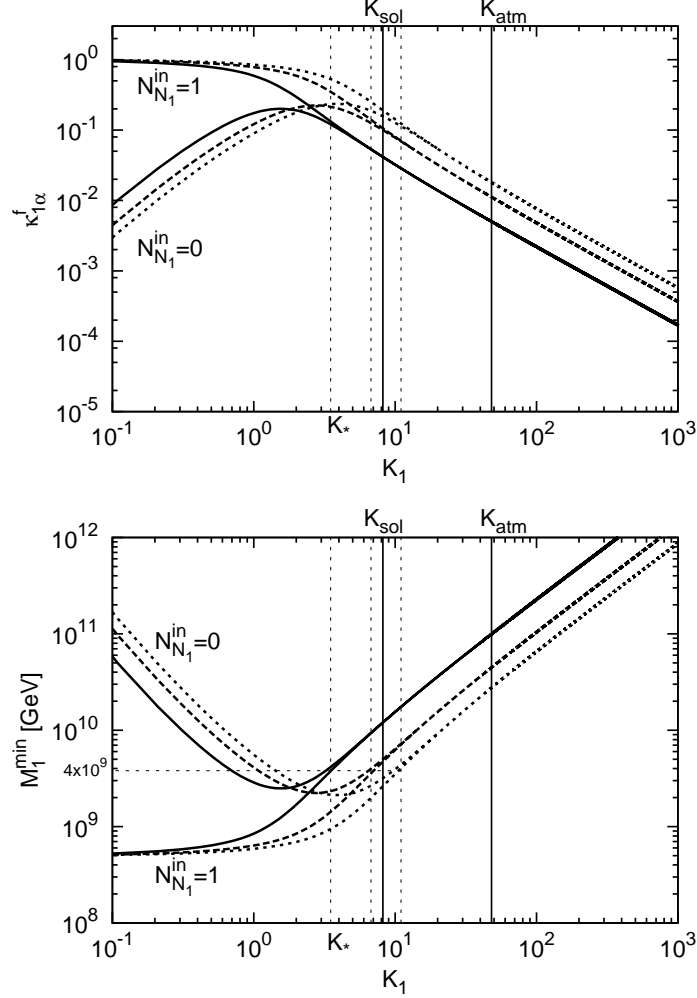


Figure 3.1: Efficiency factors (upper panel) and lower bounds on M_1 (lower panel) in the alignment (solid lines), semi-democratic (dashed lines) and democratic (short-dashed lines) cases.

In the case of alignment we are considering, we obtain $K_* \simeq 3.5$ for $\delta = 0.1$, as shown in Fig. 3.1. The value of K_* plays a relevant role since only for $K_1 \gtrsim K_*$ one has predictions from leptogenesis on the final baryon asymmetry resulting from a self-contained set of assumptions. On the other hand, for $K_1 \lesssim K_*$ leptogenesis has to be complemented with a model for the initial conditions. Additionally, the calculation of the final asymmetry in the weak washout regime requires a precise description of the RH neutrino production, potentially sensitive to many poorly known effects. It is

then interesting that current neutrino mixing data favor K_1 to be in the range $K_{\text{sol}} \simeq 8.2 \lesssim K_1 \lesssim 48 \simeq K_{\text{atm}}$ [80, 88, 93], where one can have a mild washout assuring full independence from the initial conditions, as one can see in Fig. 3.1, but still successful leptogenesis. In this case one can place constraints on the see-saw parameters which do not depend on specific assumptions for the initial conditions and with reduced theoretical uncertainties.

Since one has $\xi_1 = 1$ here [cf. Eq. (3.33)], the general lower bound on M_1 in Eq. (3.32), like all other quantities, becomes the usual lower bound derived from an unflavored treatment. In the lower panel of Fig. 3.1, we have plotted it both for $N_{N_1}^{\text{in}} = 1$ and $N_{N_1}^{\text{in}} = 0$ (solid lines). This corresponds precisely to the lower bound in the unflavored treatment shown in Fig. 2.5. One can see that the dependence on the initial conditions in $\kappa_{1\alpha}^{\text{f}}$ translates into a dependence on the initial conditions in M_1^{min} . The lowest model-independent values are then obtained for $K_1 = K_\star \simeq 3.5$ and are given by

$$M_1 \gtrsim 4 \times 10^9 \text{ GeV} \quad \text{and} \quad T_{\text{reh}} \gtrsim 1.5 \times 10^9 \text{ GeV}. \quad (3.38)$$

We did not show the lower bound on T_{reh} in Fig. 3.1, not to overload the plot, but it is precisely given by the dashed line in Fig. 2.5. Another typically quoted lower bound on M_1 is the one obtained for a thermal initial N_1 -abundance in the limit $K_1 \rightarrow 0$, given by $M_1 \gtrsim 5 \times 10^8 \text{ GeV}$ [81].

3.4.2 Democratic and semi-democratic cases

Let us now discuss another possibility. For definiteness, we assume a three-flavor regime; the extension of the results to the two-flavor regime is straightforward. Let us assume a democratic situation where $P_{1\alpha} = \bar{P}_{1\alpha} = 1/3$ for any α and consequently $\Delta P_{1\alpha} = 0$. This case was also considered in [120]. From Eq. (3.20) it follows that the three efficiency factors $\kappa_{1\alpha}^{\text{f}}$, like the three CP asymmetries $\varepsilon_{1\alpha}$, are all equal and thus Eq. (3.29) simplifies into $N_{B-L}^{\text{f}} = \varepsilon_1 \kappa_{1\alpha}^{\text{f}}$, as in the usual unflavored treatment. However, the washout is now reduced by the presence of the projector, so that $K_1 \rightarrow P_{1\alpha}^0 K_1 = K_1/3$. The result is that, in the case of a thermal initial N_1 -abundance, the efficiency factor, as a function of K_1 , is simply shifted. The same happens for vanishing initial N_1 -abundance in the strong washout regime. However, in the weak washout regime, there is not only a simple shift, since the RH neutrino production is still depending on K_1 . A plot of $\kappa_{1\alpha}^{\text{f}}$ is shown in the upper panel of Fig. 3.1 (short-dashed lines). One can see how the reduced washout increases the value of K_\star to ~ 10 , approximately $1/P_{1\alpha}^0 \simeq 3$ larger, thus compensating almost exactly the washout reduction by a factor $\sim 3^{1.2}$ [cf. Eq. (2.35)].

In this way the lowest bound on M_1 in the strong washout regime, at $K_1 = K_*$, is almost unchanged. On the other hand, for a given value $K_1 \gg K_*$, the lower bound gets approximately relaxed by a factor 3 [120]. The lower bound for the democratic case is shown in the lower panel of Fig. 3.1 (short-dashed lines). It is apparent that the lower bound for $K_1 \rightarrow 0$ and thermal initial N_1 -abundance does not change with respect to the alignment case (or the unflavored treatment). One can then say that flavor effects simply induce a shift of the dependence of the lower bound on K_1 .

The semi-democratic case is intermediate between the democratic and the alignment cases. It is obtained when one projector vanishes, for example $P_{1\beta} = 0$, and the other two are $1/2$. In this case, $K_* \sim 7$. The corresponding plots of the efficiency factor and of the lower bound on M_1 are also shown in Fig. 3.1 (dashed lines). The semi-democratic case can actually be identified with the two-flavor regime, where the two projectors are equal, $P_\tau^0 = P_{e+\mu}^0 = 1/2$.

3.4.3 One-flavor dominance

There is another potentially interesting situation that motivates an extension of the previous results to arbitrarily small values of $P_{1\alpha}^0$. This occurs when the final asymmetry is dominated by one flavor α , and Eq. (3.29) can be further simplified into

$$N_{B-L}^f \simeq \varepsilon_{1\alpha} \kappa_{1\alpha}^f, \quad (3.39)$$

analogously to the alignment case but with $P_{1\alpha}^0 \ll 1$. Notice that this cannot happen due to a dominance of one of the CP asymmetries, for example with $\varepsilon_{1\alpha}$ being close to its maximum value, Eq. (3.30), much larger than the other two that are strongly suppressed, simply because one has $\sum_\alpha \Delta P_{1\alpha} = 0$. One has then to imagine a situation where the CP asymmetry $\varepsilon_{1\alpha}$ is comparable to the sum of the other two, but $K_{1\beta \neq \alpha} \gg K_{1\alpha} \gtrsim 1$, so that $\kappa_{1\alpha}^f \gg \kappa_{1\beta}^f$. The dominance is then a result of the much weaker washout.

The analysis of the dependence on the initial conditions can then be performed as in the previous cases calculating the value of K_* for any value of $P_{1\alpha}^0$. The result is shown in Fig. 3.2. The alignment case corresponds to $P_{1\alpha}^0 = 1$, the semi-democratic case to $P_{1\alpha}^0 = 1/2$ and the democratic case to $P_{1\alpha}^0 = 1/3$. Notice that the result is very close to the simple estimation $K_*(P_{1\alpha}^0) = K_*(1)/P_{1\alpha}^0$ which would follow if $\kappa_{1\alpha}^f$ were just depending on $K_{1\alpha}$. In Fig. 3.3 we have plotted the values of the lower bounds on M_1 and T_{reh} for hierarchical light neutrinos, implying $m_3 = m_{\text{atm}}$ in Eq. (3.30). These can be obtained plugging $\xi_1 = \sqrt{P_{1\alpha}^0} \kappa_{1\alpha}^f(K_{1\alpha})/\kappa_1^f(K_1) \leq 1$ in Eq. (3.32). They correspond to the lowest values in the strong washout regime, when

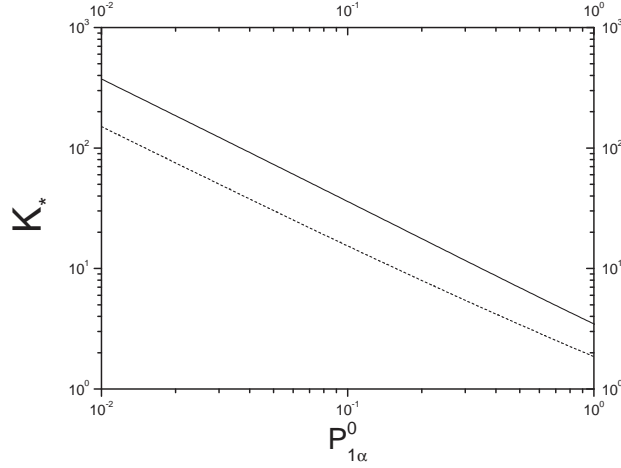


Figure 3.2: Values of K_* defining the strong washout regime, for $\delta = 10\%$ (solid line) and $\delta = 50\%$ (dashed line).

$$K_1 \geq K_*.$$

There are two possible ways to look at the results. On the one hand, flavor effects can relax the lower bounds for fixed values of $K_1 \gg 1$. Indeed, for each value $K_1 \gg 1$, one can choose $P_{1\alpha}^0 = K_*(P_{1\alpha}^0 = 1)/K_1$ such that $K_1 = K_*(P_{1\alpha}^0)$, thus obtaining the highest possible relaxation in the strong washout regime. This is shown in the right panel of Fig. 3.3. It is important to say that this relaxation is potential. A direct inspection is indeed necessary to determine whether it is really possible to achieve at the same time not only small values of $P_{1\alpha}^0$ but also a single-flavor CP asymmetry $\varepsilon_{1\alpha}$ that is not suppressed compared to $\varepsilon_{1\beta \neq \alpha}$.

On the other hand, as a function of $P_{1\alpha}^0$ the bounds get more stringent when $P_{1\alpha}^0$ decreases, so that the minimum is obtained in the alignment case, corresponding to the unflavored case. This is clearly visible in the left panel of Fig. 3.3. Therefore, it is important to emphasize here that flavor effects cannot help to alleviate the conflict of the lower bound on the reheat temperature T_{reh} from successful leptogenesis with the upper bound on T_{reh} in order not to overproduce gravitinos (see Section 2.3 for a discussion). In particular, the bounds on M_1 and T_{reh} that are usually quoted in the literature [cf. Eq. (3.38)] are not changed by flavor effects.

Notice that together with the one-flavor dominance case, one can also envisage, in the three-flavor regime, a two-flavor dominance case, where two projectors are equally small and the third is necessarily close to one, while all the three flavored CP asymmetries are comparable.

In the next section we consider a specific example that illustrates what

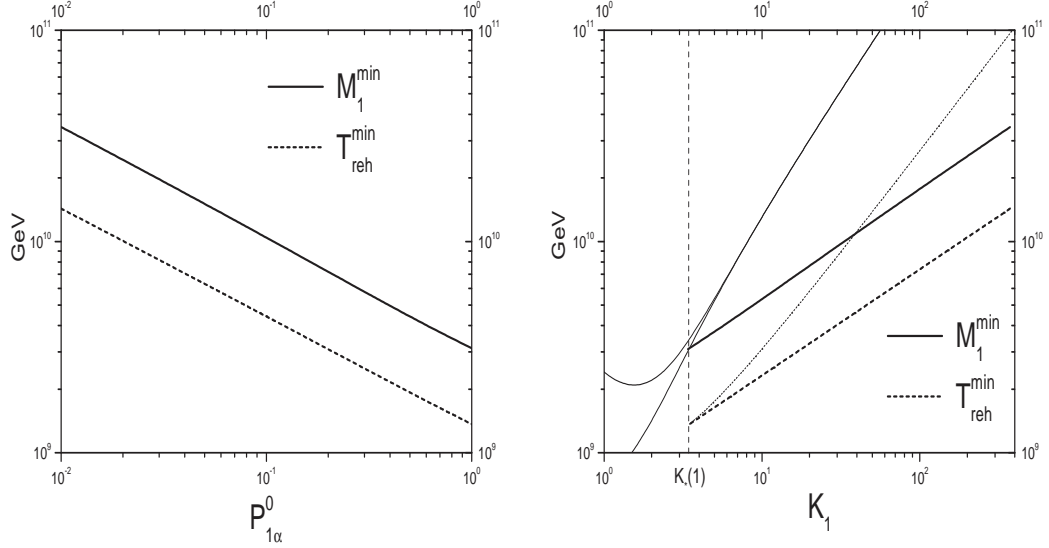


Figure 3.3: Lower bounds on M_1 and T_{reh} calculated choosing $P_{1\alpha}^0 = K_*(P_{1\alpha}^0 = 1)/K_1$ such that $K_1 = K_*(P_{1\alpha}^0)$ (thick lines) and compared with the usual bounds for $P_{1\alpha}^0 = 1$ (thin lines). In the left panel they are plotted as a function of $P_{1\alpha}^0$, while in the right panel as a function of K_1 .

we have discussed on general grounds. At the same time, it will help to understand which are realistic values for the projectors and their differences, given a specific set of see-saw parameters and using the information on the PMNS mixing matrix we have from neutrino oscillation experiments.

3.5 Study of a specific example

The previous results have been obtained assuming no restrictions on the projectors. Moreover, in the one-flavor dominance case, where there can be a relevant relaxation of the usual lower bounds derived following an unflavored treatment, we have assumed that the upper bound on $\varepsilon_{1\alpha}$, Eq. (3.30), is saturated independently of the value of the projector.

This assumption does not take into account that the values of the projectors depend on the different see-saw parameters, in particular on the neutrino mixing parameters, and that severe restrictions could apply. Let us show a definite example considering a particular form of the orthogonal matrix, $\Omega = R_{13}$ [cf. Eq. (2.21)]. This case is particularly meaningful, since it realizes one of the conditions ($\Omega_{21}^2 = 0$) to saturate the bound (2.45) for ε_1 . Moreover, the decay parameter is given by

$$K_1 = K_{\min} |1 - \omega_{31}^2| + K_{\text{atm}} |\omega_{31}^2|, \quad (3.40)$$

where $K_{\min} \equiv m_1/m_*$, and we recall that $K_{\text{atm}} \equiv m_{\text{atm}}/m_*$. The expression (3.22) for the projector gets then specialized as

$$P_{1\alpha}^0 = \frac{m_1 |U_{\alpha 1}|^2 |1 - \omega_{31}^2| + m_3 |U_{\alpha 3}|^2 |\omega_{31}^2| + 2 \sqrt{m_1 m_3} \text{Re}[U_{\alpha 1} U_{\alpha 3}^* \sqrt{1 - \omega_{31}^2} \omega_{31}^*]}{m_1 |1 - \omega_{31}^2| + m_3 |\omega_{31}^2|}, \quad (3.41)$$

while, specializing Eq. (3.28) for $\varepsilon_{1\alpha}$, one obtains

$$\begin{aligned} r_{1\alpha} = & Y_3 \frac{m_{\text{atm}}}{K_1 m_*} \left[|U_{\alpha 3}|^2 + \frac{m_1^2}{m_{\text{atm}}^2} (|U_{\alpha 3}|^2 - |U_{\alpha 1}|^2) \right] \\ & - \frac{m_{\text{atm}}}{K_1 m_*} \sqrt{\frac{m_1}{m_{\text{atm}}} \frac{m_3}{m_{\text{atm}}}} \left[\left(\frac{m_1 + m_3}{m_{\text{atm}}} \right) \text{Im} \left[\omega_{31} \sqrt{1 - \omega_{31}^2} \right] \text{Re}[U_{\alpha 1}^* U_{\alpha 3}] \right. \\ & \quad \left. + \left(\frac{m_3 - m_1}{m_{\text{atm}}} \right) \text{Re} \left[\omega_{31} \sqrt{1 - \omega_{31}^2} \right] \text{Im}[U_{\alpha 1}^* U_{\alpha 3}] \right], \end{aligned} \quad (3.42)$$

where $m_3/m_{\text{atm}} = \sqrt{1 + m_1^2/m_{\text{atm}}^2}$.

If we first consider the case of fully hierarchical light neutrinos, $m_1 = 0$, then

$$P_{1\alpha}^0 = \frac{\varepsilon_{1\alpha}}{\varepsilon_1} = |U_{\alpha 3}|^2 \quad \text{and} \quad \frac{\Delta P_{1\alpha}^0}{2 \varepsilon_1} = 0. \quad (3.43)$$

For the PMNS matrix U we adopt the parametrization Eq. (A.5). One then finds

$$P_{1e}^0 \lesssim 0.03, \quad P_{1\mu}^0 \simeq P_{1\tau}^0 \simeq 1/2. \quad (3.44)$$

The fact that the projector on the electron flavor is very small and $\Delta P_{1\alpha}^0 = 0$ for all flavors implies that the asymmetry generated in the electron flavor will be small, while the muon and tauon contributions will be equal, since the projectors on these flavors are equal. Summing Eq. (3.18) over α , one then simply recovers the unflavored case with the washout reduced by a factor of 2. This is a realization of the semi-democratic case that we were envisaging at the end of Section 3.4.2 where $K_* \simeq 7$. In this situation flavor effects do not produce large modifications to the usual results, essentially a factor of 2 reduction of the washout in the strong washout regime with a consequent equal relaxation of the lower bounds (see dashed lines in Fig. 3.1). Moreover, there is practically no difference between a calculation in the two- or three-flavor regime.

Let us now consider the effect of a non-vanishing but small lightest neutrino mass m_1 , for example $m_1 = 0.1 m_{\text{atm}}$. In this case the results can also depend on the Majorana and Dirac phases. We will show the results for ω_{31}^2 purely imaginary, the second condition that maximizes the total CP asymmetry if $m_1 \ll m_{\text{atm}}$ [93]. Notice that this is not in general the condition

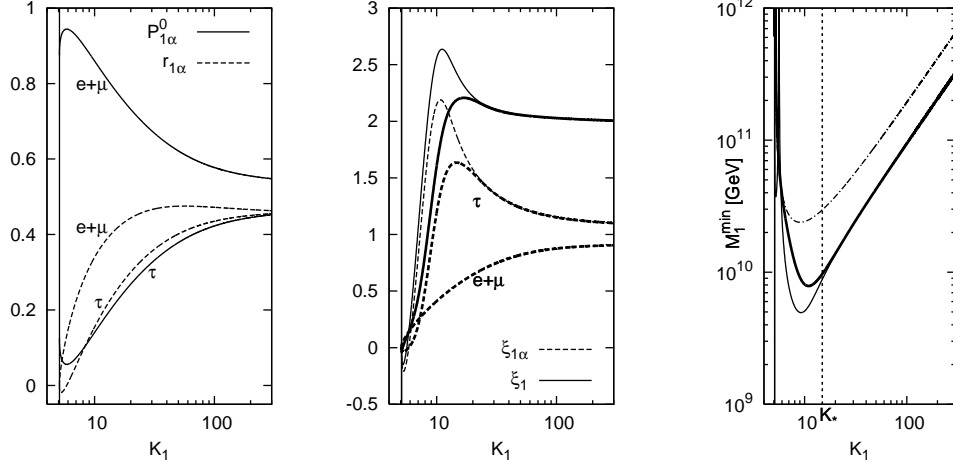


Figure 3.4: Dependence of different quantities on K_1 for $m_1/m_{\text{atm}} = 0.1$ and real U . Left panel: projectors $P_{1\alpha}^0$ and normalized CP asymmetries $r_{1\alpha}$; central panel: $\xi_{1\alpha}$ and ξ_1 as defined in Eq. (3.33) for thermal (thin) and vanishing (thick) initial N_1 -abundances; right panel: lower bound on M_1 for thermal (thin solid) and vanishing (thick solid) abundances compared with the unflavored result (dash-dotted line).

that maximizes $r_{1\alpha}$ for $m_1 \gtrsim m_{\text{atm}}$; however, we will also use it in this case for simplicity.

We first consider the case of a real U . The results are only slightly sensitive to a variation of θ_{13} within the experimentally allowed 3σ range 0–0.2. Therefore, we shall set $\theta_{13} = 0$, corresponding to $U_{e3} = 0$, in all examples. In the left panel of Fig. 3.4 we show the values of the projectors $P_{1\alpha}^0$ and of the normalized CP asymmetries $r_{1\alpha}$ as a function of K_1 . The calculations are performed in the two-flavor regime since we obtain that successful leptogenesis is possible only for $M_1 > 10^9$ GeV, where the two-flavor regime applies. Now a difference between the tauon and the sum of the muon and electron projectors and asymmetries arises. On the other hand, for $K_1 \gg 100$, this difference tends to vanish and the semi-democratic case is again recovered.

In the central panel we show the quantities $\xi_{1\alpha}$ [cf. Eq. (3.33)] and their sum ξ_1 . We recall that ξ_1 gives the deviation of the total asymmetry from an unflavored calculation for hierarchical light neutrinos. One can see how the contribution to the total asymmetry from the tauon flavor is now twice as large as from the electron plus muon flavors. For $K_1 \gg 100$, the semi-democratic case is restored, the two contributions tend to be equal to the unflavored case, and the total final asymmetry is about twice larger. Finally,

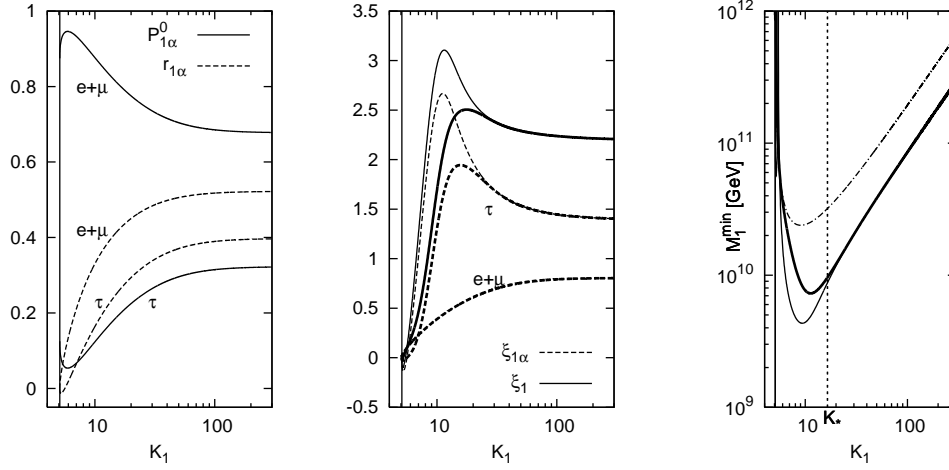


Figure 3.5: Same quantities as in the previous figure but with one non-vanishing Majorana phase: $\Phi_1 = -\pi$.

in the right panel we show the lower bound on M_1 , and compare it with the results from the unflavored analysis (dash-dotted line). At $K_* \simeq 14$, the relaxation in the strong washout is maximum, a factor ~ 3 . For $K_1 \gg K_*$, the relaxation is reduced to a factor 2, as in the semi-democratic case.

Let us now study the effect of switching on phases in the U matrix, again for $m_1 = 0.1 m_{\text{atm}}$. The most important effect arises from one of the two Majorana phases, namely Φ_1 . The other Majorana phase Φ_2 is irrelevant in the particular model we consider, $\Omega = R_{13}$. As for the Dirac phase δ , it plays a role similar to Φ_1 , but its effect is suppressed by the small angle θ_{13} . In Fig. 3.5 we show, again in three panels, the same quantities as in Fig. 3.4 for $\Phi_1 = -\pi$. One can see how this further increases the difference between the $e+\mu$ and the τ contributions and further relaxes the lower bound on M_1 . The effect is small for the considered value $m_1/m_{\text{atm}} = 0.1$. However, considering a much larger neutrino mass m_1 while keeping $\Phi_1 = -\pi$, the effect becomes dramatically bigger. In Fig. 3.6 we show the same quantities as in Fig. 3.4 and Fig. 3.5 for $m_1/m_{\text{atm}} = 10$. In the left panel one can see that now, for $K_1 \gg K_{\min}$, $|r_{1e+\mu}| \simeq |r_{1\tau}| \simeq 2$, much larger than in the previous case. This means that the dominant contribution to the flavored CP asymmetries comes now from the $\Delta P_{1\alpha}$ term [cf. Eq. (3.6)]. At the same time, very importantly, $P_{1\tau}^0 \ll P_{1e+\mu}^0$ and in this way, as one can see in the central panel, the dominant contribution to ξ_1 is given by $\xi_{1\tau}$. This case thus finally realizes a one-flavor dominance. The final effect is that the lower bound on M_1 is about three orders of magnitude relaxed compared to the unflavored case.

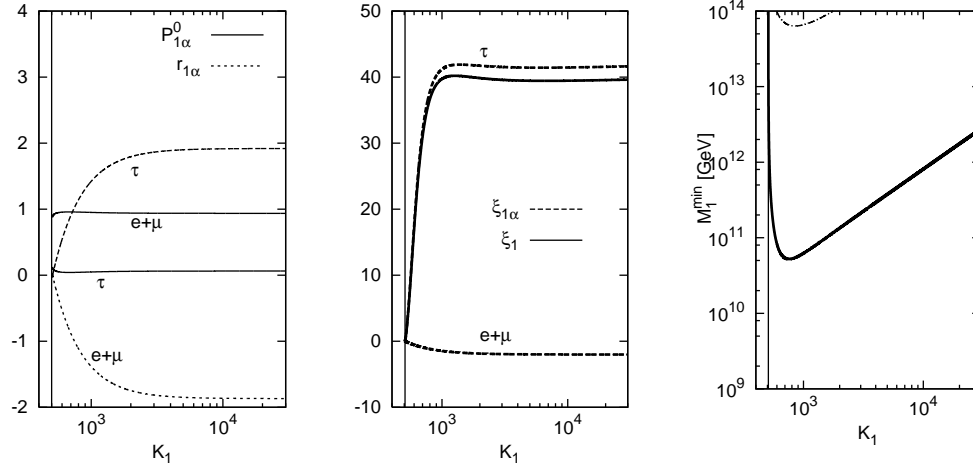


Figure 3.6: Same quantities as in the previous two figures but with $m_1/m_{\text{atm}} = 10$ and one non-vanishing Majorana phase: $\Phi_1 = -\pi$.

In Fig. 3.7 the dependence on m_1/m_{atm} of the lower bound on M_1 is summarized, showing both the case with zero Majorana phase and the case with $\Phi_1 = -\pi$. One can notice how the effect of the phase in relaxing the lower bound increases with m_1/m_{atm} .

Finally, we want to study the interesting case of a real orthogonal matrix Ω , implying $\varepsilon_1 = 0$. In the particular model we are considering, namely $\Omega = R_{13}$, there is no asymmetry produced if $m_1 = 0$, since $\varepsilon_{1\alpha} \propto \varepsilon_1 = 0$ [cf. Eq. (3.42)]. For a non-vanishing m_1 and a non-real U , we have that $\Delta P_{1\alpha} \neq 0$ and consequently $\varepsilon_{1\alpha} \neq 0$. In Fig. 3.8 we show the results for $m_1/m_{\text{atm}} = 0.1$ and $\Phi_1 = \pi/2$. We present again the same quantities as in Figs. 3.4, 3.5 and 3.6. One can see that an asymmetry can still be produced, as envisaged in [119]. However, successful leptogenesis is possible almost only in the weak washout regime. In the strong washout regime, for values $M_1 \lesssim 10^{12}$ GeV, there is a small allowed region only for $K_* \simeq 14 \leq K_1 \lesssim 30$.

Let us summarize the main results of this section, where we assumed the Ω matrix to have the simple form $\Omega = R_{13}$.

We have seen that the relaxation of the lower bounds compared to the unflavored case is only of order one for $m_1 \ll m_{\text{atm}}$, but grows to several orders of magnitude for $m_1 \gtrsim 10 m_{\text{atm}} \simeq 0.5$ eV, i.e. in the quasi-degenerate limit. The reason is that for quasi-degenerate neutrinos ($m_1 \simeq m_2 \simeq m_3$) a partial cancellation in one of the projectors, Eq. (3.22), can be more easily obtained, simply because all terms in the numerator are of the same order. When a partial cancellation occurs, one projector will be suppressed, leading

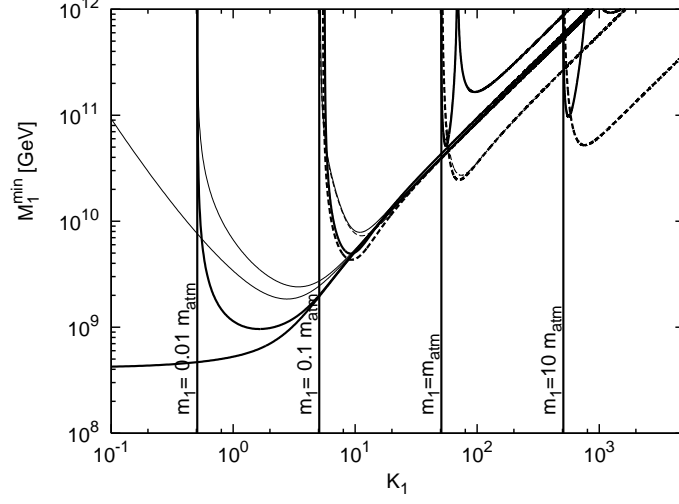


Figure 3.7: Lower bound on M_1 . The solid lines are for vanishing phase, while the dashed lines are for $\Phi_1 = -\pi$. The results for both vanishing (thick lines) and thermal (thin lines) initial abundances are presented.

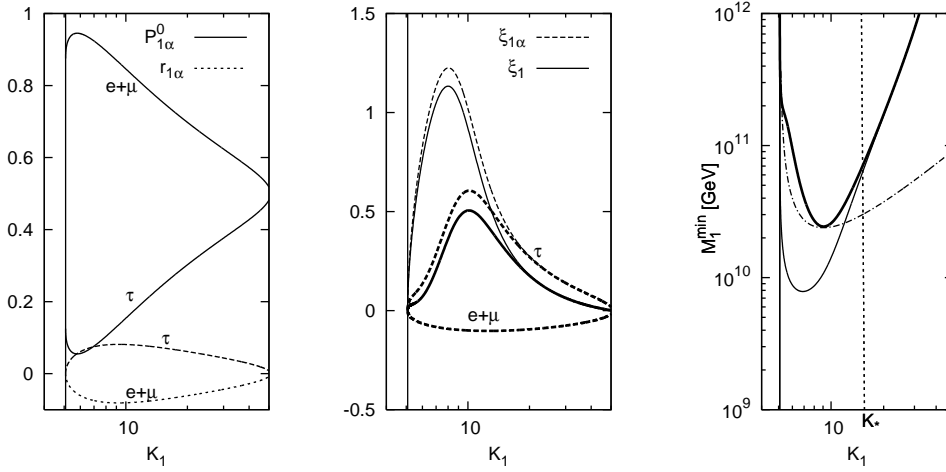


Figure 3.8: Same quantities as in Figs. 3.4, 3.5 and 3.6 in the case of real Ω for $m_1/m_{\text{atm}} = 0.1$ and $\Phi_1 = \pi/2$. The dot-dashed line still refers to the unflavored case for $\Omega = R_{13}$ and purely imaginary ω_{31}^2 .

to a one-flavor dominance and thus to a large relaxation of the lower bound at large values of K_1 . This is exactly what happened in the situation depicted in Fig. 3.6.

The role of the phases in the U matrix to achieve a cancellation in one of the projectors is crucial. For $\Omega = R_{13}$, only one Majorana phase, Φ_1 , is relevant, and the specific value it takes leads to very different results. In Fig. 3.6 we used the value $\Phi_1 = -\pi$ which approximately maximizes the asymmetry. The Dirac phase δ can also play a similar role to Φ_1 for $\Omega = R_{13}$, but its effect is always suppressed by the small angle θ_{13} . It should be noted that for more general cases like $\Omega = R_{12}R_{13}$, the cancellation in the projector leading to a one-flavor dominance is also possible when $m_1 = 0$, because there is more freedom in the Ω matrix to achieve a cancellation. Moreover, both Majorana phases in U can play a role in principle, not only Φ_1 .

It seems therefore that when flavor effects are taken into account, one obtains an opposite result compared to the unflavored analysis we performed in the previous chapter, where one had a suppression of the final asymmetry for growing absolute neutrino mass scale, leading to the stringent upper bound Eq. (2.57). This upper bound seems now to hold only for $M_1 \gtrsim 10^{12}$ GeV [120]. However, as we shall argue in the next chapter, this issue requires a full quantum kinetic calculation, in order to keep track of the correlations in flavor space and of partial losses of coherence [133].

We wish also to emphasize that, when flavor effects are included, leptogenesis is an interesting example of phenomenology, beyond neutrinoless double beta decay, where Majorana phases play an important role. The Dirac phase is also relevant, although it appears in combination with the small angle θ_{13} . The importance of the CP -violating phases in U shows up at two levels. First, as we have discussed above, they are crucial to achieve a cancellation in one of the projectors, leading to a one-flavor dominance. Second, they can provide the unique source of CP violation required for successful leptogenesis, as illustrated in Fig. 3.8. We shall come back to this interesting possibility in Chapter 6.

Chapter 4

From classical to quantum kinetic equations

We saw in the last two chapters that two quite different pictures of leptogenesis are valid in two different temperature regimes. Roughly speaking, when the temperature relevant for leptogenesis is above 10^{12} GeV, the unflavored picture should hold, whereas at lower temperatures, $T \lesssim 10^{12}$ GeV, the fully flavored regime should apply, either with two independent flavors (10^9 GeV $\lesssim T \lesssim 10^{12}$ GeV) or with three ($T \lesssim 10^9$ GeV).

The final baryon asymmetry was estimated in both regimes, unflavored and fully flavored, by means of classical Boltzmann equations. However, one could expect that quantum effects, such as correlations in flavor space and partial losses of coherence, might play some role in the intermediate regime around 10^{12} GeV. In such a case, the classical Boltzmann equation for the Δ_α asymmetry given in Eq. (3.18) is not expected to describe correctly the generation of asymmetry. One should indeed turn to a density matrix equation, which provides the right formalism to keep track of correlations in flavor space and partial losses of coherence.

In this chapter we re-visit the conditions of validity of both the unflavored and the fully flavored pictures. We shall give physical arguments why one actually expects to have a substantial part of the parameter space where quantum effects are important. Interestingly, this part of the parameter space is exactly the one relevant for a discussion about the upper bound on the absolute neutrino mass scale, which is evaded if one believes a fully flavored analysis. We shall argue that only solving the relevant density matrix equation will give a definite answer to that question. In the final section we discuss the density matrix formalism and give tentative equations for leptogenesis in the transition region.

4.1 Validity of the different pictures

Let us first discuss in some detail the quantity that will be the angular stone of the subsequent analysis, namely the washout rate by inverse decays [cf. Eq. (2.12)]. As usual, we restrict our analysis to the lightest RH neutrino N_1 .

It was shown in [80] that the inverse-decay rate reaches a maximum $W_1^{\text{ID}}(z_{\text{max}}) \simeq 0.3 K_1$ at $z_{\text{max}} \simeq 2.4$. In the weak washout regime, when $K_1 \lesssim 3.3$, one has $W_1^{\text{ID}}(z) < 1$ for any value of z . In this case the washout is negligible, and the final asymmetry depends on the initial conditions. In the strong washout regime, when $K_1 \gtrsim 3.3$, there is an interval $[z_{\text{on}}, z_{\text{off}}]$ where $W_1^{\text{ID}} \geq 1$. The asymmetry produced at $z \lesssim z_{\text{off}}$ is very efficiently washed out, and thus the final asymmetry is essentially what is produced around $z_{\text{B}} \simeq z_{\text{off}}$ by the out-of-equilibrium decays of the residual RH neutrinos, whose number corresponds approximately to the final value of the efficiency factor.

In Fig. 4.1 we show the washout term from inverse decays for three different values of K_1 . For $K_1 = 100$, we show the interval $[z_{\text{on}}, z_{\text{off}}]$. The maximum value, $W_1^{\text{ID}}(z_{\text{max}}) \simeq 33$, is reached at $z_{\text{max}} \simeq 2.4$. For $K_1 \simeq 3.3$, one has $z_{\text{on}} \simeq z_{\text{max}} \simeq z_{\text{off}}$. This can be taken as the threshold value distinguishing between the strong and the weak washout regimes. For $K_1 = 10^{-1}$, one has $W_1^{\text{ID}} \ll 1$ for any value of z . Notice however that even in this case the weak washout can be important for successful leptogenesis if the initial N_1 -abundance is zero, since it prevents a full cancellation between two different sign contributions to the final asymmetry [80].

4.1.1 When are flavor effects important?

As discussed in Section 3.1, flavor effects are caused by charged-lepton Yukawa interactions [127] that occur with the rate given in Eq. (3.1). The largest rate is for $\alpha = \tau$ where

$$\frac{\Gamma_\tau}{H} \simeq \left(\frac{10^{12} \text{ GeV}}{T} \right). \quad (4.1)$$

Therefore, if $T \gtrsim 10^{12} \text{ GeV}$, charged-lepton Yukawa interactions are not effective, and all processes in the early Universe are flavor blind, justifying the unflavored treatment. For $T \lesssim 10^{12} \text{ GeV}$, the τ -Yukawa coupling is strong enough that the scatterings $\ell_\tau \bar{e}_\tau \leftrightarrow \Phi^\dagger$ are in equilibrium. However, this condition is not necessarily sufficient for important flavor effects to occur, because we need to compare the speed of the Yukawa interactions with that of the RH neutrino decays and inverse decays. To this end, we study the

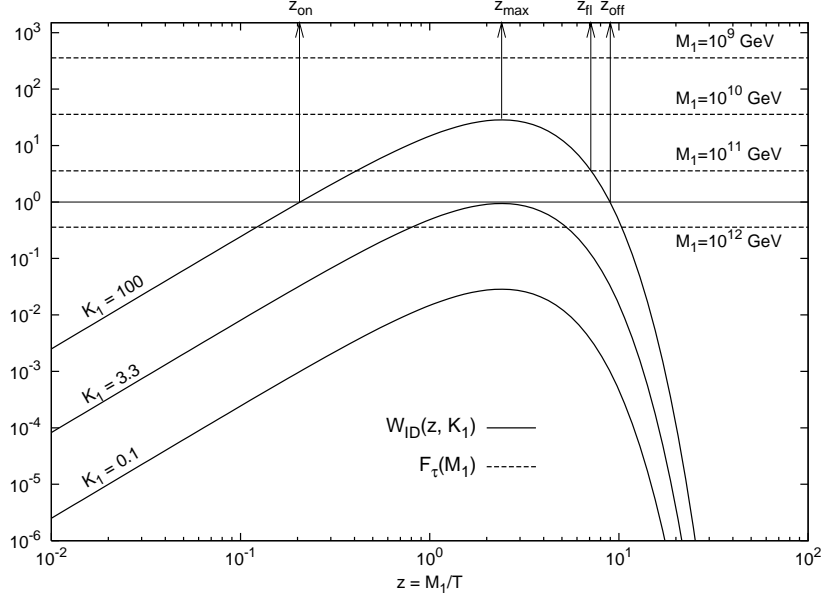


Figure 4.1: Comparison between the washout term $W_1^{ID}(z)$ (thick solid lines), defined in Eq. (2.12) and plotted for the three indicated values of K_1 , and the charged-lepton Yukawa interaction term F_τ , defined in Eq. (4.5) and plotted for the indicated values of M_1 .

weak and strong washout regimes separately and consider only a two-flavor case, because the τ -lepton Yukawa coupling causes the main modification.

In the weak washout regime, assuming a vanishing initial N_1 -abundance, the production of RH neutrinos by inverse decays occurs around $T \sim M_1$. At this epoch, inverse decays are by definition slower than the expansion rate. Therefore, the condition $T \lesssim 10^{12}$ GeV is sufficient to conclude that the charged-lepton Yukawa interactions are faster than the inverse decay rate. This translates into the condition $M_1 \lesssim 10^{12}$ GeV because the RH neutrino production occurs at $T \sim M_1$, in agreement with the previous literature [119, 120].

However, this condition does not guarantee that flavor effects indeed have an impact on the final asymmetry, because this impact depends on washout playing some role. For a vanishing initial N_1 -abundance, this is the case in that washout effects prevent a full sign cancellation between the asymmetry produced when $N_{N_1} < N_{N_1}^{\text{eq}}$ and the asymmetry produced later on. On the other hand, for a thermal initial N_1 -abundance, no such effect arises from the weak washout and flavor effects do not modify the final asymmetry. We will come back to this point later on.

In the strong washout regime, the situation is very different. The rate of RH neutrino inverse decays at $T \sim M_1$ is larger than the expansion rate. Therefore, we need to compare the charged-lepton Yukawa rate Γ_τ with the RH neutrino inverse-decay rate Γ_1^{ID} . For the unflavored treatment to be valid for $z \lesssim z_{\text{fl}} \leq z_{\text{B}}$ then requires

$$M_1 \gtrsim \frac{10^{12} \text{ GeV}}{2 W_1^{\text{ID}}(z_{\text{fl}})}, \quad (4.2)$$

where z_{fl} is that value of z where the two rates are equal, i.e. $\Gamma_1^{\text{ID}}(z_{\text{fl}}) = \Gamma_\tau(z_{\text{fl}})$. This condition guarantees that at temperatures $T > T_{\text{fl}} = M_1/z_{\text{fl}}$ flavor effects will not be able to break the coherent propagation of the lepton states. The final asymmetry is dominantly produced around $z \sim z_{\text{B}}$. Therefore, the condition for flavor effects to be negligible is

$$M_1 \gtrsim 5 \times 10^{11} \text{ GeV}, \quad (4.3)$$

similar to the weak washout regime. However, the corresponding condition on the temperature

$$T \gtrsim \frac{10^{12} \text{ GeV}}{2 z_{\text{B}}(K_1)} \quad (4.4)$$

is now less restrictive.

If one starts with a non-vanishing initial N_1 -abundance, then the final asymmetry is also determined by how efficiently the initial value is washed out; this is described by the integral in Eq. (2.29). In this case even a value of $z_{\text{fl}} < z_{\text{B}}$ would be important to determine the final asymmetry since washout in the unflavored regime would be effective for $z \lesssim z_{\text{fl}} < z_{\text{B}}$, while a reduced washout would apply in the flavored regime at lower temperatures such that $z_{\text{fl}} \lesssim z \lesssim z_{\text{B}}$.

We conclude that the condition (4.2) obeys the intuitive expectation that there is always a threshold value for K_1 above which the unflavored case is recovered. In this case the temperature below which flavor effects play a role indeed becomes smaller and smaller. The situation is illustrated in Fig. 4.1 where we compare W_{ID} with

$$F_\tau \equiv \frac{1}{2} \frac{\Gamma_\tau}{H z} \simeq \frac{5 \times 10^{11} \text{ GeV}}{M_1}, \quad (4.5)$$

the analogous quantity for the charged-lepton Yukawa interactions. For any value of M_1 and K_1 , there is a value z_{fl} such that $F_\tau \gtrsim W_{\text{ID}}$ for $z > z_{\text{fl}}$. If $M_1 \lesssim 2 \times 10^{12} \text{ GeV}/K_1$ and $K_1 \gtrsim 3.3$, corresponding to $F_\tau \gtrsim W_{\text{ID}}(z_{\text{max}})$ in the strong washout regime, then $z_{\text{fl}} = 0$, meaning that flavor effects are

important during the entire thermal history. On the other hand, for a fixed value of M_1 , one has $z_{\text{fl}} \rightarrow \infty$ for $K_1 \rightarrow \infty$, implying that flavor effects tend to disappear for sufficiently large values of K_1 . Notice however that if $M_1 \gtrsim 5 \times 10^{11} \text{ GeV}$, then $z_{\text{fl}} \gtrsim z_{\text{off}} \simeq z_{\text{B}}$ for any value of K_1 . This confirms that only for $M_1 \gtrsim 5 \times 10^{11} \text{ GeV}$ flavor effects can be neglected and the unflavored regime is recovered.

4.1.2 Maximum flavor effects

We now turn to the opposite extreme case when flavor effects are maximal, the “fully flavored regime.” In other words, the charged-lepton Yukawa interactions are now taken to be so fast that the lepton flavor content produced in $N \rightarrow \ell + \Phi$ on average fully collapses before the inverse reaction can take place, i.e., the ℓ density matrix in flavor space is to be taken diagonal in the charged-lepton Yukawa basis. In this case each single-flavor asymmetry has to be calculated separately because generally the washout by inverse decays is different for each flavor. Moreover, the single-flavor CP asymmetries now have an additional contribution compared to the total, as shown in Eq. (3.6) [119,120]. Finally, the inverse decay involving a lepton in the flavor α does not wash out as much asymmetry as the one produced by one RH neutrino decay. The reduction is quantified by the probability $P_{i\alpha}^0$, averaged over leptons and antileptons, that the lepton ℓ_i produced in the decay of N_i collapses into the flavor eigenstate ℓ_α . Focusing on the lightest RH neutrino N_1 , the fully flavored Boltzmann equations are given by Eqs. (3.17) and (3.18), with $i = 1$. Since we are dealing with the two-flavor case, here $\alpha = \tau$ or $e + \mu$ where the latter stands for a suitable superposition of the e and μ flavors, as explained after Eq. (3.18).

As in the unflavored case, we next identify the condition for the fully flavored approximation to hold. The final asymmetry in the flavor α is dominantly produced at $z \simeq z_{\text{B}\alpha} \equiv z_{\text{B}}(K_{1\alpha})$, where $K_{1\alpha} \equiv P_{1\alpha}^0 K_1$. Therefore, one must require that $\Gamma_\alpha \gtrsim \Gamma_1^{\text{ID}}$ holds already at $z \sim z_{\text{B}\alpha}$, or else the washout reduction takes place too late. We stress that flavor effects modify the final asymmetry only if the flavor projection takes place before the washout by inverse decays freezes out. Otherwise the washout epoch is over and the unflavored behavior is recovered. It is easy to verify that if the projectors are set to unity and the equations are summed over flavors, the kinetic equation (2.28) for N_{B-L} holding in the unflavored regime is recovered. Therefore, we require

$$M_1 \lesssim \frac{10^{12} \text{ GeV}}{2 W_1^{\text{ID}}(z_{\text{B}\alpha})} \quad (4.6)$$

as an approximate condition for the fully flavored behavior.

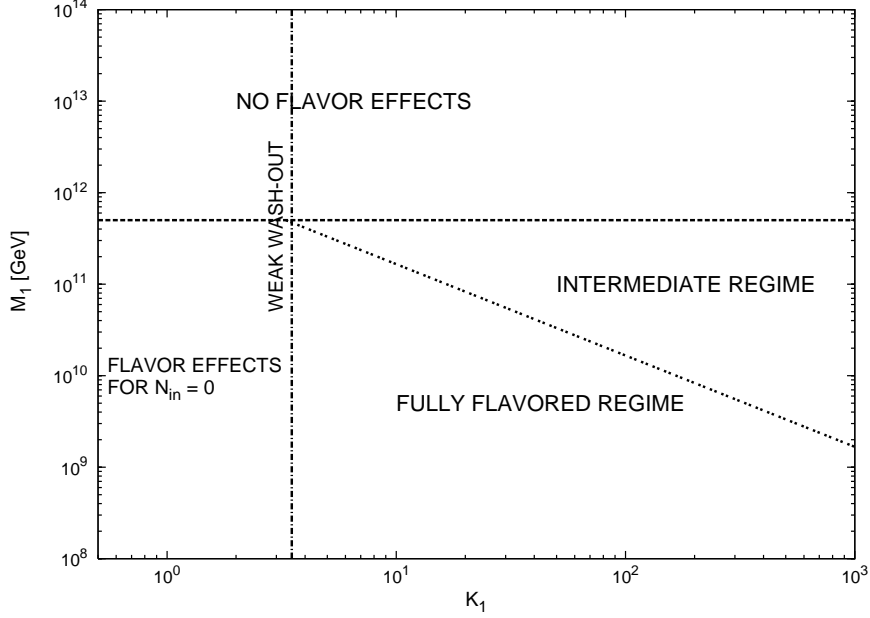


Figure 4.2: Relevance of flavor effects in schematic regions of parameters K_1 and M_1 . The region above the horizontal dashed line corresponds to the condition (4.3). The vertical dot-dashed line is the border between the weak and the strong washout regime. The region below the inclined dotted line corresponds to the condition (4.6) for $z_{B\alpha} = z_{\max}$.

In Fig. 4.2 we summarize the different possible cases in the plane of parameters K_1 and M_1 . For $M_1 \gtrsim 5 \times 10^{11}$ GeV, above the dashed line, flavor effects are not important independently of K_1 . The condition (4.6), in the most restrictive case when $z_{B\alpha} = z_{\max}$ and $W_1^{\text{ID}} \simeq 0.3 K_1$, is satisfied below the inclined dotted line. This case typically occurs in a one-flavor dominated scenario, as we explain below. The vertical dot-dashed line is the border that separates the weak from the strong washout regime in the unflavored case. In the flavored case the condition $K_1 \lesssim 3.3$ still implies a weak washout regime because flavor effects can only reduce the washout. However, the condition for the strong washout regime can be more restrictive than $K_1 \gtrsim 3.3$, as discussed in [123]. For $K_1 \lesssim 3.3$, flavor effects modify the final asymmetry only marginally and more specifically only if the initial N_1 -abundance vanishes, as indicated in Fig. 4.2. On the other hand, for $K_1 \gtrsim 3.3$ and below the diagonal line, flavor modifications of the final asymmetry can be large, especially in the one-flavor dominated scenario.

There is a region in parameter space where neither condition (4.2) nor (4.6) holds. This intermediate regime can become very large in the case

of a one-flavor dominated scenario, where several orders of magnitude enhancement of the final asymmetry compared to the unflavored calculation are possible (see Fig. 3.6). In this case one of the two projectors is very small compared to the other, and so the washout is very asymmetric in the two flavors. On the other hand, if the two flavored CP asymmetries are comparable, then the final asymmetry is dominantly produced into one flavor and deviations from the unflavored regime can become very large. This scenario is realized, in particular, when the absolute neutrino mass scale increases, relaxing the traditional neutrino mass bound.

However, the condition (4.6) strongly restricts the applicability of the one-flavor dominated scenario. Even though the reduction of the washout is driven by $K_{1\alpha} \ll K_1$, implying $z_{B\alpha} \ll z_B$, the possibility for flavor effects to be relevant relies on the dominance of the charged-lepton Yukawa interaction rate compared to the RH neutrino inverse-decay rate, which however is still driven by K_1 . Therefore, increasing K_1 , one can enhance the asymmetry in the one-flavor dominated scenario compared to the unflavored case, if smaller and smaller values of the projector $P_{1\alpha}^0$ are possible. On the other hand, the inverse-decay rate increases so that the fully flavored behavior may no longer apply. In particular notice that the maximum enhancement of the asymmetry is obtained when $K_1 \gg K_{1\alpha} \simeq 1$, when $z_{B\alpha} \simeq z_{\max}$ and the condition (4.6) is maximally restrictive.

4.2 Neutrino mass bound

One possible consequence of flavor effects is to relax the traditional upper bound on the neutrino mass that is implied by successful leptogenesis. In order to explore the impact of our modified criteria, we first recall the origin of this bound in the unflavored case. Maximizing the final value of the asymmetry over all see-saw parameters except M_1 and m_1 yields [80]

$$\begin{aligned} \frac{\eta_B^{\max}(M_1, m_1)}{\eta_B^{\text{CMB}}} &\simeq 3.8 \left(\frac{m_\star}{m_1} \right)^{1.2} \left(\frac{M_1}{10^{10} \text{ GeV}} \right) \frac{m_{\text{atm}}}{m_1 + m_3} \\ &\times \exp \left[-\frac{\omega}{z_B} \left(\frac{M_1}{10^{10} \text{ GeV}} \right) \left(\frac{\overline{m}}{\text{eV}} \right)^2 \right] \geq 1, \quad (4.7) \end{aligned}$$

where we have approximated $\kappa(K_1) \simeq 0.5 K_1^{-1.2}$ [cf. Eq. (2.35)], and we have neglected the dependence of z_B on K_1 in the derivative. This constraint translates into $m_1 < m_1^{\max}(M_1)$ shown by the curved solid line in the upper part of Fig. 4.3 where the unflavored behavior obtains. This curve sports an absolute maximum, $m_1 \lesssim 0.12 \text{ eV}$, for $M_1 \simeq 10^{13} \text{ GeV}$.

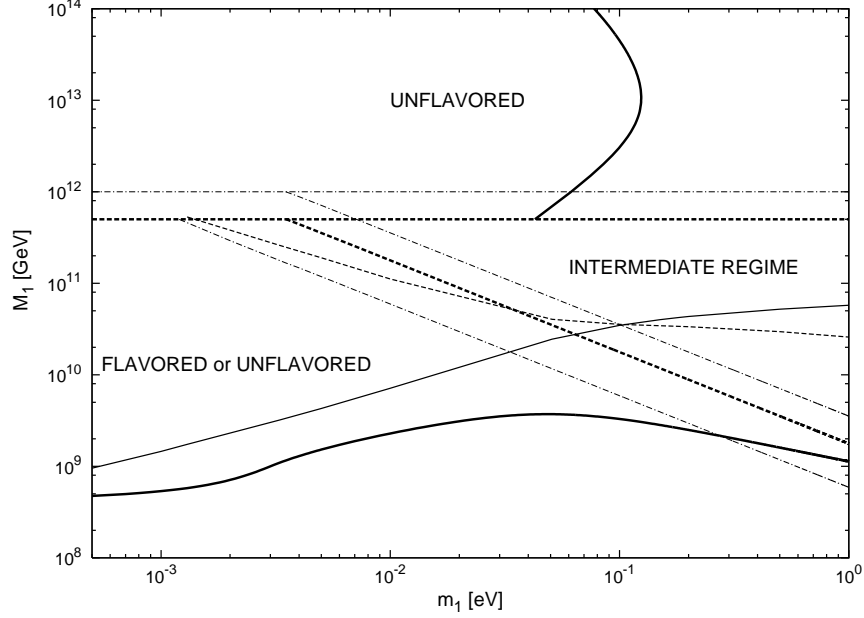


Figure 4.3: Relevance of flavor effects similar to Fig. 4.2, now mapped to schematic regions of parameters m_1 and M_1 . The region above the horizontal dashed line corresponds to the condition (4.3) for the applicability of the unflavored regime. The region below the inclined thick dashed line corresponds to the condition (4.6) calculated for that value of $z_{B\alpha}$ that maximizes the final asymmetry in the one-flavor dominated scenario and for $K_1 = m_1/m_\star$. In this same case, the lower inclined dot-dashed lines includes also the effect of scatterings in the condition (4.6), while the upper inclined and the horizontal dot-dashed lines include the effect of oscillations. The area between the two inclined dot-dashed lines gives an estimation of the uncertainty on the condition for the fully flavored regime to hold. The area between the horizontal thin dot-dashed line and the horizontal thick dashed line gives an estimation of the uncertainty on the condition for the unflavored regime to hold. The two thick solid lines borders the region where successful leptogenesis is possible: on the left in the unflavored regime and above in the fully flavored regime. The thin solid line is a more restrictive border obtained for a specific choice of the see-saw orthogonal matrix ($\Omega = R_{13}$) and the thin dashed line is the corresponding condition (4.6). In this case one has $K_1 > m_1/m_\star$.

The possibility that flavor effects could relax this bound is based on the observation that the flavored CP asymmetries, for $m_1 \gtrsim m_{\text{atm}}$, are proportional to m_1 [cf. Eq. (3.30)]. On the other hand, the total CP asymmetry is suppressed like m_1^{-1} , contributing to the upper bound in the unflavored regime. However, if m_1 increases, then K_1 has to increase as well, so that it is not guaranteed that the fully flavored treatment remains justified.

Quantitatively, the value of K_1 is bounded from below by [92]

$$K_1 \geq \frac{m_1}{m_\star}. \quad (4.8)$$

For $K_1 \geq m_1/m_\star \gg 1$, the final asymmetry is maximized when a one-flavor dominated scenario is realized. In this case the final asymmetry is approximately $N_{B-L}^f \simeq \varepsilon_{1\alpha} \kappa_{1\alpha}^f$. The bound on the single-flavor CP asymmetry was given in Eq. (3.30). It is then possible to find the value of $P_{1\alpha}^0$ that maximizes the asymmetry as a function of K_1 and the corresponding value of $z_{B\alpha}$. Imposing $\eta_B^{\text{max}} \geq \eta_B^{\text{CMB}}$ implies a lower bound on M_1 as a function of K_1 .

This limit can be translated into a lower bound on M_1 as a function of m_1 by replacing K_1 with its minimum value m_1/m_\star . In this way the washout is always minimized and the final efficiency factor and the final asymmetry are maximized. Notice that the single-flavor CP asymmetries, like the total, vanish for $K_1 = m_1/m_\star$. Therefore, this lower bound cannot be saturated. Notice moreover that for $m_1 \lesssim m_\star$ the one-flavor dominated scenario does not necessarily hold because it is possible that $K_1 \lesssim 1$. Actually, for $K_1 \rightarrow 0$, flavor effects disappear and one recovers the usual asymptotic value of the lower bound obtained in the unflavored case for thermal initial N_1 -abundance, $M_1 \gtrsim 5 \times 10^8 \text{ GeV}$ [cf. Eq. (2.53)]. For intermediate values of K_1 , one can use a simple interpolation. The final result is shown in the bottom part of Fig. 4.3 as a thick solid line.

In Fig. 4.3 we also show the condition (4.6) calculated for the same value of $z_{B\alpha}$ that maximizes the final asymmetry, but replacing K_1 with its minimum value m_1/m_\star (thick dashed line). Since W_1^{ID} increases with K_1 , this produces a necessary, but not sufficient, condition in the m_1 - M_1 plane for the fully flavored behavior. This condition matches the validity of the unflavored regime at $m_1 \simeq 3 \times 10^{-3} \text{ eV}$ and the lower bound on M_1 at $m_1 \simeq 2 \text{ eV}$. This means that for $m_1 \gtrsim 2 \text{ eV}$ the fully flavored behavior does not obtain. Notice also that this upper limit is quite conservative because the lower bound on M_1 has been obtained neglecting that, for $K_1 = m_1/m_\star$, the flavored CP asymmetry vanishes and thus the bound cannot be saturated. Moreover, we have assumed that $P_{1\alpha}^0$ can always assume the value that maximizes the asymmetry.

In Fig. 4.3 we also show (thin solid line) the lower bound $M_1(m_1)$ in

the specific scenario considered in Section 3.5, namely $\Omega = R_{13}$ and ω_{31}^2 is taken purely imaginary [cf. Eq. (2.21)]. In this case the value of $z_{B\alpha}$ is not necessarily the same as the one that maximizes the asymmetry in the one-flavor dominated scenario, and $K_1 > m_1/m_\star$. Therefore, a specific calculation is necessary in order to work out correctly the condition (4.6). The result is shown in Fig. 4.3 with a thin dashed line.

In this case the upper limit on m_1 for the applicability of the fully flavored regime is much smaller, $m_1 \simeq 0.1$ eV. Allowing for a non-vanishing real part of ω_{31}^2 , slightly larger values are possible. It should be however kept in mind that these values are indicative since they rely on a condition for the fully flavored regime that comes from a simple rate comparison.

4.3 Limitations of a simple rate comparison

We have exploited a somewhat qualitative rate comparison for the determination of the region where the fully flavored regime obtains. While we believe that our approach nicely illustrates the modifications that derive from our more restrictive criterion for the significance of flavor effects, there are also important shortcomings. First, we have simply compared the inverse-decay rate with the charged-lepton Yukawa interaction rate, ignoring flavor oscillations caused by the flavor-dependent lepton dispersion relation in the medium. If the oscillations are much faster than the inverse-decay rate, they also contribute effectively, together with inelastic scatterings, to project the lepton state on the flavor basis. Therefore, including oscillations will tend to enlarge the region where the fully flavored behavior obtains (the inclined upper dot-dashed line in Fig. 4.3) and to reduce the one where the unflavored behavior obtains (the horizontal upper dot-dashed line in Fig. 4.3). In our case, the oscillation frequency is comparable to Γ_α , and so the two estimations are not too far off.

Moreover, we have also neglected $\Delta L = 1$ scatterings. They also contribute, like inverse decays, both to generate the asymmetry and to the washout and hence, together with inverse decays, contribute to preserving the flavor direction of the leptons. At the relevant $z \sim z_{B\alpha} \sim 2$, the $\Delta L = 1$ scattering rate is actually larger than the inverse-decay rate and thus tends to reduce the region where the fully flavored behavior obtains (the lower inclined dot-dashed line in Fig. 4.3). Therefore, the effects of oscillations and of $\Delta L = 1$ scatterings may partially cancel each other. In Fig. 4.3 the region between the two inclined dot-dashed lines gives then an indication of the theoretical uncertainty on the determination of the region where the fully flavored regime holds. It can be seen that current calculations cannot estab-

lish whether the upper bound holding in the unflavored regime is nullified, just simply relaxed or still holding, when flavor effects are included.

Only a full quantum kinetic treatment can give a final verdict on the effectiveness of flavor effects in leptogenesis and its impact on the neutrino mass limit. While we have verified that our rate criteria are borne out by the quantum kinetic equations stated in Ref. [120] (see [134]), these equations are not necessarily complete in that the term describing the generation of the asymmetry has been added by hand. Moreover, the “damping rate” caused by the flavor-sensitive Yukawa interactions ultimately derives from a collision term in the kinetic equation [135]. Extending the pioneering treatment of Ref. [120] to allow for a complete understanding of flavor effects remains a challenging task. In the next section we show how such a quantum kinetic equation could be derived.

4.4 Density matrix equation

Here we aim to derive a density matrix equation for leptogenesis following [135], where the general formalism was introduced. We consider exclusively the decay of the lightest RH neutrino, N_1 , with a mass between 10^9 GeV and 10^{14} GeV where only the τ -Yukawa interactions may be faster than the Hubble rate. We are therefore either in the unflavored or in the two-flavor regime, the two flavors being τ and a combination of e and μ which we call β in the following.

We follow the definition of the matrices of densities for leptons and antileptons given in [135]:

$$\rho_l = \begin{pmatrix} \rho_{\tau\tau} & \rho_{\beta\tau} \\ \rho_{\tau\beta} & \rho_{\beta\beta} \end{pmatrix} \quad (4.9)$$

$$\rho_{\bar{l}} = \begin{pmatrix} \bar{\rho}_{\tau\tau} & \bar{\rho}_{\tau\beta} \\ \bar{\rho}_{\beta\tau} & \bar{\rho}_{\beta\beta} \end{pmatrix} \quad (4.10)$$

where $\rho_{ij} = \langle a_j^\dagger(t) a_i(t) \rangle$, $\bar{\rho}_{ij} = \langle b_i^\dagger(t) b_j(t) \rangle$, with a (a^\dagger) denoting the annihilation (creation) operator for a lepton and b (b^\dagger) the annihilation (creation) operator for an antilepton. All matrix components are implicitly given in a portion of comoving volume that would contain one heavy neutrino in ultra-relativistic thermal equilibrium. Note that we introduce here matrices of number densities, not occupation numbers as in [135]. We shall explain later on how the integration over all modes can be performed here. As usual in leptogenesis, one assumes kinetic equilibrium, an assumption which should be good at the 10% level in the strong washout regime [136]. Following this assumption, all interaction rates are thermally averaged.

Let us first study the two simplest – nevertheless very important – processes, namely decays and inverse decays: $N_1 \leftrightarrow \ell_1 + \Phi^\dagger$ and $N_1 \leftrightarrow \bar{\ell}_1 + \Phi$. The state $|\ell_1\rangle$ was defined in Eq. (2.1).

The idea is to write the equation for the generation of lepton number in the basis $\{|\ell_1\rangle, |\ell_\perp\rangle\} \equiv \{\ell_1\}$, and then rotate it into the flavor basis $\{|\ell_\tau\rangle, |\ell_\beta\rangle\} \equiv \{\ell_\alpha\}$. The unitary matrix for the change of basis is given by

$$U(\{\ell_1\} \rightarrow \{\ell_\alpha\}) = \frac{1}{\sqrt{(h^\dagger h)_{11}}} \begin{pmatrix} \langle \ell_\tau | \ell_1 \rangle & -\langle \ell_\beta | \ell_1 \rangle \\ \langle \ell_1 | \ell_\beta \rangle & \langle \ell_1 | \ell_\tau \rangle \end{pmatrix}. \quad (4.11)$$

The same can be done for antileptons, and one gets the following matrix for the change of basis:

$$U'(\{\bar{\ell}'_1\} \rightarrow \{\bar{\ell}_\alpha\}) = \frac{1}{\sqrt{(h^\dagger h)_{11}}} \begin{pmatrix} \langle \bar{\ell}_\tau | \bar{\ell}'_1 \rangle & -\langle \bar{\ell}'_1 | \bar{\ell}_\beta \rangle \\ \langle \bar{\ell}_\beta | \bar{\ell}'_1 \rangle & \langle \bar{\ell}'_1 | \bar{\ell}_\tau \rangle \end{pmatrix}, \quad (4.12)$$

where it should be remembered that $\bar{\ell}'_1$ is not the CP -conjugate of ℓ_1 at the one-loop level.

Decays and inverse decays are just source and sink terms, so one can proceed by analogy with [135] with the conventions of [80] on leptogenesis quantities. In the basis $\{\ell_1\}$, the equation tracking the density matrix for leptons is given by

$$\frac{d}{dz} \rho_\ell = \frac{1}{2}(1+\varepsilon_1)DN_{N_1} \begin{pmatrix} 1 & 0 \\ 0 & 0 \end{pmatrix} - \frac{1}{2}(1-\varepsilon_1)W_{\text{ID}} \left[\begin{pmatrix} 1 & 0 \\ 0 & 0 \end{pmatrix} \rho_\ell + \rho_\ell \begin{pmatrix} 1 & 0 \\ 0 & 0 \end{pmatrix} \right], \quad (4.13)$$

where $z = M_1/T$, and for antileptons:

$$\frac{d}{dz} \rho_{\bar{\ell}} = \frac{1}{2}(1-\varepsilon_1)DN_{N_1} \begin{pmatrix} 1 & 0 \\ 0 & 0 \end{pmatrix} - \frac{1}{2}(1+\varepsilon_1)W_{\text{ID}} \left[\begin{pmatrix} 1 & 0 \\ 0 & 0 \end{pmatrix} \rho_{\bar{\ell}} + \rho_{\bar{\ell}} \begin{pmatrix} 1 & 0 \\ 0 & 0 \end{pmatrix} \right], \quad (4.14)$$

where both equations are written to first order in the CP asymmetry parameter ε_1 , and we neglected Pauli blocking effects.

Let us now rotate these equations to the flavor basis $\{\ell_\alpha\}$, applying the transformations introduced above, Eqs. (4.11) and (4.12). It will prove useful to define the following matrices which will appear in the new equations:

$$U \begin{pmatrix} 1 & 0 \\ 0 & 0 \end{pmatrix} U^\dagger = \begin{pmatrix} P_{1\tau} & \langle \ell_\tau | \ell_1 \rangle \langle \ell_1 | \ell_\beta \rangle \\ \langle \ell_1 | \ell_\tau \rangle \langle \ell_\beta | \ell_1 \rangle & P_{1\beta} \end{pmatrix} \equiv \mathcal{P}, \quad (4.15)$$

and

$$U' \begin{pmatrix} 1 & 0 \\ 0 & 0 \end{pmatrix} U'^\dagger = \begin{pmatrix} \bar{P}_{1\tau} & \langle \bar{\ell}'_1 | \bar{\ell}_\tau \rangle \langle \bar{\ell}_1 | \bar{\ell}_\beta \rangle \\ \langle \bar{\ell}'_1 | \bar{\ell}_\tau \rangle \langle \bar{\ell}_1 | \bar{\ell}_\beta \rangle & \bar{P}_{1\beta} \end{pmatrix} \equiv \bar{\mathcal{P}}, \quad (4.16)$$

where the projectors are defined as $P_{1\alpha} = |\langle \ell_\alpha | \ell_1 \rangle|^2$ and $\bar{P}_{1\alpha} = |\langle \bar{\ell}_\alpha | \bar{\ell}_1 \rangle|^2$ [cf. Eqs. (3.3) and (3.4)]. At tree level, the two matrices just defined are equal and given by

$$\mathcal{P}^0 = \frac{1}{(h^\dagger h)_{11}} \begin{pmatrix} |h_{\tau 1}|^2 & h_{\tau 1}^* h_{\beta 1} \\ h_{\tau 1} h_{\beta 1}^* & |h_{\beta 1}|^2 \end{pmatrix}. \quad (4.17)$$

In the flavor basis, Eqs. (4.13) and (4.14) become

$$\frac{d}{dz} \rho_\ell = \frac{1}{2} (1 + \varepsilon_1) D N_{N_1} \mathcal{P} - \frac{1}{2} (1 - \varepsilon_1) W_{\text{ID}} [\mathcal{P} \rho_\ell + \rho_\ell \mathcal{P}], \quad (4.18)$$

and

$$\frac{d}{dz} \rho_{\bar{\ell}} = \frac{1}{2} (1 - \varepsilon_1) D N_{N_1} \bar{\mathcal{P}} - \frac{1}{2} (1 + \varepsilon_1) W_{\text{ID}} [\bar{\mathcal{P}} \rho_{\bar{\ell}} + \rho_{\bar{\ell}} \bar{\mathcal{P}}]. \quad (4.19)$$

Subtracting the first equation with the second, and defining $\rho_\ell - \rho_{\bar{\ell}} \equiv \rho_{\ell - \bar{\ell}}$, one obtains

$$\frac{d}{dz} \rho_{\ell - \bar{\ell}} = \varepsilon_1 D (N_{N_1} + N_{N_1}^{\text{eq}}) \mathcal{P}^0 + \frac{\mathcal{P} - \bar{\mathcal{P}}}{2} D (N_{N_1} - N_{N_1}^{\text{eq}}) - \frac{1}{2} W_{\text{ID}} \{\mathcal{P}^0, \rho_{\ell - \bar{\ell}}\}, \quad (4.20)$$

to first order both in ε_1 and $\mathcal{P} - \bar{\mathcal{P}}$. Note that we used the fact that $\rho_\ell + \rho_{\bar{\ell}} \simeq 2N_\ell^{\text{eq}} \mathbb{1}$, where we neglected contributions of $\mathcal{O}(\varepsilon_1)$, because the whole term is already at first order in ε_1 . As usual in leptogenesis, one notices that there is an asymmetry production even in thermal equilibrium [82]. This is due to the missing contribution from the on-shell $\Delta L = 2$ processes $\bar{\ell} \Phi \leftrightarrow \ell \Phi^\dagger$. Properly accounting for them yields [120, 127]

$$\frac{d}{dz} \rho_{\ell - \bar{\ell}} = \varepsilon_1 D (N_{N_1} - N_{N_1}^{\text{eq}}) \left(\mathcal{P}^0 + \frac{\mathcal{P} - \bar{\mathcal{P}}}{2\varepsilon_1} \right) - \frac{1}{2} W_{\text{ID}} \{\mathcal{P}^0, \rho_{\ell - \bar{\ell}}\}, \quad (4.21)$$

which looks intuitively correct, with both the reduction of the washout by the projector (a matrix now!) and the additional contribution to the source term, of the type ΔP (also a matrix). If the off-diagonal elements are quickly damped (see below), one recovers exactly the fully flavored equations on the diagonal entries [cf. Eq. (3.18) with $i = 1$].

Actually, the matrix of CP asymmetries, which can be defined as

$$\epsilon \equiv \varepsilon_1 \left(\mathcal{P}^0 + \frac{\mathcal{P} - \bar{\mathcal{P}}}{2\varepsilon_1} \right), \quad (4.22)$$

was proposed in [120] for the three-flavor regime to be given by

$$\epsilon_{\alpha\beta} = \frac{3}{32\pi} \frac{1}{(h^\dagger h)_{11}} \sum_{j \neq 1} \frac{M_1}{M_j} \text{Im} (h_{\alpha 1}^* (h^\dagger h)_{1j} h_{\beta j} - h_{\beta 1} (h^\dagger h)_{j1} h_{\alpha j}^*), \quad (4.23)$$

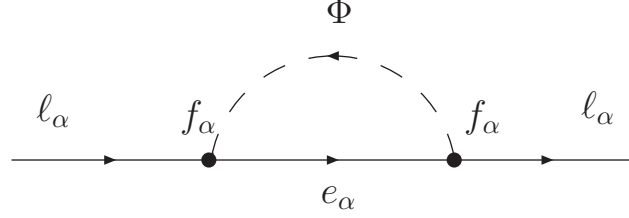


Figure 4.4: Flavor diagonal contribution to the refractive index for the leptons.

in the HL, $M_1 \ll M_2 \ll M_3$, where $\alpha, \beta = e, \mu, \tau$. It is straightforward to check that the diagonal elements correspond to the single-flavor CP asymmetries shown in Eq. (3.25).

Let us now examine the effect of the term $f_\alpha \overline{\ell_{L\alpha}} e_{R\alpha} \Phi$, which we said in Section 3.1 is responsible for flavor effects to manifest themselves. This interaction is flavor diagonal, and we expect it to affect Eq. (4.21) in two ways. First, it induces a contribution to the refractive index for the lepton doublet ℓ_α , and, second, it makes the lepton doublet interact with the lepton singlet e_α .

Starting with the index of refraction effect, in perfect analogy with [135], one has a contribution in the form of a commutator both for leptons and antileptons:

$$\frac{d}{dz} \rho_\ell = [\text{RHS of Eq. (4.18)}] - i[\Lambda_\omega^\tau, \rho_\ell] \quad (4.24)$$

$$\frac{d}{dz} \rho_{\bar{\ell}} = [\text{RHS of Eq. (4.19)}] + i[\Lambda_\omega^\tau, \rho_{\bar{\ell}}], \quad (4.25)$$

where

$$\Lambda_\omega^\tau \simeq \frac{1}{Hz} \begin{pmatrix} \langle M_\tau^2/2p \rangle & 0 \\ 0 & 0 \end{pmatrix} \simeq \frac{1}{Hz} \frac{T}{64} \begin{pmatrix} f_\tau^2 & 0 \\ 0 & 0 \end{pmatrix} \quad (4.26)$$

The effective mass M_α acquired by the lepton in the medium due to the Yukawa coupling f_α was calculated in [137] from the real part of the diagram shown in Fig. 4.4 and used in the second equality.

It is important to be aware that the possibility to use a density matrix of number densities, i.e. to have been able to integrate over the 3-momentum of the leptons, is non-trivial and comes from [138], where it was noticed that when gauge interactions are very fast, all modes oscillate at the same frequency, given by the thermal average $\langle M^2/2p \rangle$ in this case.

Similar to the effect of a vacuum mass, leptons and antileptons oscillate in opposite directions, so that subtracting Eq. (4.25) to Eq. (4.24) leads to

$$\frac{d}{dz}\rho_{\ell-\bar{\ell}} = [\text{RHS of Eq. (4.21)}] - i[\Lambda_{\omega}^{\tau}, \rho_{\ell} + \rho_{\bar{\ell}}] = [\text{RHS of Eq. (4.21)}] - i[\Lambda_{\omega}^{\tau}, \rho_{-}], \quad (4.27)$$

where, in the second equality, we defined $\rho_{-} \equiv \rho_{\ell} + \rho_{\bar{\ell}} - 2N_{\ell}^{\text{eq}}\mathbb{1}$, which has all elements of $\mathcal{O}(\varepsilon_1)$ since the diagonal part of $\rho_{\ell} + \rho_{\bar{\ell}}$ has a part proportional to $2N_{\ell}^{\text{eq}}$ which drops out of the commutator. In order to have a closed set of equations, we must give the equation of evolution of ρ_{-} ,

$$\frac{d}{dz}\rho_{-} = i[\Lambda_{\omega}^{\tau}, \rho_{\ell-\bar{\ell}}]. \quad (4.28)$$

As for the new interactions between lepton doublets and singlets, they yield again two terms, one source and one sink term, which describe how the lepton asymmetry is shared between the doublets and the singlets. As we already mentioned, only the τ -Yukawa coupling is relevant for the range of RH neutrino masses we consider, and thus the relevant interaction rate is given by F_{τ} , which we defined in Eq. (4.5). Assuming a negligible asymmetry in the Higgs field, the resulting term can be written in the form

$$\begin{aligned} \frac{d}{dz}\rho_{\ell-\bar{\ell}} \simeq & \epsilon D (N_{N_1} - N_{N_1}^{\text{eq}}) - \frac{1}{2}W_{\text{ID}} \{\mathcal{P}^0, \rho_L\} - i[\Lambda_{\omega}^{\tau}, \rho_{-}] \\ & + 2F_{\tau}(N_{e_{\tau}} - N_{\bar{e}_{\tau}}) \left(\begin{pmatrix} 1 & 0 \\ 0 & 0 \end{pmatrix} \right) - \frac{1}{2}F_{\tau} \left\{ \left(\begin{pmatrix} 1 & 0 \\ 0 & 0 \end{pmatrix} \right), \rho_{\ell-\bar{\ell}} \right\}. \end{aligned} \quad (4.29)$$

The asymmetry in the lepton singlets is found by solving the following Boltzmann equation:

$$\frac{d}{dz}(N_{e_{\tau}} - N_{\bar{e}_{\tau}}) = F_{\tau} [(N_{\ell_{\tau}} - N_{\bar{\ell}_{\tau}}) - 2(N_{e_{\tau}} - N_{\bar{e}_{\tau}})], \quad (4.30)$$

where $N_{\ell_{\tau}} - N_{\bar{\ell}_{\tau}}$ is the upper left component of the density matrix $\rho_{\ell-\bar{\ell}}$. Clearly, this equation will tend to equalize $N_{\ell_{\tau}} - N_{\bar{\ell}_{\tau}}$ and $2(N_{e_{\tau}} - N_{\bar{e}_{\tau}})$. It is interesting to notice that when the latter two quantities are equal, Eq. (4.29) can be written as

$$\begin{aligned} \frac{d}{dz}\rho_L \simeq & \epsilon D (N_{N_1} - N_{N_1}^{\text{eq}}) - \frac{1}{2}W_{\text{ID}} \{\mathcal{P}^0, \rho_L\} - i[\Lambda_{\omega}^{\tau}, \rho_{-}] \\ & - \frac{1}{2}F_{\tau} \left[\left(\begin{pmatrix} 1 & 0 \\ 0 & 0 \end{pmatrix} \right), \left[\left(\begin{pmatrix} 1 & 0 \\ 0 & 0 \end{pmatrix} \right), \rho_L \right] \right], \end{aligned} \quad (4.31)$$

where the total lepton number N_L is defined as $(N_{\ell} - N_{\bar{\ell}}) + (N_e - N_{\bar{e}})$. In particular, this means that the upper left component of ρ_L is given by

$2(N_\ell - N_{\bar{\ell}})/3$. The coefficient $2/3$ translates the fact that some of the lepton asymmetry, being stored in the right-handed fields, escapes the washout by inverse decays. This is nothing else than an effect caused by one spectator process, as discussed in Section 3.2, with the difference that we consider here a simplified situation where the asymmetry stored in the Higgs is assumed to be zero.

Eq. (4.31) is very illustrative in that it includes all the well-known contributions discussed in [135] in a completely different context, namely the production (source term), the washout (sink term), the double commutator, which damps the off-diagonal elements, and the commutator, which drives the oscillations in flavor space.

In the transition region $T \sim 10^{12}$ GeV, one cannot assume $N_{\ell_\tau} - N_{\bar{\ell}_\tau} = 2(N_{e_\tau} - N_{\bar{e}_\tau})$, and one has to solve simultaneously four coupled equations, Eqs. (3.7), (4.28), (4.29) and (4.30). They constitute the system of equations to solve in order to have a correct description of leptogenesis at the transition between the fully flavored and the unflavored regime, with an approximate treatment of spectator processes.

The system of equations we propose differ from what can be found in the present literature [120, 134] in that

1. we explicitly include the effect of oscillations in flavor space, which adds one equation, since leptons and antileptons oscillate in different directions in flavor space;
2. we keep track of the asymmetry in e_τ , which adds another equation, as should be done in the transition regime around $T \sim 10^{12}$ GeV.

The second point is actually the addition of one spectator process to the picture. In principle, all spectator processes should be taken into account, and a large number of Boltzmann equations should be solved simultaneously. In particular, sphalerons should be included and the final asymmetry obtained would then be in $\Delta_\alpha \equiv B/3 - L_\alpha$, as required. We did not include these effects here for the sake of simplicity and clarity, as well as because the difference is expected to be of order 20–30%.

The conditions for the validity of the different pictures of leptogenesis which we discussed in the previous sections can be put in perspective by looking at Eq. (4.29). Roughly speaking, if $W_{\text{ID}} \gg F_\tau, \Lambda_\omega^\tau$, one expects the unflavored regime to be recovered, whereas in the opposite situation, the fully flavored regime should hold. To follow up on the comments made in the last section about the inclusion of $\Delta L = 1$ scatterings, it should be noted that, even though we did not include them for simplicity in our analysis, their addition is straightforward in that one has to replace $D_1 \rightarrow D_1 + S_1$

and $W_1^{\text{ID}} \rightarrow W_1^{\text{ID}} + W_1^{\Delta L=1} = j(z)W_{\text{ID}}$, with the corresponding analytic expressions given in Eqs. (2.6) and (2.11), respectively.

Finally, let us note that there is another quantum limit which can be considered for the Boltzmann equations relevant for leptogenesis. It relies on the closed time path formalism for non-equilibrium quantum field theory. Within such an approach, the so-called “memory effects” are for instance accounted for. In the case of leptogenesis, these effects translate into a time-dependent CP asymmetry. This quantum limit was studied in [139, 140], and the main conclusion reached there is that memory effects have some impact in the case of resonant leptogenesis in the weak washout regime. In all other cases, they can be safely neglected.

Chapter 5

Going beyond vanilla leptogenesis

We have always assumed up to now that the final $B - L$ asymmetry was predominantly produced by the lightest RH neutrino, N_1 . A N_1 -dominated scenario typically follows from the assumption of hierarchical heavy neutrino masses, $M_1 \ll M_2 \ll M_3$. Actually, it can even be enforced by setting $R_{23} = \mathbb{1}$, since a large contribution from N_2 is then unprobable, as we explained in Section 2.1. This is “vanilla” leptogenesis, where successful leptogenesis requires high-scale values of the lightest RH neutrino mass, M_1 , and of the reheat temperature, T_{reh} . Moreover, the upper bound on the absolute neutrino mass scale implied by successful leptogenesis was discussed in Section 2.2 within an unflavored treatment and in Section 4.2 including flavor effects.

In this chapter we would like to go beyond this picture. Actually, flavor effects themselves allow that to some extent. For example, they might modify the upper bound on the absolute neutrino mass scale, and they open new ways to have N_2 - and N_3 -dominated scenarios. First, we want to relax the assumption of a hierarchical heavy neutrino mass spectrum, and concentrate on quasi-degenerate spectra, $M_1 \simeq M_2 \simeq M_3$. Then, we discuss the implications of having $R_{23} \neq \mathbb{1}$, opening the way to the N_2 -dominated scenario. Actually, we also analyze this possibility within a flavored perspective and notice that the window for N_2 - and N_3 -leptogenesis opens up compared to the unflavored case. Finally, we discuss the possible effects coming from one element of the Ω matrix, namely Ω_{22} .

5.1 Degenerate limit for the heavy neutrinos

On theoretical grounds it is not difficult to motivate models with a quasi-degenerate heavy neutrino mass spectrum. For example, a slightly broken $U(1)_L$ lepton flavor symmetry is enough to achieve this goal [141–143]. Note that this possibility has other implications as well, as we shall see below. Such a spectrum can also be motivated in the context of “radiative leptogenesis” [144, 145].

In leptogenesis a quasi-degenerate mass spectrum for the heavy neutrinos leads to important qualitative and quantitative differences with respect to the vanilla picture described in Chapters 2 and 3, because all heavy neutrino contributions must be taken into account, both at the production and washout levels.

It is straightforward to generalize, including flavor effects, a result obtained in [94] for the efficiency factors within an unflavored treatment in the degenerate limit, $(M_3 - M_1)/M_1 \lesssim 0.1$, and for $K_i \gg 1$, for all i . Indeed, one can now approximate $dN_i/dz' \simeq dN_i^{\text{eq}}/dz'$ in Eq. (3.20), obtaining that

$$\kappa_{i\alpha}^{\text{f}} \simeq \kappa(K_{1\alpha} + K_{2\alpha} + K_{3\alpha}). \quad (5.1)$$

The function $\kappa(x)$ was defined in Eq. (2.31), and it approximates $\kappa_{1\alpha}^{\text{f}}$ in the hierarchical limit when $x = K_{1\alpha}$. In the degenerate limit (DL) one has then only to replace $K_{1\alpha}$ with the sum $K_{1\alpha} + K_{2\alpha} + K_{3\alpha}$. The number of efficiency factors to be calculated reduces from 6 to 2 in the two-flavor case and from 9 to 3 in the three-flavor case, i.e. one for each flavor, like in the hierarchical limit. If, instead of a full degeneracy, one has only a partial degeneracy, $M_1 \simeq M_2 \ll M_3$, then

$$\kappa_{3\alpha}^{\text{f}} \ll \kappa_{1\alpha}^{\text{f}} \simeq \kappa_{2\alpha}^{\text{f}} \simeq \kappa(K_{1\alpha} + K_{2\alpha}). \quad (5.2)$$

It is interesting to notice that, as a consequence of the orthogonality of Ω , one has

$$K_{1\alpha} + K_{2\alpha} + K_{3\alpha} = \sum_k \frac{m_k}{m_\star} |U_{\alpha k}|^2. \quad (5.3)$$

This means that the sum over the decay parameters will typically be in the strong washout range, $K_{1\alpha} + K_{2\alpha} + K_{3\alpha} \gtrsim 3$. This is a nice property of leptogenesis with degenerate heavy neutrinos which still holds when flavor effects are included. Consequently, we do not need to introduce analytic expressions for a vanishing initial number of heavy neutrinos, since it will give the same result as $\kappa(K_{1\alpha} + K_{2\alpha} + K_{3\alpha})$, which was derived for a thermal initial N_1 -abundance.

Concerning the flavored CP asymmetries, one can rewrite the general expression (3.24) in the DL,

$$\varepsilon_{i\alpha} = \frac{1}{16\pi(h^\dagger h)_{ii}} \sum_{j \neq i} \left\{ \text{Im} [h_{\alpha i}^* h_{\alpha j} (h^\dagger h)_{ij}] + \text{Im} [h_{\alpha i}^* h_{\alpha j} (h^\dagger h)_{ji}] \right\} \delta_{ji}^{-1}, \quad (5.4)$$

where we used the fact that $\xi(x_j/x_i) \simeq 1/(3\delta_{ji})$ and we defined

$$\delta_{ji} \equiv \frac{M_j - M_i}{M_i} = \sqrt{\frac{x_j}{x_i}} - 1. \quad (5.5)$$

As it is clear from Eq. (5.4), there can be an enhancement of the CP asymmetry proportional to δ_{ji}^{-1} [87] for quasi-degenerate heavy neutrino masses. This enhancement originates from the one-loop self energy contribution. Note however that an enhancement of the CP asymmetry might require that all three heavy neutrinos are quasi-degenerate. As a matter of fact, when $\Omega = R_{13}$, there is no enhancement when $M_2 \rightarrow M_1$, but only when $M_3 \rightarrow M_1$ [94].

We can now write in general for the final $B-L$ asymmetry

$$N_{B-L}^f = \sum_{\alpha} \left\{ \left(\sum_k \varepsilon_{k\alpha} \right) \kappa \left(\sum_i K_{i\alpha} \right) \right\}, \quad (5.6)$$

where the sums over i and k run from 1 to 3 in the case of full DL and from 1 to 2 in the case of partial DL. When computing the final asymmetry and the lower bound on M_1 in the DL, there will be a competition between two effects, namely the increase of the washout because of the sum of the decay parameters in the efficiency factor, and the enhancement of the CP asymmetry. The second effect will become dominant once the first one saturates, which occurs for $\delta_{ji} \sim 0.01$ [94]. From this point going to higher degeneracies will lower the bounds proportionally to δ_{ji} . Therefore, as we pointed out in Section 2.3, it is possible to relax the lower bound on the reheat temperature in such a way that the gravitino problem is avoided.

One can go even further and look for the most extreme relaxation one can achieve. This occurs when the resonance in the CP asymmetry is reached, for $M_j - M_i \simeq \Gamma_j/2$ [117, 118]. We shall use a slightly modified condition,

$$\delta_{ji}^{\text{res}} \simeq d \bar{\varepsilon}(M_i)/3, \quad (5.7)$$

where we introduced the uncertainty parameter $d = 1 \div 10$ because of the claim in [85] that it is not possible to be exactly on resonance without breaking perturbation theory, contrary to what was stated in [76, 117]. We do not aim here at a resolution of this discrepancy and therefore introduced the parameter d .

It is straightforward to check that the resonance condition (5.7) implies that $\varepsilon_1 = 1/d$ in the unflavored case with maximal phase. In other words, the resonance condition simply cancels out the dependence on the heavy neutrino mass scale in the CP asymmetry and therefore also in the final baryon asymmetry. Hence, in resonant leptogenesis there is essentially no lower bound on M_1 and T_{reh} and one can go down to the TeV scale [76, 117]. The only requirement is actually to let the heavy neutrinos decay before the freeze-out of the sphalerons (at around 100 GeV), in order to produce not only lepton number but also baryon number. In [76] the authors followed an unflavored treatment where the third heavy neutrino N_3 is decoupled and the other two are quasi-degenerate. In such a scenario one cannot avoid the fact that the Yukawa coupling must be quite small in order to have a successful leptogenesis.

Accounting for flavor effects in the case of resonant leptogenesis, it was realized in [132, 146] that an even more dramatic situation could be envisaged. If three quasi-degenerate RH neutrinos are considered, it is possible to have some of the Yukawa couplings of order one, leading to phenomenological implications, such as a rate for the lepton flavor violating decay $\mu \rightarrow e\gamma$ within reach of future experiments, as well as successful leptogenesis at the TeV scale. The crucial point there was to have one flavor, the τ , that is very weakly washed out thanks to a very small projector $P_{1\tau}$, and one heavy neutrino, N_3 , that is weakly coupled. However, the latter condition does not necessarily imply that the CP asymmetry ε_3 is suppressed because it receives other contributions when $M_3 \simeq M_{1,2}$, as we will explain in Section 5.3. It must be said, however, that the extreme situation needed seems to occur in a region of the parameter space where the condition of validity (4.6) which was derived in the previous chapter is not satisfied.

Actually, strictly speaking, the possibility of explaining the smallness of neutrino masses with large Yukawa couplings and relatively light RH neutrino masses (TeV scale) does not involve a conventional “see-saw mechanism”, even though the same matrix for the light neutrinos applies, Eq. (B.5). The point is that the neutrino masses are not in this case small because of the suppression due to the heavy neutrino mass, but because of a very large cancellation due to the Ω matrix. The elements of the Ω matrix can indeed be arbitrarily large, as long as they satisfy $\Omega^T \Omega = \Omega \Omega^T = \mathbb{1}$. This can be theoretically motivated by a slightly broken $U(1)_L$ lepton flavor symmetry [141–143]. It is interesting that this type of model may lead to possible signatures of heavy neutrinos at future colliders [143, 147, 148].

5.2 N_2 -dominated scenario

In this section we consider again a hierarchical heavy neutrino mass spectrum, $M_1 \ll M_2 \ll M_3$. In the unflavored regime, this assumption typically implies a N_1 -dominated scenario, where the final asymmetry is dominated by the contribution from the lightest RH neutrino decays, Eq. (3.29). Indeed, in general, in the HL one has two effects. The first effect is that the asymmetry production from the two heavier RH neutrinos, N_2 and N_3 , is typically later on washed out by the N_1 inverse processes, implying $\kappa_3^f, \kappa_2^f \ll \kappa_1^f$. The second effect is a consequence of the fact that the total CP asymmetries vanish in the limit when all particles running in the loops become massless, and this yields typically $|\varepsilon_3| \ll |\varepsilon_2| \ll |\varepsilon_1|$.

However, for a particular choice of the see-saw parameters, $\Omega = R_{23}$ [cf. Eq. (2.22)] and $m_1 \ll m_\star$ [cf. Eq. (1.27)], the contribution to the final asymmetry from the next-to-lightest RH neutrino N_2 is not only non-negligible but even dominant, giving rise to a N_2 -dominated scenario [93]. Indeed, for $\Omega = R_{23}$, different things happen simultaneously. First, N_2 , even though decoupled from N_1 , is still coupled to N_3 and in the HL the total CP asymmetry ε_2 not only does not vanish, since it receives an unsuppressed contribution from graphs where N_3 runs in the loops, but can even be maximal [cf. Eq. (2.25)]. On the other hand, one has now $\varepsilon_1 = 0$, since N_1 is essentially decoupled from the other two RH neutrinos. At the same time, one has $K_1 = m_1/m_\star \ll 1$, so that the washout from N_1 inverse processes is negligible. The final result is that $|\varepsilon_2 \kappa_2| \gg |\varepsilon_{i \neq 2} \kappa_{i \neq 2}^f|$, and the final asymmetry is dominantly produced from N_2 -decays.

A nice feature of this model is that the lower bound on M_1 does not hold anymore, being replaced by a lower bound on M_2 that, however, still implies a lower bound on T_{reh} [93]. If one switches on some small R_{12} and R_{13} complex rotations, then the lower bounds on M_2 and T_{reh} become necessarily more stringent. Therefore, there is a border beyond which this scenario is not viable and one is forced to go back to the usual N_1 -dominated scenario for successful leptogenesis.

Within an unflavored treatment and in the HL, the condition $w_{32} \simeq 0$ in the Ω -matrix parametrization [cf. Eq. (2.19)], implying $R_{23} \simeq \mathbb{1}$, is sufficient to have a negligible asymmetry production from the two heavier RH neutrinos and to guarantee that the N_1 -dominated scenario holds. This condition is even not necessary for $m_1 \gg m_\star$, since in this case, due to the fact that $\tilde{m}_1 \geq m_1$, one has necessarily $K_1 \gg 1$ and the washout from N_1 inverse processes is strong enough to suppress a possible contribution to the final asymmetry from N_2 -decays.

When flavor effects are taken into account, the domain of applicability

of the N_1 -dominated scenario reduces because the importance of N_2 and N_3 increases. There are two aspects to be considered.

The first aspect is that the washout from N_1 inverse processes becomes less efficient. Indeed, the projectors $P_{1\alpha}$ can considerably reduce the washout of the asymmetry produced in the flavor α from N_2 -decays [149]. This turns the condition $m_1 \gg m_\star$ into a looser condition $m_1 \gg m_\star/P_{1\alpha}$. Another effect is that N_1 inverse processes can be fast enough to quickly destroy the coherence of ℓ_2 . Then a statistical mixture of ℓ_1 and of the state orthogonal to ℓ_1 builds up, and hence part of the asymmetry produced in N_2 -decays is protected from the washout from N_1 inverse processes [6, 127, 150]. These effects may occur in the unflavored regime ($M_1 \gtrsim 10^{12}$ GeV) or in the two-flavor regime (10^9 GeV $\lesssim M_1 \lesssim 10^{12}$ GeV), but disappear in the three-flavor regime, where the full flavor basis is resolved, since no direction in flavor space is protected from the N_1 -washout. Recently, it has been also pointed out that the off-diagonal elements in the matrix C^ℓ introduced in Eq. (3.15) and which encodes the effects of all spectator processes can lead to a reduction of the washout from N_1 inverse processes as well [151]. One can therefore conclude that the assumption $\kappa_{2\alpha} \ll \kappa_{1\alpha}$ is not valid in general, even when $M_1 \ll M_2$.

The second aspect concerns the flavored CP asymmetries. Even though the results obtained at the end of Section 2.1 in the particular cases $\Omega = R_{23}$ and $\Omega = R_{13}$ are still valid in the flavored case, i.e. $\varepsilon_{1\alpha} = 0$ for $\Omega = R_{23}$, and $\varepsilon_{2\alpha} = 0$ for $\Omega = R_{13}$, there are other effects to keep in mind. As we shortly mentioned in Section 3.3, the flavored CP asymmetries $\varepsilon_{2\alpha}$ are not necessarily suppressed by factors M_1/M_2 compared to $\varepsilon_{1\alpha}$, as it is the case in the unflavored regime for ε_2 compared to ε_1 . This observation [123] can also potentially contribute to enlarge the domain of applicability of the N_2 -dominated scenario when flavor effects are taken into account. Another related observation is that the $\varepsilon_{3\alpha}$'s, contrarily to ε_3 , are not suppressed in the HL. This could open the door even to a N_3 -dominated scenario, although this is possible only for $M_3 \lesssim 10^{12}$ GeV, when flavor effects affect the generation of asymmetry by N_3 .

Therefore, when flavor effects are taken into account, the conditions of applicability of the N_1 -dominated scenario become potentially more restrictive than in the unflavored case. There is a clear choice of the parameters, for $\Omega = R_{13}$ and $M_3 \gtrsim 10^{12}$ GeV, where the N_1 -dominated scenario holds. Indeed, in this case, one has that $\varepsilon_{2\alpha} = 0$ and ε_3 is suppressed as M_1/M_3 . This can be considered somehow opposite to the case $\Omega = R_{23}$, where the N_2 -dominated scenario holds [93].

In general, one can say that the asymmetry produced from the two heavier RH neutrinos is non-negligible if two conditions are satisfied:

- (i) The asymmetry generated from $N_{2,3}$ -decays at $T \sim M_{2,3}$ is non-negligible compared to the asymmetry generated at $T \sim M_1$ from N_1 -decays. This depends on an evaluation of the CP asymmetries $\varepsilon_{2,3}^\alpha$ and of the washout due to the same $N_{2,3}$ inverse processes.
- (ii) The asymmetry produced from $N_{2,3}$ -decays is not afterwards washed out by N_1 inverse processes. Notice that this second condition is subordinate to the first condition.

5.3 Effects of $|\Omega_{22}|$

The general formula for the total CP asymmetry ε_1 was given in Eq. (2.16) with $i = 1$. It can be rewritten in the illustrative form Eq. (2.40), where the second term was said to be usually negligible for hierarchies larger than $3M_1 \lesssim M_2$. In fact, there is a situation where the term $[\xi(x_3) - \xi(x_2)]\Delta\varepsilon_1$ in Eq. (2.40) becomes dominant over $\xi(x_2)\varepsilon_1^{\text{HL}}$ and one has to require a stronger hierarchy than $3M_1 \lesssim M_2$ to recover the results presented in Section 2.2 [98]. From another perspective one can say that the second term in Eq. (2.40) offers a way to evade the bound on the CP asymmetry Eq. (2.45) for mild hierarchies.

The term proportional to $\Delta\varepsilon_1$ is maximized when $x_3 \gg 1$, implying $\xi(x_3) \simeq 1$. Moreover, if for definiteness one imposes $\Omega_{21} = 0$ and $\text{Re}[\Omega_{31}^2] = 0$, so that $\sin \delta_L = 1$ [cf. Eq.(2.47)], then

$$\xi_{\varepsilon_1} \equiv \frac{\varepsilon_1}{\bar{\varepsilon}(M_1)} = \xi(x_2) + [1 - \xi(x_2)](\text{Re}[\Omega_{22}^2] + \tilde{m}_1/m_{\text{atm}} \text{Im}[\Omega_{22}^2]). \quad (5.8)$$

One can immediately see that when $\text{Re}[\Omega_{22}^2] = 1$ and $\text{Im}[\Omega_{22}^2] = 0$, corresponding to $\Omega = R_{13}$, one recovers $\xi_{\varepsilon_1} = 1$, independently of the value of x_2 . Notice also that when $M_2 = M_3$, the $\Delta\varepsilon_1$ term vanishes. However, one can now perceive another possibility: if $|\Omega_{22}| \gg 1$, then the CP asymmetry can be enhanced, i.e. $\xi_{\varepsilon_1} > 1$, even when $x_2 \gg 1$.

This possibility is interesting because having large $|\Omega_{22}|$ values does not imply that the washout is large. As a matter of fact, the decay parameter K_1 does not depend on Ω_{22} . So there can be an enhancement of the CP asymmetry without any enhancement of the washout. This observation was made in [98] and supplemented with theoretical motivations for models with large $|\Omega_{22}|$ in [152]. These models make possible to evade the bound on the CP asymmetry Eq. (2.45) without reducing the efficiency factor, thus relaxing the lower bounds Eqs. (2.54) and (2.55). It was found that values of $M_1 \simeq 10^6$ GeV for mild hierarchies $M_2/M_1 \sim 10$ were possible, hence avoiding the gravitino problem. Note moreover that models with large $|\Omega_{22}|$ can

yield observable signals at experiments searching for lepton flavor violating decays $\mu \rightarrow e\gamma$, $\tau \rightarrow \mu\gamma$ and $\tau \rightarrow e\gamma$ [5, 153, 154].

There is another important consequence of the term $\Delta\varepsilon_1$, which concerns the upper bound on the absolute neutrino mass scale, Eq. (2.57). First, when the absolute neutrino mass scale increases, it is well known that the upper bound on the CP asymmetry decreases [cf. Eq. (2.45)]. Thus, a dominance of the $\Delta\varepsilon_1$ term over the first term in Eq. (2.40) can be more easily obtained when m_1 is larger, even for moderate values $|\Omega_{22}| \sim 1$. The term $\Delta\varepsilon_1$ is indeed not suppressed at large m_1 . Second, it can be argued that when $m_1 \sim 0.1$ eV, the light neutrinos are quasi-degenerate, so that quasi-degenerate heavy neutrinos with a mild degeneracy are more natural. Under the assumption of ‘natural’ mild degeneracy, the effect of the $\Delta\varepsilon_1$ term has to be included and leads to a relaxed upper bound $m_1 \lesssim 0.6$ eV [98]. Note that the washout from the heavier RH neutrino N_2 must be taken into account for degeneracies $\delta_{21} \lesssim 0.1$, as emphasized in Section 5.1.

The bottom line is that there are situations where the $\Delta\varepsilon_1$ term in Eq. (2.40) is crucial and hence should not be neglected. The first situation is when a large $|\Omega_{22}|$ allows to evade the upper bound on the CP asymmetry even when $m_1 \rightarrow 0$ and for moderate hierarchies $M_2/M_1 \simeq 10$, without reducing the efficiency factor. The lower bounds on M_1 and T_{reh} can then be relaxed by a few orders of magnitude. The second situation is when a quasi-degenerate mass spectrum for the heavy neutrinos is considered, $\delta_{ji} \lesssim 1$, and $|\Omega_{22}| \sim 1$. Then the contribution from the $\Delta\varepsilon_1$ term can be large, especially for quasi-degenerate light neutrinos.

We think it is judicious to recall that Eq. (2.40) is only a convenient rewriting of the general expression (2.16). All the effects discussed in this section are of course present in the general expression, but they can be overseen when the basic assumptions behind some simplified expressions like $\varepsilon_1^{\text{HL}}$ in Eq. (2.40) are forgotten, such as a sufficiently large hierarchy $M_1 \ll M_2 \ll M_3$.

Chapter 6

Leptogenesis from low-energy CP -violating phases

The possibility of relating the CP violation required for successful leptogenesis with the one that could be seen in future neutrino experiment is very attractive. However, in the context of unflavored leptogenesis (see Chapter 2), we saw that the PMNS matrix, which includes the observable CP -violating phases [cf. Eq. (A.5)], cancels out in the general case. Yet, even in this unfavorable situation, there have been attempts to relate low-energy CP -violating phases with the baryon asymmetry of the Universe produced through leptogenesis [79, 155–160]. It must be however said that a link could only be made for specific textures of the Dirac mass matrix.

As discussed in Chapter 3, flavor effects have modified the conventional picture of leptogenesis in a number of ways. In particular, the fact that the final asymmetry in the fully flavored regime depends explicitly on the PMNS mixing matrix is interesting. Thanks to the new source of CP violation implied by flavor effects, namely the ΔP contribution, Eq. (3.6), one can imagine a situation where the *only* source of CP violation comes from the PMNS matrix or, equivalently, where the contributions from the unobservable phases in the Ω matrix are negligible. This leads to the exciting possibility of explaining the baryon asymmetry of the Universe thanks to CP -violating phases that are accessible in neutrino experiments. This scenario has attracted some attention recently [123, 161–166].

In this chapter we first introduce the concepts of low-energy CP violation due to the Dirac phase and to the Majorana phases. Then, we study the possibility that the Dirac phase, which offers the best prospects for a possible measurement in the next years, provides the unique source of CP violation required for leptogenesis. This can be considered as the most conservative case, since we know that the Dirac phase comes always together with the

small angle θ_{13} [cf. Eq. (1.8)]. Afterwards, we shortly comment on the role played by the Majorana phases as sole sources of CP violation in leptogenesis. Finally, we discuss the theoretical relevance of models where Ω is real.

6.1 CP violation in neutrino physics

6.1.1 Neutrino oscillations and the Dirac phase

Searching for CP -violating effects in neutrino oscillations is the only practical way to get information about Dirac CP violation in the lepton sector, associated with the phase δ in the PMNS mixing matrix U [cf. Eq. (A.5)]. A measure of CP and T violation is provided by the asymmetries [167–169]

$$\begin{aligned} A_{CP}^{(\alpha,\alpha')} &= P(\nu_\alpha \rightarrow \nu_{\alpha'}) - P(\bar{\nu}_\alpha \rightarrow \bar{\nu}_{\alpha'}), \\ A_T^{(\alpha,\alpha')} &= P(\nu_\alpha \rightarrow \nu_{\alpha'}) - P(\nu_{\alpha'} \rightarrow \nu_\alpha), \end{aligned}$$

where $\alpha \neq \alpha' = e, \mu, \tau$. For three-neutrino oscillations in vacuum, which respect the CPT symmetry, one has [170]

$$\begin{aligned} A_T^{(e,\mu)} &= A_T^{(\mu,\tau)} = -A_T^{(e,\tau)} = J_{CP} F_{\text{osc}}^{\text{vac}}, \quad A_{CP}^{(\alpha,\alpha')} = A_T^{(\alpha,\alpha')}, \\ J_{CP} &= \text{Im}(U_{e1}U_{\mu 2}U_{e2}^*U_{\mu 1}^*) = \frac{1}{4} \sin 2\theta_{12} \sin 2\theta_{23} \cos^2 \theta_{13} \sin \theta_{13} \sin \delta, \\ F_{\text{osc}}^{\text{vac}} &= \sin\left(\frac{\Delta m_{21}^2}{2E}x\right) + \sin\left(\frac{\Delta m_{32}^2}{2E}x\right) + \sin\left(\frac{\Delta m_{13}^2}{2E}x\right), \end{aligned}$$

where x is the distance travelled by the neutrinos, and E is their common energy [cf. Eq. (1.11)]. Thus, the magnitude of the CP -violating effects in neutrino oscillations is controlled by the rephasing invariant associated with the Dirac phase δ , the so-called *Jarlskog invariant* J_{CP} [171]. The existence of Dirac CP violation in the lepton sector would be established if, e.g., some of the vacuum oscillation asymmetries $A_{CP,T}^{(\alpha,\alpha')}$ are proven experimentally to be non-zero. This would imply that $J_{CP} \neq 0$ and, consequently, that $\sin \theta_{13} \sin \delta \neq 0$. Without doubt, the search for CP -violating effects due to the Dirac phase in U represents one of the major goals of the future experimental studies of neutrino oscillations [172], in experiments like T2K [173] or NO ν A [174] as well as in the (far) future neutrino factories and/or beta beam experiments [175].

6.1.2 Neutrinoless double-beta decay and the Majorana phases

Theories with neutrino mass generation of the see-saw type predict the massive neutrinos ν_j to be Majorana particles. Determining the nature of massive neutrinos is one of the most formidable and pressing problems in today's neutrino physics (see, e.g., [172, 176, 177]). Even if neutrinos are proven to be Majorana fermions, getting information about the Majorana CP -violating phases in U , Φ_1 and Φ_2 [cf. Eq. (A.5)], will be very difficult. Moreover, the oscillations of flavor neutrinos, $\nu_\alpha \rightarrow \nu_{\alpha'}$ and $\bar{\nu}_\alpha \rightarrow \bar{\nu}_{\alpha'}$, $\alpha, \alpha' = e, \mu, \tau$, are insensitive to the Majorana phases [168, 178]. On the other hand, they can affect significantly the predictions for the rates of lepton-flavor-violating decays $\mu \rightarrow e + \gamma$, $\tau \rightarrow \mu + \gamma$, etc. in a large class of supersymmetric theories with type-I see-saw mechanism (see, e.g., [179–181]).

In the case of three-neutrino mixing under discussion, there are, in principle, three independent CP violation rephasing invariants. The first is J_{CP} , the Dirac one, associated with the Dirac phase δ , which we discussed in the previous subsection. The existence of two additional invariants, S_1 and S_2 , is related to the two Majorana CP -violating phases in U . The invariants S_1 and S_2 can be chosen as [182]

$$S_1 = \text{Im}(U_{\tau 1}^* U_{\tau 2}), \quad S_2 = \text{Im}(U_{\tau 2}^* U_{\tau 3}). \quad (6.1)$$

The rephasing invariants associated with the Majorana phases are not uniquely determined. Instead of the flavor τ involved in both S_1 and S_2 , one could have chosen e or μ . Note also that CP violation due to the Majorana phases imply that both $S_1 = \text{Im}(U_{\tau 1}^* U_{\tau 2}) \neq 0$ and $\text{Re}(U_{\tau 1}^* U_{\tau 2}) \neq 0$, and similarly for S_2 .

The only feasible experiments which, at present, have the potential of establishing the Majorana nature of light neutrinos and of providing information on the Majorana CP -violating phases in U are the experiments searching for neutrinoless double-beta ($0\nu\beta\beta$) decay, $(A, Z) \rightarrow (A, Z + 2) + 2e^-$. The $0\nu\beta\beta$ -decay effective Majorana mass, $|\langle m \rangle|$, as defined in Eq. (1.18), which contains all the dependence of the $0\nu\beta\beta$ -decay amplitude on the neutrino mixing parameters, is given by the following expressions for a normal hierarchical (NH, $m_1 \ll m_2 \ll m_3$), inverted hierarchical (IH, $m_1 \ll m_2 \ll m_3$, but the U matrix changes, as explained in Appendix A) and quasi-degenerate (QD, $m_{1,2,3} \simeq m \gtrsim 0.1$ eV) neutrino mass spectra:

$$|\langle m \rangle| \simeq \left| \sqrt{\Delta m_{\text{sol}}^2} \sin^2 \theta_{12} e^{i\Phi_2} + \sqrt{\Delta m_{\text{atm}}^2} \sin^2 \theta_{13} e^{-2i\delta} \right|, \quad (\text{NH}), \quad (6.2)$$

$$|\langle m \rangle| \simeq \sqrt{\Delta m_{\text{atm}}^2} |\cos^2 \theta_{12} e^{i\Phi_1} + e^{i\Phi_2} \sin^2 \theta_{12}|, \quad (\text{IH}), \quad (6.3)$$

$$|\langle m \rangle| \simeq m \left| \cos^2 \theta_{12} e^{i\Phi_1} + e^{i\Phi_2} \sin^2 \theta_{12} \right|, \text{ (QD)}. \quad (6.4)$$

Obviously, $|\langle m \rangle|$ depends strongly on the Majorana phases: the CP -conserving values of $\Phi_2 - \Phi_1 = 0, \pm\pi$ [183], for instance, determine the range of possible values of $|\langle m \rangle|$ in the case of IH and QD spectra, while the CP -conserving values of $\Phi_2 = 0, \pm\pi$, can be important in the case of NH spectrum.

The planned $0\nu\beta\beta$ -decay experiments of the next generation such as GERDA [49], MAJORANA [50] or CUORE [51] are aiming to probe the QD and IH ranges of $|\langle m \rangle|$ (see, e.g., [176, 177]). If the $0\nu\beta\beta$ -decay is observed in these experiments, the measurement of the $0\nu\beta\beta$ -decay half-life might then allow to obtain constraints on the combination of Majorana phases $\Phi_2 - \Phi_1$.

6.2 Dirac phase leptogenesis

In this section we would like to investigate in detail a scenario of leptogenesis where the CP violation necessary for leptogenesis is exclusively provided by the Dirac phase δ , hence the name δ -leptogenesis. Following closely [164] we start analysing the case where the heavy neutrino mass spectrum is hierarchical, i.e. $M_1 \ll M_2 \ll M_3$, which, in the fully flavored regime, does not necessarily lead to a N_1 -dominated scenario. Therefore, we shall not only consider the decay of the lightest RH neutrino, but that of all three RH neutrinos. Then, we will assume a quasi-degenerate mass spectrum for the heavy neutrinos, $M_1 \simeq M_2 \simeq M_3$, and perform the same analysis.

6.2.1 The hierarchical limit

Throughout this section, we will always assume that the fully flavored regime holds. However, the condition of validity of the fully flavored regime, Eq. (4.6), is qualitative. One should not expect it to be exact. For example, this simple condition neglects the effect of $\Delta L = 1$ scatterings and of refractive effects, the first contributing with inverse decays to preserve the quantum state coherence, the second, conversely, in projecting it on the flavor basis. Both of them can be as large as the effect from inverse decays. Moreover, in a rigorous quantum kinetic description, it is likely that other subtle effects will contribute to the determination of the exact value of M_1 below which the fully flavored regime can be assumed. Only making a precise study of the transition region between the unflavored and the fully flavored regimes solving the full system of equations, which includes the density matrix equation (4.29), will allow to derive a better condition of validity.

In the plots showing the lower bound on M_1 , we will then distinguish four regions. All plots will be cut at $M_1 = 10^{12}$ GeV, since above this value, according to the condition (4.3), the unflavored regime is recovered and the asymmetry production has to switch off, since only the phases in the Ω matrix can make the total CP asymmetries ε_i non-zero. On the other hand, when the condition (4.6) is satisfied, one can expect the fully flavored regime to hold. There is an intermediate regime where a transition between the fully flavored regime and the unflavored regime takes place. This regime will be indicated in all plots with a squared region. This signals that, even though we still show the results obtained in the fully flavored regime, important corrections are expected, especially when M_1 gets close to $\sim 10^{12}$ GeV. Since this region describes a transition towards the unflavored regime, where the asymmetry production has to switch off, these corrections are expected to reduce the final asymmetry, making more stringent the lower bounds shown in the plots. Furthermore, since large corrections to the condition (4.6) cannot be excluded, we will also indicate, with a hatched region, the area where the condition (4.6) holds but a very conservative condition,

$$M_1 \lesssim \frac{10^{11} \text{ GeV}}{W_1^{\text{ID}}(z_B(K_{1\alpha}))} \quad (6.5)$$

does not. In this region some corrections to the results presented cannot be excluded, but the fully flavored regime should represent a good approximation.

We anticipate that, in the N_1 -dominated scenario, successful leptogenesis always requires $M_1 \gtrsim 10^9$ GeV, where the two-flavor regime applies. Therefore, considering that we are assuming $\varepsilon_1 = \varepsilon_{1\tau} + \varepsilon_{1,e+\mu} = 0$, Eq. (3.29) can be specialized into

$$N_{B-L}^f|_{N_1} \simeq (\kappa_{1\tau}^f - \kappa_{1,e+\mu}^f) \varepsilon_{1\tau}, \quad (6.6)$$

showing that, in order to have a non-vanishing final asymmetry it is necessary to have that $P_{1\tau}^0 \neq P_{1,e+\mu}^0$. Indeed, the efficiency factors crucially depend on $K_{1\alpha}$. Useful analytical expressions for the flavored efficiency factors, both for a vanishing and a thermal initial N_1 -abundance can be found in Section 3.4. As for the flavored decay parameters in the usual orthogonal parametrization, Eq. (2.18), they were given in Eq. (3.23).

The parameter $r_{1\alpha}$ defined in Eq. (3.31) is convenient to describe the behavior of the CP asymmetry $\varepsilon_{1\alpha}$. Using Eq. (3.28) for real Ω , one obtains [129]

$$r_{1\alpha} = - \sum_{h < l} \frac{\sqrt{m_l m_h} (m_l - m_h)}{\tilde{m}_1 m_{\text{atm}}} \Omega_{h1} \Omega_{l1} \text{Im}[U_{\alpha h} U_{\alpha l}^*]. \quad (6.7)$$

Taking $\alpha = \tau$ and specifying the matrix elements $U_{\alpha j}$ from Eq. (A.5), one has

$$r_{1\tau} = -\frac{m_{\text{atm}}}{\tilde{m}_1} [A_{12} + A_{13} + A_{23}], \quad (6.8)$$

where, in the case of normal hierarchy for the light neutrinos¹,

$$\begin{aligned} A_{12} &= -\frac{\sqrt{m_1 m_2} (m_2 - m_1)}{m_{\text{atm}}^2} \Omega_{11} \Omega_{21} \text{Im}[(s_{12} s_{23} - c_{12} c_{23} s_{13} e^{i\delta}) \\ &\quad \times (c_{12} s_{23} + s_{12} c_{23} s_{13} e^{-i\delta}) e^{-\frac{i}{2}(\Phi_2 - \Phi_1)}], \\ A_{13} &= \frac{\sqrt{m_1 m_3} (m_3 - m_1)}{m_{\text{atm}}^2} \Omega_{11} \Omega_{31} c_{23} c_{13} \text{Im}[(s_{12} s_{23} - c_{12} c_{23} s_{13} e^{i\delta}) e^{\frac{i}{2}\Phi_1}], \\ A_{23} &= -\frac{\sqrt{m_2 m_3} (m_3 - m_2)}{m_{\text{atm}}^2} \Omega_{21} \Omega_{31} c_{23} c_{13} \text{Im}[(c_{12} s_{23} + s_{12} c_{23} s_{13} e^{i\delta}) e^{\frac{i}{2}\Phi_2}]. \end{aligned}$$

In the case of δ -leptogenesis ($\Phi_1 = \Phi_2 = 0$), these expressions further specialize into

$$\begin{aligned} A_{12} &= \frac{\sqrt{m_1 m_2} (m_2 - m_1)}{m_{\text{atm}}^2} \Omega_{11} \Omega_{21} s_{23} c_{23} \Delta, \\ A_{13} &= -\frac{\sqrt{m_1 m_3} (m_3 - m_1)}{m_{\text{atm}}^2} \Omega_{11} \Omega_{31} c_{23}^2 c_{12} c_{13} \Delta, \\ A_{23} &= -\frac{\sqrt{m_2 m_3} (m_3 - m_2)}{m_{\text{atm}}^2} \Omega_{21} \Omega_{31} c_{23}^2 s_{12} c_{13} \Delta, \end{aligned}$$

where we defined $\Delta \equiv \sin \theta_{13} \sin \delta$.

It is now instructive to make some general considerations. Looking at the expression Eq. (6.6), one can see that in order for the final B – L asymmetry to be non-zero, two conditions have to be simultaneously satisfied : $\varepsilon_{1\tau} \neq 0$ and $\kappa_{1\tau}^f \neq \kappa_{1,e+\mu}^f$. These two conditions are a specialization of two of Sakharov's necessary conditions for baryogenesis to the case of δ -leptogenesis.

The first condition is the requirement to have CP violation and, as one could expect, from the expressions found for the terms A_{ij} , one can have $\varepsilon_{1\tau} \neq 0$ only if $\Delta \neq 0$.

The second condition is a specialization of the condition of departure from thermal equilibrium in quite a non-trivial way. Indeed, in the case of δ -leptogenesis, in a fully out-of-equilibrium situation where only decays are active, no final asymmetry is generated since $\varepsilon_1 = 0$, implying that there is an equal number of decays into leptons and antileptons. However, the presence of inverse processes can remove this balance, yielding a different washout rate

¹For an inverted hierarchy, the elements A_{ij} must be computed using a modified U matrix, as explained at the end of Appendix A.

for the τ asymmetry and for the $e + \mu$ asymmetry, so that, if $K_{1\tau} \neq K_{1,e+\mu}$, one has a dynamical net lepton number generation. From the flavored decay parameters Eq. (3.23), it can be seen that this is possible independently of the value of the Dirac phase, which is therefore directly responsible only for CP violation and not for lepton number violation, exactly as in neutrino mixing, where lepton number is conserved.

It should also be noticed that the $\varepsilon_{1\alpha}$'s are expressed through quantities $\text{Im}[U_{\alpha h} U_{\alpha l}^*]$ that are invariant under a change of the PMNS matrix parametrization [161, 182]. Actually, the CP asymmetry itself is an invariant quantity [184]. Therefore, the final $B-L$ asymmetry depends only on physical quantities, as it should be.

Maximizing the asymmetry over all involved parameters at fixed M_1 and K_1 and imposing $\eta_B^{\text{max}} \geq \eta_B^{\text{CMB}}$ [cf. Eqs. (2.15) and (1.6)], a lower bound on M_1 is obtained, which can be conveniently expressed as in Eq. (3.32). Notice that $r_{1\tau} \propto \Delta$, implying $N_{B-L}^f \propto \Delta$ as well. Therefore, the maximum asymmetry is obtained for $|\delta| = \pi/2$ and $s_{13} = 0.20$.

As we explained in Section 5.2, accounting for flavor effects it is not clear whether the contribution from the lightest RH neutrino, N_1 , is the only one that matters. Since we want our analysis to be as general as possible, we will always estimate the asymmetry produced by the two heavier neutrinos N_2 and N_3 .

The calculation of the contribution to the asymmetry from N_2 -decays proceeds in an analogous way. It can be again calculated in the two-flavor regime, since, in the HL, successful leptogenesis always implies $M_2 \gtrsim 10^9$ GeV. Therefore, one can write an expression similar to Eq. (6.6) for the contribution to the final asymmetry from N_2 -decays,

$$N_{B-L}^f|_{N_2} \simeq (\kappa_{2\tau}^f - \kappa_{2,e+\mu}^f) \varepsilon_{2\tau}. \quad (6.9)$$

The difference is now in the calculation of the efficiency factors as they are suppressed by the washout from the N_1 inverse processes. In the HL this additional washout factorizes and [94, 123, 149]

$$\kappa_{2\alpha}^f \simeq \kappa(K_{2\alpha}) \exp\left(-\frac{3\pi}{8} K_{1\alpha}\right), \quad (6.10)$$

where $K_{2\alpha} \equiv P_{2\alpha}^0 K_2$. The tree-level projectors $P_{2\alpha}^0$ can be readily evaluated using the general expression (3.22).

The calculation of the contribution to the final asymmetry from N_3 -decays proceeds in a similar way and analogous expressions hold. The only non-trivial difference is that now, in the calculation of the efficiency factors, one

has also to include the washout from N_2 inverse processes, so that

$$\kappa_{3\alpha}^f \simeq \kappa(K_{3\alpha}) \exp \left[-\frac{3\pi}{8} (K_{1\alpha} + K_{2\alpha}) \right]. \quad (6.11)$$

Notice that in the calculation of $\kappa_{2\alpha}^f$ ($\kappa_{3\alpha}^f$) we are not including a possible effect where part of the asymmetry in the flavor $\alpha = e + \mu$ produced in N_2 - or N_3 -decays is orthogonal to N_1 inverse decays [127, 150] and is not washed out. This washout avoidance does not apply to the asymmetry in the τ -flavor. Since in all cases we shall consider, a τ -dominated scenario will be realized, we shall simply neglect this effect. For a short discussion about these effects, see Section 5.2.

Let us now calculate the final asymmetry in some interesting cases.

$$\Omega = R_{13}$$

The first case we consider is $\Omega = R_{13}$ [cf. Eq. (2.21)], implying $A_{12} = A_{23} = 0$ in Eq. (6.8). It is easy to check from Eq. (3.26) that $\varepsilon_{2\tau} = 0$, and therefore there is no asymmetry production from N_2 -decays even if $M_2 \lesssim 10^{12}$ GeV. On the other hand, one obtains

$$r_{3\tau} = -\frac{2}{3} \frac{\sqrt{m_1 m_3} (m_3 - m_1)}{\tilde{m}_3 m_{\text{atm}}} \omega_{31} \sqrt{1 - \omega_{31}^2} c_{12} c_{23}^2 c_{13} \Delta, \quad (6.12)$$

essentially the same expression as for $r_{1\tau}$ but with \tilde{m}_1 replaced by \tilde{m}_3 . Therefore, for $M_3 \lesssim 10^{12}$ GeV, one has to worry about a potential non-negligible contribution from N_3 -decays. However, when the washout from N_1 and N_2 inverse processes is taken into account [cf. Eq. (6.11)], we always find that the contribution from N_3 -decays is negligible and the N_1 -dominated scenario holds.

The results are shown in Fig. 6.1 for $s_{13} = 0.20$, $\delta = -\pi/2$ and $m_1/m_{\text{atm}} = 0.1$, a choice of values that approximately maximizes the final asymmetry and yields the lower bound $M_1^{\text{min}}(K_1)$. In the left panel we show the tree-level projectors $P_{1\alpha}^0$ and the normalized CP asymmetries $r_{1\alpha}$ [cf. Eq. (3.31)]. It can be seen how for $K_1 \gg 10$ one has $P_{1\tau}^0 \simeq P_{1,e+\mu}^0 \simeq 1/2$, while for $K_1 \sim 10$ one has $P_{1\tau}^0 \ll P_{1,e+\mu}^0$. In the central panel ξ_1 and the $\xi_{1\alpha}$'s are plotted [cf. Eq. (3.33)], and one can see how for $K_1 \simeq 10$ a τ -dominance is realized. Finally, in the right panel, we show $M_1^{\text{min}}(K_1)$ and we compare it with the lower bound from an unflavored calculation where ω_{31}^2 is taken purely imaginary [93]. One can see how, at $K_1 \gg 10$, the asymmetry production rapidly dies, so that $\xi_1 \rightarrow 0$ and $M_1^{\text{min}}(K_1) \rightarrow \infty$. Notice that we have plotted the lower bound both for thermal and vanishing initial N_1 -abundances.

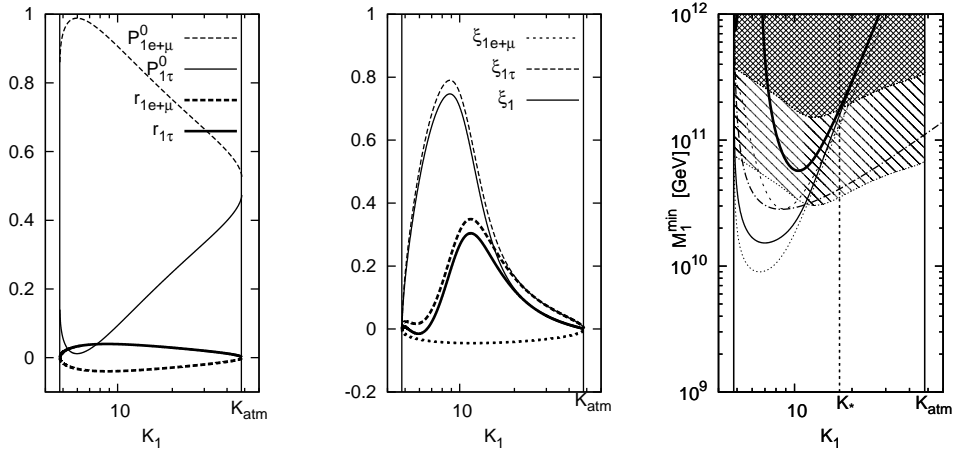


Figure 6.1: Dependence of different quantities on K_1 for $m_1/m_{\text{atm}} = 0.1$, $s_{13} = 0.2$, $\delta = -\pi/2$ and real $\Omega = R_{13}$ with $\omega_{31} < 0$. Left panel: projectors $P_{1\alpha}^0$ and normalized CP asymmetries $r_{1\alpha}$; central panel: $\xi_{1\alpha}$ and ξ_1 as defined in Eq. (3.33) for thermal (thin) and vanishing (thick) initial N_1 -abundance; right panel: lower bound on M_1 for thermal (thin solid) and vanishing (thick solid) initial N_1 -abundance compared with the unflavored result (dash-dotted line) obtained for complex $\Omega = R_{13}$. In the squared region the condition (4.6) is not satisfied, and in the hatched region even the more conservative condition (6.5) is not satisfied. The dotted lines (thick for vanishing and thin for thermal initial N_1 -abundance) correspond still to a real $\Omega = R_{13}$ but this time $\delta = 0$ while the only non-vanishing low-energy phase is the Majorana phase $\Phi_1 = -\pi/2$.

We also indicated K_* , defined as that value of K_1 such that for $K_1 \gtrsim K_*$ the dependence on the initial conditions can be neglected and the strong washout regime holds. One can notice that the intermediate regime between a fully flavored regime and the unflavored regime, the squared area, is quite extended. In this regime corrections to the results we are showing, obtained in the fully flavored regime, are expected in a way that the unflavored regime should be recovered for $M_1 \rightarrow 10^{12}$ GeV. In this limit the asymmetry production has to switch off and thus one expects that the lower bound on M_1 becomes more restrictive and eventually, for $M_1 \rightarrow 10^{12}$ GeV, the allowed region has to close up. One can see that there is essentially no allowed region in the strong washout regime outside the squared area. The hatched area, where corrections cannot be excluded within current theoretical uncertainties, cuts away almost completely any allowed region even in the weak washout regime.

In conclusion, the allowed region where one can safely rely on the fully flavored regime according to current calculations is very restricted and confined only to a small region in the weak washout regime.

$$M_3 \gg 10^{14} \text{ GeV}$$

The second case we consider is the limit $M_3 \gg 10^{14}$ GeV. This corresponds to an effective 2-RH neutrino model, where the third RH neutrino is decoupled. In this limit one has necessarily $m_1 \ll m_{\text{sol}}$, implying $m_3 \simeq m_{\text{atm}}$, and the Ω matrix takes the special form [160, 185, 186]

$$\Omega = \begin{pmatrix} 0 & 0 & 1 \\ \sqrt{1 - \Omega_{31}^2} & -\Omega_{31} & 0 \\ \Omega_{31} & \sqrt{1 - \Omega_{31}^2} & 0 \end{pmatrix}. \quad (6.13)$$

Notice that this form of Ω corresponds to set $\omega_{32} = 1$ and $\omega_{21} = 1$ in Eq. (2.19). In the expression (6.8) for $r_{1\tau}$, one has now $A_{12} = A_{13} = 0$, and hence

$$r_{1\tau} \simeq \frac{m_{\text{atm}}}{\tilde{m}_1} \sqrt{\frac{m_2}{m_{\text{atm}}}} \left(1 - \frac{m_2}{m_{\text{atm}}} \right) \Omega_{31} \sqrt{1 - \Omega_{31}^2} c_{23}^2 c_{13} s_{12} \Delta. \quad (6.14)$$

If $M_2 \gtrsim 10^{12}$ GeV, there is no contribution from the next-to-lightest RH neutrino decays, since these occur in the unflavored regime where $\varepsilon_2 \simeq 0$. On the other hand, if $M_2 \lesssim 10^{12}$ GeV, then one has to worry about a (flavored) asymmetry generation from N_2 -decays. A calculation of $\varepsilon_{2\alpha}$ shows that the first term in Eq. (3.26) vanishes while the second term gives

$$r_{2\tau} = -\frac{2}{3} \frac{m_{\text{atm}}}{\tilde{m}_2} \sqrt{\frac{m_2}{m_{\text{atm}}}} \left(1 - \frac{m_2}{m_{\text{atm}}} \right) \Omega_{31} \sqrt{1 - \Omega_{31}^2} c_{23}^2 s_{12} \Delta. \quad (6.15)$$

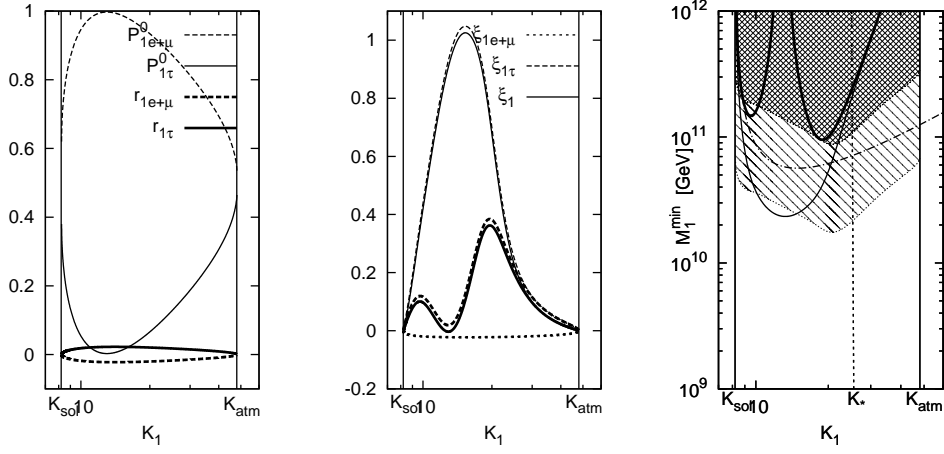


Figure 6.2: Same quantities as in Fig. 6.1 but for the case $M_3 \gg 10^{14}$ GeV, corresponding to the special form of Ω in Eq. (6.13). Here we are moreover assuming $M_2 \gtrsim 10^{12}$ GeV and a normal hierarchy for the light neutrinos. The lower bound $M_1^{\min}(K_1)$ is obtained for $\omega_{31} > 0$ and $\delta = \pi/2$.

This is an example of how the second term in Eq. (3.26) is not suppressed in the HL like the first term. However, like for the contribution from N_3 -decays in the case $\Omega = R_{13}$, when the washout from N_1 inverse processes is taken into account, one finds $N_{B-L}^f|_{N_2} \ll N_{B-L}^f|_{N_1}$ and a N_1 -dominated scenario is realized.

Notice that there is a strong dependence whether one assumes a normal or an inverted hierarchy. For normal hierarchy the results are shown in Fig. 6.2 for $\omega_{31} > 0$ and $\delta = \pi/2$. For inverted hierarchy the asymmetry is so suppressed that there is no allowed region. This means that for any choice of the parameters one always obtains $M_1^{\min} \gtrsim 10^{12}$ GeV.

Notice that some results for δ -leptogenesis in the particular case where $M_3 \gg 10^{14}$ GeV have been recently presented in [163] for vanishing initial N_1 -abundance. For example the authors obtain a lower bound $\sin \theta_{13} \gtrsim 0.09$ imposing the existence of an allowed region for $M_1 \lesssim 5 \times 10^{11}$ GeV, while we would obtain $\sin \theta_{13} \gtrsim 0.05$. Different reasons might explain this discrepancy. First, we are using a ($\sim 30\%$) more conservative lower bound on \overline{M}_1 [cf. Eq. (2.53)]. Second, we do not include the effects of $\Delta L = 1$ scatterings on the efficiency factors, which might produce some difference when $K_{1\alpha} \sim 1$, even though in the strong washout regime this effect should be negligible. Finally, another likely minor source of difference is that we are not accounting for the effect of spectator processes encoded in the matrix C^ℓ [cf. Eq. (3.15)] that relates the $B/3 - L_\alpha$ asymmetries to the L_α asymmetries [127]. However,

notice that we do not want here to emphasize too much a precise value of this lower bound on $\sin \theta_{13}$, since we believe that it is anyway affected by much larger theoretical uncertainties on the validity of the fully flavored regime.

$$\Omega = R_{12}$$

The third case we consider is $\Omega = R_{12}$ [cf. Eq. (2.20)]. This time one has $A_{13} = A_{23} = 0$ in Eq. (6.8). In the case of normal hierarchy, the CP asymmetry, compared to the case $\Omega = R_{13}$, is suppressed by a factor $(m_{\text{sol}}/m_{\text{atm}})^{3/2}$, while it is essentially the same for inverted hierarchy. The projectors present very similar features to the case $\Omega = R_{13}$. One can also again calculate, for $M_2 \lesssim 10^{12}$ GeV, the contribution from N_2 -decays to the final asymmetry, and one finds again that the first term in Eq. (3.26) vanishes, while the second produces a term $\propto M_1$, so that

$$r_{2\tau} = \frac{2}{3} \frac{\sqrt{m_1 m_2} (m_2 - m_1)}{\tilde{m}_2 m_{\text{atm}}} \omega_{21} \sqrt{1 - \omega_{21}^2} s_{23} c_{23} \Delta. \quad (6.16)$$

When the efficiency factors are taken into account, one finds that only in the case of normal hierarchy the contribution to the final asymmetry from N_2 -decays can be comparable to the one from N_1 -decays. However, in this case both productions are suppressed and there is no allowed region in the end. In the case of inverted hierarchy, the contribution from N_2 -decays is always negligible compared to the one from N_1 -decays. Notice, moreover, that $\varepsilon_{3\alpha} = 0$ for $\Omega = R_{12}$, and hence there is no contribution from N_3 -decays.

In conclusion, for $\Omega = R_{12}$, the lower bound on M_1 for normal hierarchy is much more restrictive than in the case $\Omega = R_{13}$, while it is very similar for inverted hierarchy. A production from the two heavier RH neutrinos can be neglected and the N_1 -dominated scenario always applies when the asymmetry is maximized.

$$\Omega = R_{23}$$

The last interesting case is $\Omega = R_{23}$ [cf. Eq. (2.22)]. From Eq. (3.28) one can easily check that $\varepsilon_{1\alpha} = 0$. One can also check that, contrarily to the case $\Omega = R_{12}$, the second term in Eq. (3.26) vanishes while the first term does not and yields

$$r'_{2\tau} \equiv \frac{\varepsilon_{2\tau}}{\bar{\varepsilon}(M_2)} = \frac{\sqrt{m_2 m_3} (m_3 - m_2)}{\tilde{m}_2 m_{\text{atm}}} \omega_{32} \sqrt{1 - \omega_{32}^2} s_{12} c_{23}^2 c_{13} \Delta. \quad (6.17)$$

Notice that this time $\varepsilon_{2\tau} \propto M_2$ and actually, more generally, one can see that this expression is obtained from Eq. (6.8) for $r_{1\tau}$ in the case $\Omega = R_{13}$,

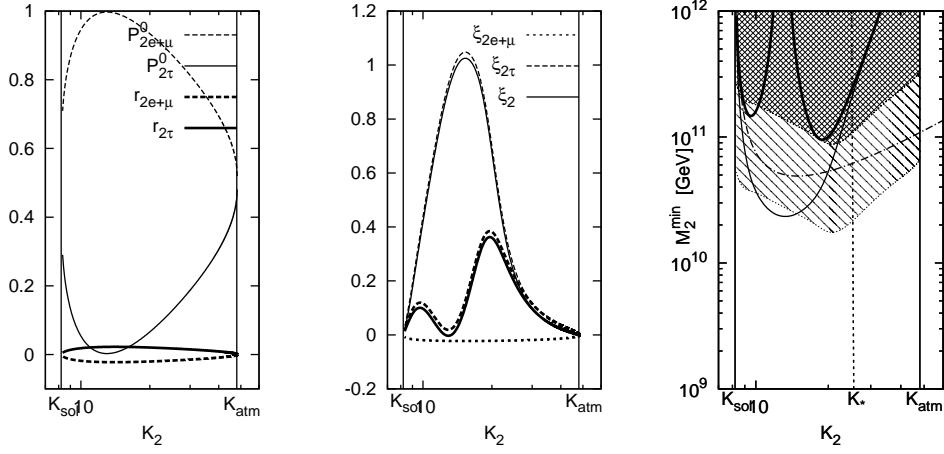


Figure 6.3: Dependence of different quantities on K_2 for $m_1 = 0$, $s_{13} = 0.2$, $\delta = \pi/2$ and real $\Omega = R_{23}$ with $\omega_{32} > 0$. Left panel: projectors $P_{2\alpha}^0$ and quantities $r'_{2\alpha}$; central panel: $\xi_{2\alpha}$ and ξ_2 for thermal (thin) and vanishing (thick) initial N_1 -abundance; right panel: lower bound on M_2 for thermal (thin solid) and vanishing (thick solid) abundance compared with the unflavored result (dash-dotted line) as obtained in [93].

just with the replacement $(M_1, \tilde{m}_1) \rightarrow (M_2, \tilde{m}_2)$. At the same time, one has $K_1 = m_1/m_*$, so that the washout from N_1 inverse processes vanishes for $m_1 \rightarrow 0$. For $M_3 \lesssim 10^{12}$ GeV, one has to worry about a possible contribution to the asymmetry from N_3 -decays. A straightforward calculation shows that $\varepsilon_{3\alpha} = (2/3)\varepsilon_{2\alpha}$, and therefore an asymmetry is produced at $T \sim M_3$. However, we verified once more that the washout from N_2 inverse processes is always strong enough for the contribution to the final asymmetry from N_3 -decays to be negligible.

In complete analogy with the unflavored case [93], one has that the lower bound $M_1^{\text{min}}(K_1)$ is replaced by a lower bound $M_2^{\text{min}}(K_2)$ obtained for $\omega_{32} > 0$ and shown in the right panel of Fig. 6.3. One can see that also in this case, within the validity of the condition (4.6), the allowed region is constrained to a small portion falling in the weak washout regime. Assuming the very conservative condition of validity for the fully flavored regime outside the squared and hatched regions, there is essentially no allowed region even in the weak washout regime.

One can wonder whether there is some choice of Ω beyond the special cases we analyzed where the final asymmetry is much higher and the lower bound on M_1 much more relaxed, especially in the strong washout regime. We have checked different intermediate cases, and we can exclude such a possibility.

Therefore, the lower bound shown in Fig. 6.1 has to be considered, with good approximation, the lowest bound for any choice of real Ω .

Another legitimate doubt is whether going beyond the approximations we made the lower bound in Fig. 6.1 can be considerably relaxed. The inclusion of non-resonant $\Delta L = 2$ or $\Delta L = 1$ scatterings is not expected to produce large corrections. Recently the effect of the off-diagonal terms in the matrix C^ℓ [cf. Eq. (3.15)] has been considered, but it has been shown that it does not produce any relevant change in the final asymmetry [130].

Relevant corrections, as already pointed out, can only come from a full quantum kinetic treatment, which should describe accurately the transition between the unflavored regime and the fully flavored regime.

The same kind of considerations holds for the N_2 -dominated scenario, realized for $\Omega = R_{23}$. As soon as Ω deviates from R_{23} , the washout from N_1 inverse processes comes into play suppressing the final asymmetry and, at the same time, $\varepsilon_{2\tau}$ gets also suppressed. Therefore, the lower bound on M_2 is necessarily obtained for $\Omega = R_{23}$ in complete analogy with the unflavored treatment [93].

In conclusion, δ -leptogenesis in the HL is severely constrained, confirming the conclusions of [123] and [122]. In particular, imposing independence from the initial conditions, then not even a marginally allowed region seems to survive. Notice moreover that all plots have been obtained for $s_{13} = 0.2$, the current 3σ upper limit. Assuming that for values of M_1 above the condition (4.6) the unflavored regime is quickly recovered and therefore that the asymmetry production quickly switches off, then a one-order-of-magnitude improvement of the upper limit on $\sin\theta_{13}$ would essentially rule out δ -leptogenesis in the HL, even the marginally allowed regions falling in the weak washout regime.

In the next section we consider the effect of close heavy neutrino masses in enhancing the CP asymmetries and relaxing the lower bounds on M_1, M_2 as well as the related one on T_{reh} . But before concluding this section, we want to mention that in the more general case of real Ω with non-vanishing Majorana phases, an upper bound $m_1 \lesssim 0.1$ eV has been obtained in the fully flavored regime [162] and for a hierarchical heavy neutrino mass spectrum. This bound clearly applies also to δ -leptogenesis, but in this case, considering the results we have obtained and the expected quantum kinetic corrections to the fully flavored regime, the issue is actually whether an allowed region exists at all in the HL, even for $m_1 = 0$. Therefore, we do not even try to place an upper bound on m_1 in the HL. In the next section we show that an upper bound on m_1 from successful δ -leptogenesis actually holds even in the resonant limit, where the CP asymmetries are maximally enhanced.

6.2.2 The degenerate limit

We would like to show that going beyond the HL, the lower bound on M_1 (or on M_2) can be considerably relaxed. Nevertheless, we shall see that some interesting constraints on the involved parameters still apply. For simplicity, we assume from the beginning that M_1 (or M_2) $\ll 10^9$ GeV, so that the three-flavor regime applies, where the muon-Yukawa interactions are also faster than inverse decays. Therefore, when we show the flavor index α , we mean $\alpha = e, \mu, \tau$. This assumption simplifies the calculation, since we do not have to describe a transition between the two and the three-flavor regime, and because we can completely neglect the effect envisaged in [127, 150] where part of the asymmetry produced from N_2 -decays is not touched by N_1 inverse decays.

In order to go beyond the HL, it is convenient to use the quantity δ_{ji} defined in Eq. (5.5). We are interested in the degenerate limit (DL), where at least one δ_{ji} is small enough that both the asymmetry production from $N_{i,j}$ -decays and the washout from the corresponding inverse processes can be approximately treated as if they occurred at the same temperature, so that they can be simply added up. The DL is a good approximation for $|\delta_{ji}| \lesssim 0.01$ [94].

If $i, j \neq 3$ and $M_1 \simeq M_2 \ll M_3$, then one has a partial DL, where the efficiency factors can be approximated as in Eq. (5.2) for thermal initial N_1 -abundance. In all the cases we shall consider, we will always have $K_{i\alpha} + K_{j\alpha} \gg 1$, so that the strong washout regime applies, and there is no need to consider the case of vanishing initial N_1 -abundance.

Another possibility is to have a partial DL with $i, j \neq 1$, so that $M_1 \ll M_2 \simeq M_3$. In this case one has to take into account the washout from the lightest RH neutrino, implying

$$\kappa_{i\alpha}^f \simeq \kappa_{j\alpha}^f \simeq \kappa(K_{i\alpha} + K_{j\alpha}) \exp\left(-\frac{3\pi}{8}K_{1\alpha}\right). \quad (6.18)$$

Finally, in the full DL, $M_1 \simeq M_2 \simeq M_3$, and the efficiency factor is given by Eq. (5.1).

Let us now calculate the flavored CP asymmetries. In the case of real Ω , which implies real $(h^\dagger h)_{ij} = (h^\dagger h)_{ji}$, the expression (5.4) becomes

$$\varepsilon_{i\alpha} \simeq \frac{1}{8\pi(h^\dagger h)_{ii}} \sum_{j \neq i} (h^\dagger h)_{ij} \operatorname{Im}[h_{\alpha i}^* h_{\alpha j}] \delta_{ji}^{-1}. \quad (6.19)$$

We can again express the neutrino Yukawa coupling matrix through the orthogonal representation. This time the presence of the factor δ_{ji}^{-1} does not

allow to remove the sum on j , as it has been possible in the HL in order to derive Eq. (3.28). However, considering the same special cases as in the HL, only one term $j \neq i$ survives, and we can write

$$\varepsilon_{i\alpha} \simeq \frac{2\bar{\varepsilon}(M_i)}{3\delta_{ji}} \sum_{n,h<l} \frac{m_n \sqrt{m_h m_l}}{\tilde{m}_i m_{\text{atm}}} \Omega_{ni} \Omega_{nj} [\Omega_{hi} \Omega_{lj} - \Omega_{li} \Omega_{hj}] \text{Im}[U_{\alpha h}^* U_{\alpha l}]. \quad (6.20)$$

The same expression holds for $\varepsilon_{j\alpha}$ simply exchanging the i and j indexes. We can always choose $j > i$ such that $M_j \geq M_i$. In all the particular cases we shall consider, we will have that $\varepsilon_{k\alpha} = 0$ for $k \neq i, j$, and moreover the following simplifications apply:

$$\sum_n m_n \Omega_{ni} \Omega_{nj} = (m_q - m_p) \Omega_{ji} \Omega_{jj} \quad (6.21)$$

$$\sum_{h<l} \sqrt{m_h m_l} [\Omega_{hi} \Omega_{lj} - \Omega_{li} \Omega_{hj}] = \sqrt{m_q m_p}, \quad (6.22)$$

with $q > p$. Except for the case $M_3 \gg 10^{14}$ GeV, we will always have $q = j$ and $p = i$. The final $B-L$ asymmetry can then be expressed as

$$N_{B-L}^f \simeq \sum_{\alpha} (\varepsilon_{i\alpha} + \varepsilon_{j\alpha}) \kappa_{\alpha}^f(K_{i\alpha} + K_{j\alpha}, K_{k\alpha}) = \frac{\bar{\varepsilon}(M_i)}{3\delta_{ji}} g(m_1, \Omega_{ji}, \theta_{13}, \delta) \Delta, \quad (6.23)$$

where

$$\begin{aligned} g(m_1, \Omega_{ji}, \theta_{13}, \delta) &\equiv \frac{2 K_{\text{atm}} (K_i + K_j)}{K_i K_j} \frac{(m_q - m_p) \sqrt{m_q m_p}}{m_{\text{atm}}^2} \Omega_{ji} \sqrt{1 - \Omega_{ji}^2} \\ &\times \sum_{\alpha} \kappa_{\alpha}^f(K_{i\alpha} + K_{j\alpha}, K_{k\alpha}) \frac{\text{Im}[U_{\alpha p}^* U_{\alpha q}]}{\Delta} \end{aligned} \quad (6.24)$$

and where $\kappa_{\alpha}^f(K_{i\alpha} + K_{j\alpha}, K_{k\alpha}) = \kappa_{i\alpha}^f = \kappa_{j\alpha}^f$ is given by one of the three expressions Eq. (5.1), Eq. (5.2) or Eq. (6.18) according to the particular case.

It is interesting to notice that because of the unitarity of U , the sum over i of the flavored decay parameters, Eq. (5.3), tends to m/m_{\star} in the degenerate limit for the light neutrinos (m is the common mass scale) independently of the flavor. Therefore, the sum over the flavor in Eq. (6.24) tends to vanish. This will contribute, as we shall see, to place a stringent upper bound on the absolute neutrino mass scale in the full DL.

It is also worthwhile to notice that the sign of Δ cannot be predicted from the sign of the observed baryon asymmetry, since the sign of $g(m_1, \Omega_{ji}, \theta_{13}, \delta)$ depends on the sign of Ω_{ji} , which is undetermined. Notice

also that $\text{Im}[U_{\alpha h}^* U_{\alpha l}]/\Delta$ does not depend on Δ , but nevertheless there is a dependence of $g(m_1, \Omega_{ji}, \theta_{13}, \delta)$ on δ and on θ_{13} coming from the tree-level projectors $P_{i\alpha}^0$ in the sum $K_{i\alpha} + K_{j\alpha}$. However, in any case, for $\Delta \rightarrow 0$ one has that $g(m_1, \Omega_{ji}, \theta_{13}, \delta) \Delta \rightarrow 0$, since the final asymmetry has to vanish when $\sin \theta_{13}$ or $\sin \delta$ vanishes.

The function $|g(m_1, \Omega_{ji}, \theta_{13}, \delta)|$ can be maximized over Ω_{ji} . Indeed for $m_1 = 0$, since $\kappa < 1$ and $K_i + K_j \leq K_{\text{atm}}$, one has $g(m_1 = 0, K_i, \theta_{13}, \delta) < 4$. Increasing m_1 there is a suppression due to the fact that $K_i \geq m_1/m_*$, and $g_{\text{max}}(m_1, \theta_{13}, \delta)$ decreases monotonically. Therefore, for any m_1 , there is a lower bound on M_1 given by

$$M_1 \geq M_1^{\min}(m_1, \theta_{13}, \delta) \equiv \frac{3 \overline{M}_1}{g_{\text{max}}(m_1, \theta_{13}, \delta)} \frac{\delta_{j1}}{|\Delta|}. \quad (6.25)$$

The CP asymmetries, and consequently the final baryon asymmetry, are maximally enhanced in the extreme case of resonant leptogenesis [76, 117, 118], when the heavy neutrino mass degeneracy is comparable to the decay widths. An approximate resonance condition was given in Eq. (5.7), where the uncertainty parameter $d = 1 \div 10$ was introduced because of a discrepancy in the literature [85, 117]. When the resonance condition is satisfied, one has $\varepsilon_1 = 1/d$ in the unflavored case with maximal phase. This can be taken as a conservative limit that implies, maximizing over δ , a lower bound

$$\sin \theta_{13} \geq \sin \theta_{13}^{\min} = \frac{d \eta_B^{\text{CMB}} N_{\gamma}^{\text{rec}}}{a_{\text{sph}} \max_{\delta} [g_{\text{max}}(m_1, \theta_{13}^{\min}, \delta) \sin \delta]}. \quad (6.26)$$

Let us now specialize the expressions for the four special cases we have already analyzed in the HL.

$$M_3 \gg 10^{14} \text{ GeV}$$

Remember that in this case one has $(h^\dagger h)_{3j} = 0$, implying $\varepsilon_{3\alpha} = 0$, a consequence of the fact that the heaviest RH neutrino decouples. Moreover, one has $m_1 \ll m_{\text{sol}}$, so that terms $\propto m_1$ can be neglected, $m_3 \simeq m_{\text{atm}}$ and $m_2 \simeq m_{\text{sol}}$ for normal hierarchy or $m_2 \simeq m_{\text{atm}} \sqrt{1 - m_{\text{sol}}^2/m_{\text{atm}}^2}$ for inverted hierarchy. Therefore, there is actually no dependence on m_1 in $g(m_1, \Omega_{ji}, \theta_{13}, \delta)$, which is given by Eq. (6.24) with $(i, j) = (1, 2)$ and $(p, q) = (2, 3)$,

$$\begin{aligned} g(\Omega_{21}, \theta_{13}, \delta) &\simeq \frac{2(K_1 + K_2) K_{\text{atm}}}{K_1 K_2} \left(1 - \frac{m_2}{m_{\text{atm}}}\right) \sqrt{\frac{m_2}{m_{\text{atm}}}} \Omega_{21} \sqrt{1 - \Omega_{21}^2} \\ &\times \sum_{\alpha} \kappa(K_{1\alpha} + K_{2\alpha}) \frac{\text{Im}[U_{\alpha 2}^* U_{\alpha 3}]}{\Delta}. \end{aligned} \quad (6.27)$$

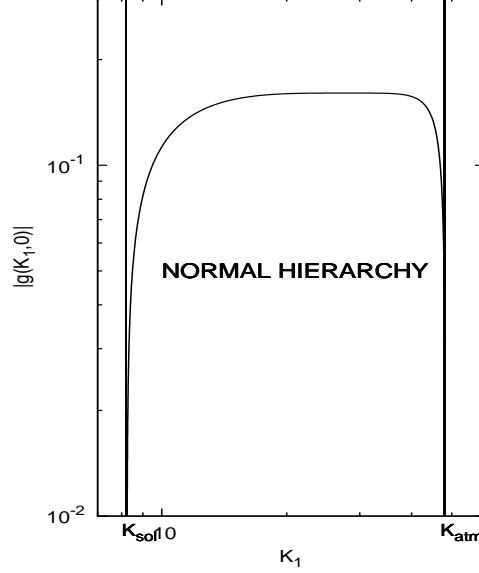


Figure 6.4: Case $M_3 \gg 10^{14}$ GeV for normal hierarchy in the DL. Plot of the function $|g(K_1, \theta_{13}, \delta)|$ in the limit $\Delta \rightarrow 0$. The maximum gives the lower bound on M_1 [cf. Eq. (6.28)] and on $\sin \theta_{13}$ [cf. Eq. (6.30)].

In the case of normal hierarchy, $|g(\Omega_{21}, \theta_{13}, \delta)|$ slightly decreases when Δ increases, and so the maximum is found for $\Delta = 0$ and the dependence on θ_{13} and δ disappears. Replacing the dependence on Ω_{21} with a dependence on K_1 , we have plotted $|g(K_1, \Delta = 0)|$ in Fig. 6.4 for central values of m_{sol} and m_{atm} . Including the errors, one finds $g_{\text{max}} \simeq 0.160 \pm 0.005$.

The (3σ) lower bound on M_1 for normal hierarchy, from the general expression (6.25), is then given by

$$M_1 \geq 0.9 \times 10^{10} \text{ GeV} \frac{\delta_{21}}{|\Delta|}. \quad (6.28)$$

In the case of inverted hierarchy, the situation is somehow opposite, since for $\theta_{13} = 0$ the electron flavor contribution vanishes in Eq. (6.27) and there is an exact cancellation between the τ and μ contributions. Consequently, the asymmetry increases for increasing values of θ_{13} and the maximum is found for $\sin \theta_{13} = 0.2$ and $\delta \simeq \pi/4$. In this case one has that $\max_{\theta_{13}, \delta} [g_{\text{max}}(m_1 = 0, \theta_{13}, \delta) \Delta] \simeq (9 \pm 2) \times 10^{-8}$, which, plugged into Eq. (6.25), gives at 3σ

$$M_1 \geq 6 \times 10^{15} \text{ GeV} \delta_{21}. \quad (6.29)$$

It should be remembered that these conditions have been obtained in the three-flavor regime and in the DL, i.e. they are valid for $M_{1,2} \lesssim 10^9 \text{ GeV}$. This implies that $\delta_{21} \lesssim 10^{-1} |\Delta|$ for normal hierarchy and $\delta_{21} \lesssim 10^{-7}$ for inverted hierarchy.

Analogously, the general expression (6.26) gives the following (3σ) lower bounds on $\sin \theta_{13}$ for normal and inverted hierarchy, respectively:

$$\sin \theta_{13} \gtrsim 3.3 \times 10^{-7} d \quad \text{and} \quad \sin \theta_{13} \gtrsim 0.06 d. \quad (6.30)$$

$$\Omega = R_{13}$$

In this particular case, the next-to-lightest RH neutrino is decoupled from the other two heavy neutrinos, which implies that $\varepsilon_{2\alpha} = 0$ for any α and that $\varepsilon_{1\alpha}$ does not depend on M_2 ; in particular, it does not get enhanced if $\delta_{21} \rightarrow 0$. Therefore, one has necessarily to consider $\delta_{31} \lesssim 0.01$, implying a full DL with all three RH neutrino masses quasi-degenerate. The function $g(m_1, \Omega_{ji}, \theta_{13}, \delta)$ is now obtained from Eq. (6.24) with $j = q = 3$ and $i = p = 1$ and $\kappa_\alpha^f = \kappa(K_{1\alpha} + K_{2\alpha} + K_{3\alpha})$, or explicitly

$$\begin{aligned} g(m_1, \Omega_{31}, \theta_{13}, \delta) &\equiv \frac{2 K_{\text{atm}} (K_1 + K_3)}{K_1 K_3} \frac{(m_3 - m_1) \sqrt{m_3 m_1}}{m_{\text{atm}}^2} \Omega_{31} \sqrt{1 - \Omega_{31}^2} \\ &\times \sum_{\alpha} \kappa(K_{1\alpha} + K_{2\alpha} + K_{3\alpha}) \frac{\text{Im}[U_{\alpha 1}^* U_{\alpha 3}]}{\Delta}. \end{aligned} \quad (6.31)$$

It is interesting to notice that in this case an e -dominance is realized. Moreover, one has that the dependence of $|g(m_1, \Omega_{31}, \theta_{13}, \delta)|$ on θ_{13} and δ is slight, and the maximum is for $\Delta = 0$ and $m_1 = 0$. We find $g_{\text{max}}(0) = 0.24 \pm 0.01$ for normal hierarchy and $g_{\text{max}}(0) = (3.1 \pm 0.2) \times 10^{-3}$ for inverted hierarchy. The lower bound on M_1 in Eq. (6.25) yields then at 3σ for normal and inverted hierarchy, respectively,

$$M_1 \gtrsim 5.5 \times 10^9 \text{ GeV} \frac{\delta_{31}}{|\Delta|} \quad \text{and} \quad M_1 \gtrsim 5 \times 10^{11} \text{ GeV} \frac{\delta_{31}}{|\Delta|}, \quad (6.32)$$

while in the case of resonant leptogenesis Eq. (6.26) yields

$$\sin \theta_{13} \gtrsim 2.3 \times 10^{-7} d \quad \text{and} \quad \sin \theta_{13} \gtrsim 1.5 \times 10^{-5} d. \quad (6.33)$$

Increasing m_1 , the value of $g_{\text{max}}(m_1)$ decreases, and the lower bound on $\sin \theta_{13}$ in resonant leptogenesis becomes more and more restrictive. This dependence is shown in Fig. 6.5 both for normal (left panel) and inverted (right panel) hierarchies and for $d = 1$ (solid line) and $d = 10$ (short-dashed line). Interestingly, imposing the experimental (3σ) upper limit $\sin \theta_{13} \lesssim 0.20$, one

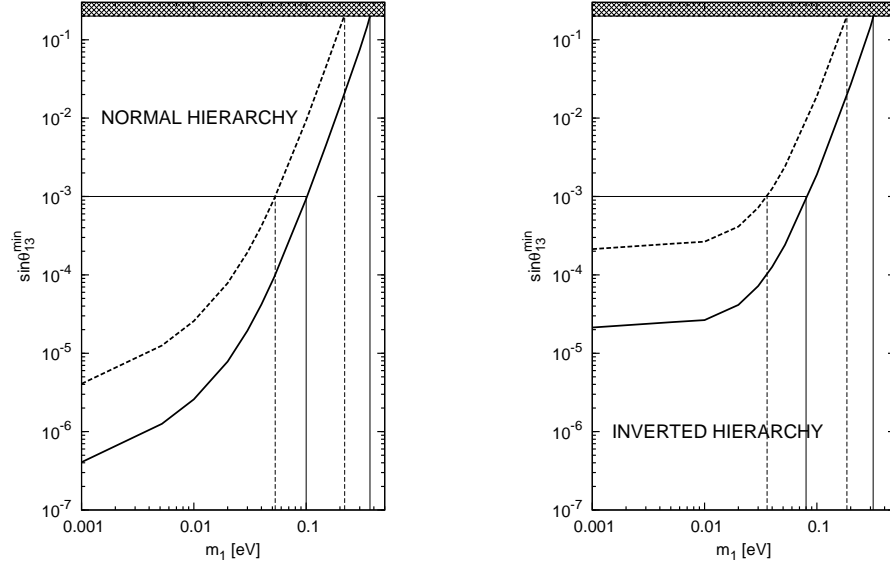


Figure 6.5: Case $\Omega = R_{13}$ in the full DL. Lower bound on $\sin \theta_{13}$ versus m_1 obtained in resonant leptogenesis for $d = 1$ (solid line) and $d = 10$ (short-dashed line). Values $\sin \theta_{13} > 0.20$ are excluded at 3σ by current experimental data.

obtain the upper bound $m_1 \lesssim 0.2\text{--}0.4$ eV, depending on the value of d . This upper bound will become more stringent if no signal for a non-vanishing mixing angle θ_{13} is seen in future neutrino oscillation experiments, since the experimental limit on $\sin \theta_{13}$ will then go down. Assuming no discovery, the most stringent experimental upper limit is expected to be reached in neutrino factories, where one could obtain $\sin \theta_{13} < 10^{-3}$ [187]. This asymptotical upper limit is also shown in Fig. 6.5 and would imply an upper bound $m_1 \lesssim 0.05\text{--}0.1$ eV for normal hierarchy and $m_1 \lesssim 0.03\text{--}0.08$ eV for inverted hierarchy. Therefore, an interesting interplay between two measurable quantities is realized, making δ -leptogenesis falsifiable independently of the RH neutrino mass spectrum.

In the more conservative case of normal hierarchy (see left panel of Fig. 6.5), a good approximation for the upper bound on m_1 ($d = 1$) is given by the fit

$$m_1 \lesssim 0.6 \left(\sin \theta_{13} - 2.3 \times 10^{-7} \right)^{0.25} \text{ eV}. \quad (6.34)$$

It is interesting that this upper bound holds in the extreme case of resonant leptogenesis and therefore holds for any RH neutrino spectrum. However, we still have to verify if it holds also for a different choice of Ω .

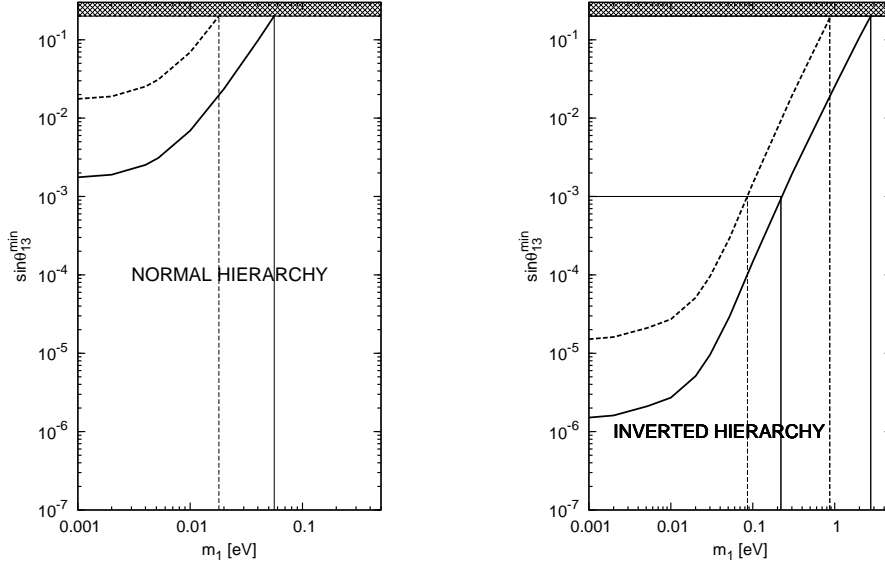


Figure 6.6: Case $\Omega = R_{12}$ in the partial DL. Lower bound on $\sin \theta_{13}$ versus m_1 obtained in resonant leptogenesis. Same conventions as in the previous figure.

$$\Omega = R_{12}$$

The situation for $\Omega = R_{12}$ is quite different compared to the previous two cases. One has now $i = p = 1$ and $j = q = 2$, and it is possible to have both a partial DL with $M_1 \simeq M_2 \ll M_3 \lesssim 10^{14}$ GeV and a full DL. In the first case, the general expression (6.24) becomes

$$g(m_1, \Omega_{21}, \theta_{13}, \delta) \equiv \frac{2 K_{\text{atm}} (K_1 + K_2)}{K_1 K_2} \frac{(m_2 - m_1) \sqrt{m_2 m_1}}{m_{\text{atm}}^2} \Omega_{21} \sqrt{1 - \Omega_{21}^2} \times \sum_{\alpha} \kappa(K_{1\alpha} + K_{2\alpha}) \frac{\text{Im}[U_{\alpha 1}^* U_{\alpha 2}]}{\Delta}. \quad (6.35)$$

This time the contribution from the electron flavor vanishes. Furthermore, for normal hierarchy, there is an almost perfect cancellation between the μ and the τ contributions. In the left panel of Fig. 6.6, we show the lower bound on $\sin \theta_{13}$ versus m_1 , and one can see that it is more restrictive than in the previous case, $\Omega = R_{13}$. In particular, imposing $\sin \theta_{13} < 0.2$, one obtains now a much more stringent upper bound $m_1 \lesssim 0.06$ eV. On the other hand, for inverted hierarchy, the cancellation between the μ and the τ flavors does not occur, and one has a lower bound on $\sin \theta_{13}$ for $m_1 \ll 0.01$ eV that is similar to what has been obtained in the case $\Omega = R_{13}$ (see the right panel of

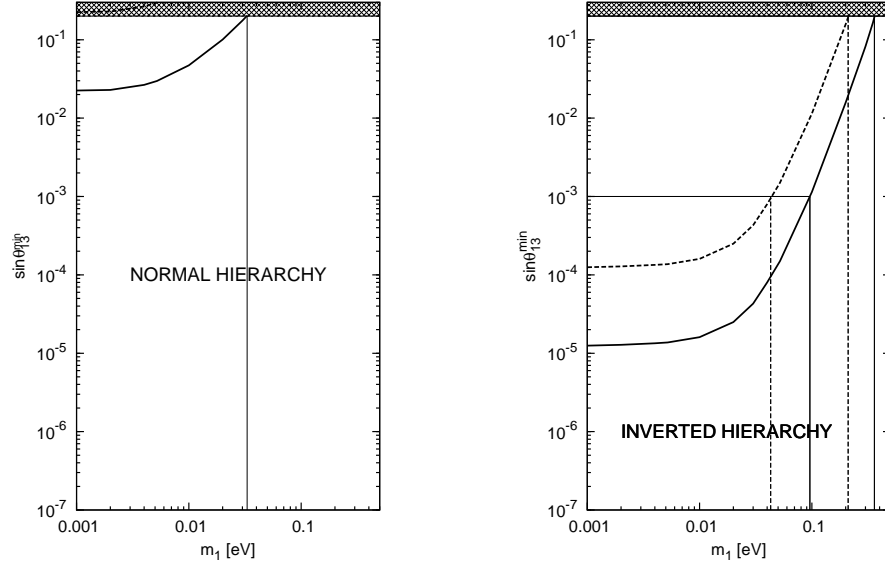


Figure 6.7: Case $\Omega = R_{12}$ in the full DL. Lower bound on $\sin\theta_{13}$ versus m_1 obtained in resonant leptogenesis. Same conventions as in the previous figures.

Fig. 6.6). However, here there is no flavor cancellation for increasing values of m_1 because $K_{1\alpha} + K_{2\alpha}$ does not tend to a common value like $K_{1\alpha} + K_{2\alpha} + K_{3\alpha}$. Therefore, one can see in Fig. 6.6 that this time the upper bound on m_1 is much looser, both compared to normal hierarchy and compared to $\Omega = R_{13}$.

In the full DL the flavor cancellation at large m_1 occurs. The results are shown in Fig. 6.7. One can notice that the upper bound on m_1 is very restrictive for normal hierarchy, and one has a situation similar to the case $\Omega = R_{13}$ for inverted hierarchy.

$$\Omega = R_{23}$$

When $\Omega = R_{23}$, the lightest RH neutrino decouples and $\varepsilon_{1\alpha} = 0$ independently of M_1 . Therefore, there is no contribution to the final asymmetry from N_1 -decays. On the other hand, $\varepsilon_{2\alpha}$ and $\varepsilon_{3\alpha}$ do not vanish and hence there is a contribution from the decays of the two heavier RH neutrinos. Still N_1 inverse processes have to be taken into account since they contribute to the washout. There are two different possibilities.

In the full DL the washout from N_1 inverse decays just cumulates with the washout from the two heavier. Therefore, using expression (6.24) with

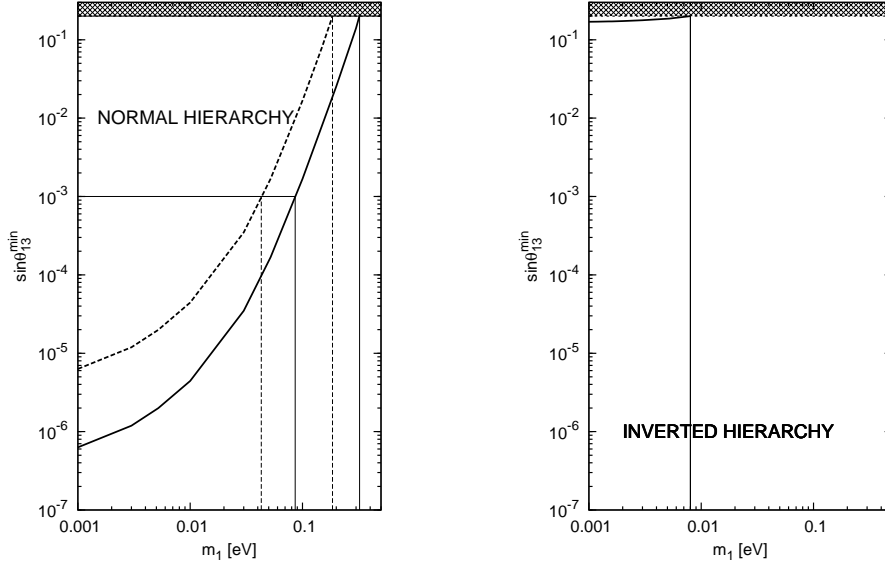


Figure 6.8: Case $\Omega = R_{23}$ in the full DL. Lower bound on $\sin \theta_{13}$ versus m_1 obtained in resonant leptogenesis. Same conventions as in the previous figures.

$i = p = 2$ and $j = q = 3$ and $\kappa_\alpha^f = \kappa(K_{1\alpha} + K_{2\alpha} + K_{3\alpha})$, one obtains

$$g(m_1, \Omega_{32}, \theta_{13}, \delta) \equiv \frac{2 K_{\text{atm}} (K_2 + K_3)}{K_2 K_3} \frac{(m_3 - m_2) \sqrt{m_3 m_2}}{m_{\text{atm}}^2} \Omega_{32} \sqrt{1 - \Omega_{32}^2} \times \sum_{\alpha} \kappa(K_{1\alpha} + K_{2\alpha} + K_{3\alpha}) \frac{\text{Im}[U_{\alpha 2}^* U_{\alpha 3}]}{\Delta}. \quad (6.36)$$

In Fig. 6.8 we show the lower bound on $\sin \theta_{13}$ versus m_1 for successful resonant leptogenesis. This time there is a bigger suppression than in the case $\Omega = R_{13}$, especially for inverted hierarchy.

In the case $M_1 \ll M_2 \simeq M_3$, one has

$$g(m_1, \Omega_{32}, \theta_{13}, \delta) \equiv \frac{2 K_{\text{atm}} (K_2 + K_3)}{K_2 K_3} \frac{(m_3 - m_2) \sqrt{m_3 m_2}}{m_{\text{atm}}^2} \Omega_{32} \sqrt{1 - \Omega_{32}^2} \times \sum_{\alpha} \kappa(K_{2\alpha} + K_{3\alpha}) \exp\left(-\frac{3\pi}{8} K_{1\alpha}\right) \frac{\text{Im}[U_{\alpha 2}^* U_{\alpha 3}]}{\Delta}. \quad (6.37)$$

The lower bound on $\sin \theta_{13}$ versus m_1 is shown in Fig. 6.9 for normal hierarchy. One notices that the upper bound on m_1 is slightly less stringent than in the full DL. For inverted hierarchy the asymmetry production is so suppressed that there is no allowed region.

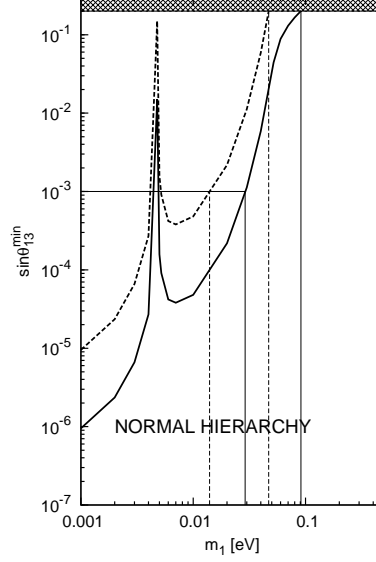


Figure 6.9: Case $\Omega = R_{23}$ in the partial DL. Lower bound on $\sin \theta_{13}$ versus m_1 obtained in resonant leptogenesis. Same conventions as in the previous figures.

We can conclude this section noticing that our results show that δ -leptogenesis can be falsified. In the case of normal hierarchy, the current upper limit $\sin \theta_{13} \lesssim 0.2$ implies $m_1 \lesssim 0.1\text{--}0.3\text{ eV}$, while, in future, a potential upper limit $\sin \theta_{13} \lesssim 10^{-3}$ would imply $m_1 \lesssim 0.01\text{--}0.1\text{ eV}$, with a more precise determination depending on the possibility of improving the current estimation of the parameter d in resonant leptogenesis.

6.3 Leptogenesis from the Majorana phases

It is apparent from the elements A_{ij} in Eq. (6.8) that the Majorana phases in U also contribute to the CP violation necessary for leptogenesis. Actually, they can also play the role of unique source of CP violation, as illustrated in Fig. 3.8 for $\Omega = R_{13}$ real and non-zero Majorana phase Φ_1 ($\Phi_1 = \pi/2$). One can even say quite generally that the Majorana phases can be more easily responsible for enough CP violation than the Dirac phase, simply because they are not associated with the small mixing angle θ_{13} . To illustrate this, we have plotted in the right panel of Fig. 6.1 with dotted lines the case of $\Phi_1 = -\pi/2$ and $\delta = 0$, compared with $\delta = -\pi/2$ and $\Phi_1 = 0$ for $\sin \theta_{13} = 0.2$, i.e. the maximal allowed value. One notices that the lower bounds on M_1 for

the case of non-vanishing Majorana phase is about a factor of 2 lower than in the case of non-vanishing Dirac phase, even for the maximal value of θ_{13} .

We do not aim here at making a thorough study of the role of the Majorana phases as the sole source of CP violation for leptogenesis. We think that the case of the Dirac phase, which we analysed in detail in the previous section, represents a more conservative situation, and the prospects for a measurement seem to be more encouraging. However, for completeness, we would like to report some results obtained in [163] and [166] concerning exclusively the Majorana phase and where only the limit of hierarchical heavy neutrinos and a vanishing initial N_1 -abundance were considered.

When a fully hierarchical light neutrino spectrum ($m_1 \ll m_{\text{sol}}$) is considered, the authors in [163] obtain two main results: for a normal hierarchy (real Ω matrix), they find the lower bound $M_1 \gtrsim 3.6 \times 10^{10}$ GeV for successful leptogenesis, whereas for inverted hierarchy (purely imaginary $\Omega_{12}\Omega_{13}$), they find $M_1 \gtrsim 5.3 \times 10^{10}$ GeV. It should be noted that for inverted hierarchy and real Ω , there is no allowed region below 10^{12} GeV.

In [166] the study was extended to arbitrary m_1 , and some new effects were found. In particular, even in the case of inverted hierarchy and real Ω , an allowed range was found, with the lower bound $M_1 \gtrsim 3 \times 10^{10}$ GeV. In the case of normal hierarchy, no such relaxation occurs and the bounds quoted above still hold.

6.4 Discussion

We have discussed situations where the “observable” CP -violating phases, δ , Φ_1 and Φ_2 , act as the only source of CP violation responsible for the matter-antimatter asymmetry of the Universe. Such possibilities, especially for the Dirac phase, which can be realistically discovered in the future, represent by themselves a strong motivation. We may indeed soon be in the situation to probe the second of Sakharov’s necessary conditions for baryogenesis (see Section 1.1).

As we have seen, successful leptogenesis from low-energy phases is only marginally possible in the HL, $M_1 \ll M_2 \ll M_3$, and with dependence on the initial conditions. This is especially true when the only source of CP violation is the Dirac phase δ . We have also argued that a definite conclusion on the existence of such a marginally allowed region requires a quantum kinetic treatment, which is expected to shrink the already quite restricted allowed region.

Therefore, δ -leptogenesis and more generally leptogenesis from low-energy phases motivate models with quasi-degenerate RH neutrino masses, the ex-

treme limit being resonant leptogenesis. Even in this extreme limit, imposing successful δ -leptogenesis we could derive interesting conditions on quantities accessible in low-energy neutrino experiment: $\sin \theta_{13}$, the absolute neutrino mass scale, normal or inverted hierarchy, the Dirac phase itself. An interesting aspect of δ -leptogenesis is then that it is falsifiable independently of the heavy neutrino mass spectrum.

There are however some objections to the scenario of leptogenesis exclusively from low-energy phases. At the moment, it still lacks a strong theoretical motivation. In [162] a model where such a situation naturally arises was shortly discussed. There, it was said that the simplest way of restricting the number of CP -violating phases is through the assumption that CP is a good symmetry of the Lagrangian, only broken by the vacuum. For example, one can add to the standard type-I see-saw framework three Higgs doublets, together with a Z_3 symmetry under which the left-handed fermion doublets ψ_{Lj} transform as $\psi_{Lj} \rightarrow e^{i2\pi j/3} \psi_{Lj}$ and the Higgs doublets as $\phi_j \rightarrow e^{-i2\pi j/3} \phi_j$, while all other fields transform trivially. It can be readily shown that there is a region of parameters where the vacuum violates CP through complex vacuum expectation values $\langle \phi_i^0 \rangle = v_i e^{i\theta_i}$. Due to the Z_3 restrictions on the Yukawa couplings, the combination $h^\dagger h$ is real, thus implying a real Ω matrix, but keeping U complex. Of course, even though such a model might work, it is not the simplest and most economical one.

There has been a recent claim that sequential dominance models [188] (see [189] for a more complete discussion) could represent a theoretical framework for leptogenesis from low-energy phases. In [184] it was shown that these models correspond to have an Ω matrix that slightly deviates from the unit matrix or from all the other five that can be obtained from the unit matrix exchanging rows or columns. However, it has been noticed in [88, 93] that in the limit $\text{Im}[\Omega] \rightarrow 0$, the total CP asymmetries ε_i do not necessarily vanish. Writing $\Omega_{ij}^2 = |\Omega_{ij}^2| e^{i\phi_{ij}}$, the correct condition to enforce $\varepsilon_i \rightarrow 0$ is to take the limit $\phi_{ij} \rightarrow 0$. This is a more demanding limit than $\text{Im}[\Omega] \rightarrow 0$, and it is not currently motivated by generic sequential dominance models. This limit is not motivated either by radiative leptogenesis [144, 145] within the context of minimal flavor violation [190], as recently considered in [165, 191, 192]. It must however be said that the limit $\text{Im}[\Omega] \rightarrow 0$, when assuming a vanishing initial abundance of RH neutrinos, as done in the works cited above, can effectively mimic the condition $\varepsilon_i \rightarrow 0$ because the efficiency factor $\kappa_i \rightarrow 0$, when $\text{Im}[\Omega] \rightarrow 0$ and $\text{Re}[\Omega] \rightarrow 0$, implying $K_i \rightarrow 0$.

Another possible objection to leptogenesis from low-energy phases is that it cannot be distinguished from the general scenario where both high- and low-energy phases are present. In particular, the Dirac phase will likely give in this case only a subdominant contribution, since its effect is always sup-

pressed by the small θ_{13} mixing angle. Following this approach, one can even say that the baryon asymmetry produced through leptogenesis is not sensitive to the phases in U [193], in the sense that the baryon asymmetry can be accounted for with the phases of U having any value. Conversely, if the phases in U are measured, the baryon asymmetry is still not constrained. The hope is then that the theoretical framework supporting leptogenesis from low-energy phases has some other testable predictions. An experimental support for this model would then represent a support for leptogenesis from low-energy phases.

However, even if a model supports leptogenesis from low-energy phases, how can one know if the source of CP violation comes from the Dirac phase or from the Majorana phases? Actually, it was noticed that the contribution to the final asymmetry from Majorana phases is in general dominant compared to the one coming from the Dirac phase (see right panel of Fig. 6.1). Thus, it will be only possible to tell if δ -leptogenesis really occurs once the Majorana phases are constrained from neutrinoless double-beta decay experiments to give small contributions.

One can even imagine a situation where there is an exact cancellation between the Dirac and Majorana contributions. It would be however strange to think that nature disposes a sufficient source of CP violation, sets up a second source that exactly cancels the first one, and the observed asymmetry is explained by yet a third one, e.g. the phases in Ω .

Chapter 7

Conclusion

The amount of baryonic matter in the Universe which we infer, for instance, from the CMB temperature anisotropies represents one of the most important puzzles of modern cosmology. In order to explain this number, one needs a *baryogenesis* mechanism which generates dynamically a small baryon asymmetry in the early Universe. We discussed in the introduction that a solution to this problem necessarily leads to physics beyond the SM. It is very exciting that this puzzle of cosmology may actually be related to the existence of tiny but non-zero neutrino masses, which are now established. As a matter of fact, a simple extension of the SM naturally leads to small neutrino masses via the see-saw mechanism, and its cosmological consequence is *leptogenesis*, which elegantly yields the required baryon asymmetry.

In the present thesis, we have thoroughly discussed the mechanism of leptogenesis, where a lepton asymmetry is produced by the decays of heavy right-handed (RH) neutrinos and then transferred to a baryon asymmetry by the non-perturbative sphaleron processes. Let us now summarize the main points discussed throughout the thesis.

First, we have presented the unflavored treatment of leptogenesis, where the leptons produced in the decays of the heavy neutrinos have no flavor structure. It was shown that in the hierarchical limit for the heavy neutrino mass spectrum, $M_1 \ll M_2 \ll M_3$, it is typically enough to consider only the decay of the lightest RH neutrino (N_1 -dominated scenario), with a reduction of the number of parameters relevant for the computation. In this minimal scenario, which we refer to as the “vanilla” scenario, the contribution from the lightest RH neutrino washes out all previous asymmetry and, for the theoretically favored values of the effective neutrino mass [cf. Eq. (1.26)] $m_{\text{sol}} \lesssim \tilde{m}_1 \lesssim m_{\text{atm}}$, where m_{sol} and m_{atm} stand for the solar and atmospheric neutrino mass scales, respectively, the strong washout regime is obtained, with no dependence of the final asymmetry on the initial conditions. Ad-

ditionally, the strong washout regime implies that the simple picture with only decays and inverse decays, i.e. neglecting all scattering processes, and without including thermal corrections yields a very good estimation of the final asymmetry.

Interestingly, in the N_1 -dominated scenario, general constraints on a few parameters of the model can be derived. For successful leptogenesis, the mass of the lightest RH neutrino, M_1 , cannot be smaller than about 4×10^9 GeV for the strong washout to be obtained [81, 96]. This lower bound leads to a related lower bound on the initial temperature of leptogenesis, $T_{\text{in}} > 1.5 \times 10^9$ GeV, which can be identified with a lower bound on the reheat temperature T_{reh} within inflation. Such a high value of the reheat temperature may be in conflict with locally supersymmetric theories due to an overproduction of gravitinos.

The baryon asymmetry produced through leptogenesis is also sensitive to the absolute neutrino mass scale. In the context of vanilla leptogenesis, the stringent upper bound $m_1 \lesssim 0.12$ eV was obtained [75, 88, 99].

Then, we introduced the “flavored” picture of leptogenesis, which has been understood only recently to be the correct one for a large fraction of the parameter space (roughly when $M_1 \lesssim 10^{12}$ GeV) [119, 120]. Flavor effects introduce a dependence of the final asymmetry on essentially all parameters of the model. On the one hand, this makes the computation more involved, but, on the other hand, some interesting parameters, such as the CP -violating phases in the PMNS matrix, become accessible. About flavor effects, one can say in general:

- In most of the parameter space they lead to modifications of the predictions by a factor 2–3 compared to the unflavored analysis, due to a reduction of the washout by this factor. Incidentally, the region of independence from the initial conditions shrinks by the same amount [123].
- Large modifications are possible in two cases: i) when the high-energy phases in the Ω matrix are zero or close to zero; ii) when a one-flavor dominance is obtained.
- The usually quoted values of the lower bounds on M_1 and T_{reh} (see above) do not change when flavor effects are included [123].

Next, we re-analysed the conditions on the temperature T and on M_1 for flavor effects to be important. We found that there should be a region in the parameter space where classical Boltzmann equations (“fully flavored regime”) are not enough to describe the generation of asymmetry [133]. Correlations in flavor space and partial losses of coherence might indeed be relevant there, so that a quantum kinetic equation in the form of a density matrix

equation should be used. Interestingly, the region concerned is exactly the one where the upper bound on the absolute neutrino mass scale seems to be evaded. Therefore, at the moment it is not clear whether the upper bound on m_1 from successful vanilla leptogenesis quoted above disappears, is simply relaxed, or still holds.

Then, we went beyond the minimal picture where only the lightest RH neutrino is considered. In the quasi-degenerate limit, $M_1 \simeq M_2 \simeq M_3$, the contributions from all RH neutrinos have to be included. Due to the enhancement of the CP asymmetry in this limit [87], the lower bounds on M_1 and T_{reh} can be lowered down to the TeV scale in the extreme case of resonant leptogenesis [76, 117]. Accounting for flavor effects, this might even be possible without having all Yukawa couplings unnaturally small [132, 146], even though it remains to be proven that the condition of validity of the fully flavored equations is satisfied in this case.

Actually, the production of asymmetry from the heavier RH neutrinos N_2 and N_3 is not only important when considering quasi-degenerate heavy neutrinos. Even for hierarchical heavy neutrinos, it was noticed in [93] that a particular choice of the Ω matrix leads to production of asymmetry by N_2 instead of N_1 . This implies that the lower bound on M_1 does not apply anymore and is replaced by a lower bound on M_2 , which still yields a lower bound on T_{reh} [93]. When flavor effects are included, the contributions from N_2 and N_3 are potentially more important, due to the reduced washout from N_1 [149, 150]. Specifically, the domain of applicability of the N_2 -dominated scenario is expected to be enlarged, and N_3 might be important as well, even though it seems complicated to avoid the washout both from N_1 and N_2 .

The last possibility of going beyond the typical scenario that we discussed is when one element of the Ω matrix, namely Ω_{22} , has a non-trivial value different from 0 or 1. It turns out that making $|\Omega_{22}|$ large opens the possibility of relaxing the lower bound on M_1 by 3 orders of magnitude even for $M_1 \ll M_2$ [152]. Moreover, with moderate values of $|\Omega_{22}|$ and moderate degeneracies $M_1 \simeq M_2$, the upper bound on the neutrino mass can be evaded [98].

Finally, we studied the special case where the source of CP violation required for leptogenesis stems exclusively from the phases in the PMNS matrix. We focused on the Dirac phase, for which the prospects of measurement are the most promising. We found that for hierarchical heavy neutrino masses leptogenesis from the Dirac phase (δ -leptogenesis) is only marginally allowed and in the weak washout regime. For quasi-degenerate heavy neutrinos, the strong washout is recovered, and we could even derive a upper bound on m_1 dependent on θ_{13} for successful resonant leptogenesis, which is the most favorable case one can imagine. Roughly speaking, for the 3σ upper limit

$\sin \theta_{13} = 0.2$, resonant δ -leptogenesis only works for $m_1 \lesssim 0.2$ eV [164]. If the experimental upper limit on $\sin \theta_{13}$ decreases in the future, so does the upper bound on m_1 for successful δ -leptogenesis.

The see-saw mechanism and leptogenesis have very appealing features. However, in their vanilla form, they seem very difficult to prove or disprove. The scale of the heavy neutrinos necessary for leptogenesis, as well as to have a “natural” see-saw mechanism, is too large to be accessible at future colliders. The only possibility to produce heavy neutrinos at colliders would be to have at the same time TeV masses and large Yukawa couplings. Even though such a possibility relies on a cancellation mechanism rather than a see-saw mechanism [143, 148], the question whether it is imaginable to have signals from heavy RH neutrinos at colliders is very exciting by itself [143, 147, 148]. The inclusion of successful leptogenesis in the picture certainly deserves investigation.

Another way of probing directly leptogenesis would be to measure a primordial lepton asymmetry of the order of the baryon asymmetry. The relic neutrino background would carry such an information. Although the sole detection of relic neutrinos is in principle possible [194–196], measuring an asymmetry of order 10^{-10} in it seems hopeless.

If a direct test of leptogenesis seems to be out of reach, then one has to wait for an accumulation of indirect hints in favor of this scenario.

First, the observation of neutrinoless double-beta decay would establish the Majorana nature of light neutrinos, hence supporting the see-saw mechanism and leptogenesis. The next-generation experiments such as GERDA [49] or CUORE [51] are likely to observe a signal if the light neutrino mass hierarchy is quasi-degenerate or inverted. Furthermore, the discovery of the Majorana nature of neutrinos would immediately tell that lepton number is violated, hence verifying the first Sakharov’s condition, thanks to the presence of sphalerons.

Second, the discovery of CP violation in the neutrino sector in future long-baseline neutrino experiments such as T2K [173] or NO ν A [174] will certainly strengthen the case for leptogenesis. It will indeed tell that the second Sakharov’s condition is verified. Moreover, the source of CP violation in neutrino mixing might be sufficient to explain the origin of the matter-antimatter asymmetry of the Universe without resorting to the unobservable high-energy phases in the Ω matrix.

Conversely, it is interesting to ask oneself if there are ways to disprove leptogenesis. A non-observation of neutrinoless double-beta decay in the next-generation experiments would not disprove by itself the see-saw mechanism and leptogenesis. The mass hierarchy might simply be normal, hence out of reach of the next-generation experiments. However, if neutrino oscillation

experiments determine the mass hierarchy to be inverted [197, 198], but no signal is found in neutrinoless double beta decay experiments, then one would conclude that the see-saw mechanism is not at the origin of the neutrino masses, and that leptogenesis is not responsible for the baryon asymmetry of the Universe.

As concerns CP violation, the non-observation of leptonic CP violation in future neutrino experiments will not weaken the case for leptogenesis in a significant way. Instead, it would mean that the Dirac phase and/or the angle θ_{13} are too small to give an noticeable contribution to the final asymmetry. The source of CP violation responsible for leptogenesis can be still given by the remaining 5 CP -violating phases present in the model.

The absolute neutrino mass scale may also provide a way to constrain significantly leptogenesis. As a matter of fact, we have seen that the latter scenario leads to an upper bound on the absolute neutrino mass scale of about 0.1 eV, which is however subject to modification due to flavor effects. Assuming that the upper bound remains below roughly 0.3 eV, implying $m_{\nu_e} \lesssim 0.3$ eV, a signal in the future KATRIN experiment [41], which claims a discovery potential down to about 0.35 eV, would severely constrain leptogenesis in its minimal version. On the other hand, other versions, such as the one with quasi-degenerate heavy neutrinos, would still remain viable.

Even though the production of heavy neutrinos at future colliders seems to be unlikely, the LHC experiment at CERN will still have an indirect impact on leptogenesis. Indeed, if supersymmetry is discovered and the parameters measured are consistent with successful electroweak baryogenesis (e.g. light stop and light Higgs [199, 200]), then the case for leptogenesis will become weaker. On the other hand, if electroweak baryogenesis is ruled out at the LHC, then leptogenesis, as one of the remaining possibilities to explain the baryon asymmetry of the Universe, will become stronger.

In conclusion, since leptogenesis is unavoidable when considering the see-saw mechanism for the generation of neutrino masses, it provides a very elegant explanation to one of the outstanding problems of modern cosmology, the origin of the matter-antimatter asymmetry of the Universe. Even though a direct test is challenging, there is no doubt that in the next few years more experimental evidence will become available to weaken or strengthen the case for leptogenesis.

Appendix A

Neutrino mixing parameters

The currently existing data from neutrino oscillation experiments can be well described by the Lagrangian,

$$\mathcal{L} = -\frac{g}{\sqrt{2}}\overline{\ell}_L\gamma^\mu\nu_L W_\mu - \frac{1}{2}\overline{(\nu_L)^c}m_\nu\nu_L - \overline{\ell}_R m_\ell \ell_L + h.c. , \quad (\text{A.1})$$

which includes the weak charged current interaction in the lepton sector, a Majorana mass term for neutrinos, and a Dirac mass term for charged leptons. When diagonalizing the neutrino and charged lepton mass matrices via $m_\nu = U_\nu^\star m_\nu^{\text{diag}} U_\nu^\dagger$ and $m_\ell = V_\ell m_\ell^{\text{diag}} U_\ell^\dagger$, one obtains the lepton mixing matrix, known also as the Pontecorvo-Maki-Nakagawa-Sakata (PMNS) mixing matrix [17–19], in the weak charged lepton current

$$U = U_\ell^\dagger U_\nu. \quad (\text{A.2})$$

The charged current interaction can then be written in the mass basis as

$$-\frac{g}{\sqrt{2}}\overline{\ell}_{L\alpha}\gamma^\mu U_{\alpha i}\nu_{Li} W_\mu. \quad (\text{A.3})$$

Note that it is conventional to choose the basis where the mass matrix for the charged leptons is diagonal, in which case $U = U_\nu$, i.e. the PMNS matrix is the matrix that diagonalizes the neutrino mass matrix. Neutrinos with a given flavor are then related to neutrinos with a given mass through the PMNS matrix,¹

$$\nu_{\alpha L} = \sum_{j=1}^3 U_{\alpha j}\nu_{jL}, \quad \alpha = e, \mu, \tau. \quad (\text{A.4})$$

¹If one wants the relation between the flavor eigenstates and the mass eigenstates, it is given by $|\nu_\alpha\rangle = \sum_{j=1}^3 U_{\alpha j}^\star |\nu_j\rangle$, $\alpha = e, \mu, \tau$. At first sight, this may seem surprising, but it is simply due to the fact that, by convention, field operators create antiparticles, or annihilate particles! [23]

Note also that the number of neutrino flavor states with mass below $M_Z/2$ is known to be three from the precise measurement of the Z -width at LEP I [5].

The standard parametrization of the PMNS matrix was given in Eq. (1.8). Carrying out the matrix product, one obtains

$$U = V \times \text{diag}(e^{i\frac{\Phi_1}{2}}, e^{i\frac{\Phi_2}{2}}, 1), \quad (\text{A.5})$$

$$V = \begin{pmatrix} c_{12} c_{13} & s_{12} c_{13} & s_{13} e^{-i\delta} \\ -s_{12} c_{23} - c_{12} s_{23} s_{13} e^{i\delta} & c_{12} c_{23} - s_{12} s_{23} s_{13} e^{i\delta} & s_{23} c_{13} \\ s_{12} s_{23} - c_{12} c_{23} s_{13} e^{i\delta} & -c_{12} s_{23} - s_{12} c_{23} s_{13} e^{i\delta} & c_{23} c_{13} \end{pmatrix}.$$

We shall use in all calculations $\theta_{12} = \pi/6$ and $\theta_{23} = \pi/4$, compatible with the results from neutrino oscillation experiments discussed in the introduction, Eqs. (1.13) and (1.15). For the third angle, we shall use the 3σ range $s_{13} = 0\text{--}0.2$ obtained from Eq. (1.16).

Concerning the mass spectrum of light neutrinos, we shall use the convention that $m_1 \leq m_2 \leq m_3$, whatever the hierarchy is. This means that when a normal hierarchy is considered, one has $m_3^2 - m_2^2 = \Delta m_{\text{atm}}^2$ and $m_2^2 - m_1^2 = \Delta m_{\text{sol}}^2$ [cf. Eqs. (1.12) and (1.14)], whereas for an inverted hierarchy, one has $m_3^2 - m_2^2 = \Delta m_{\text{sol}}^2$ and $m_2^2 - m_1^2 = \Delta m_{\text{atm}}^2$. Defining the two convenient quantities

$$m_{\text{atm}} \equiv \sqrt{\Delta m_{\text{atm}}^2 + \Delta m_{\text{sol}}^2} = (0.052 \pm 0.002) \text{ eV}, \quad (\text{A.6})$$

and

$$m_{\text{sol}} \equiv \sqrt{\Delta m_{\text{sol}}^2} = (0.0089 \pm 0.0002) \text{ eV}, \quad (\text{A.7})$$

one has that the light neutrino spectrum is quasi-degenerate when $m_1 \gg m_{\text{atm}}$, while for $m_1 \ll m_{\text{sol}}$ it is fully hierarchical.

Within the convention for the light neutrino masses we are using, it must be pointed out that the case of inverted hierarchy is obtained by performing a cyclic permutation of the columns in the PMNS matrix Eq. (A.5), such that the i -th column becomes the $(i+1)$ -th [164].

Finally, let us note that we shall always neglect the effect of the running of neutrino parameters from high energy to low energy [90, 91].

Appendix B

The see-saw mechanism with three RH neutrinos

The (type-I) see-saw mechanism is based on the following extension of the SM:

$$\mathcal{L} = \mathcal{L}_{\text{SM}} + i\overline{N_{Ri}}\gamma_\mu\partial^\mu N_{Ri} - h_{\alpha i}\overline{\ell_{L\alpha}}N_{Ri}\tilde{\Phi} - \frac{1}{2}M_{\text{Mi}}\overline{(N_{Ri})^c}N_{Ri} + h.c. , \quad (\text{B.1})$$

where $\alpha = e, \mu, \tau$, three new fields N_{Ri} , $i = 1, 2, 3$,¹ a Majorana mass matrix M_{M} and a Yukawa coupling matrix h have been introduced. We chose here the basis where the charged-lepton Yukawa matrix and the Majorana mass matrix are diagonal. The superscript c denotes charge conjugation, defined as $\phi^c \equiv C\bar{\phi}^T$, where the charge conjugation matrix C satisfies

$$C^{-1}\gamma_\mu C = -\gamma_\mu^T, \quad C^T = -C, \quad C^\dagger = C^{-1}. \quad (\text{B.2})$$

The subscripts L and R denote the left-handed and right-handed chiral projections, respectively: $P_{L,R} \equiv (1 \pm \gamma_5)/2$. Finally, the $SU(2)_L \times U(1)_Y$ charge assignments are as follows:

$$\begin{aligned} \tilde{\Phi} \equiv i\sigma_2\Phi^* &= \begin{pmatrix} \phi_0^* \\ \phi_+^* \end{pmatrix}, & (2, -1), \\ \ell_{L\alpha} &= \begin{pmatrix} \nu_\alpha \\ \alpha^- \end{pmatrix}_L, & (2, -1), \\ N_{Ri}, & & (1, 0). \end{aligned}$$

It should be stressed that the new fields N_{Ri} , often called right-handed (RH) neutrinos, are singlets under $SU(2)_L \times U(1)_Y$.

¹In principle, it would be possible to consider the addition of only two RH neutrinos, since only two light neutrinos are known to be massive. But, in the following, we want to be slightly more general and therefore keep three RH neutrinos.

In Eq. (B.1) the Yukawa-type term is simply the analog of the other mass terms for fermions in the SM. Concerning the Majorana mass term, it is new and unique, but in full generality there is no reason why it should be absent. This particularity for neutrinos is due to the fact that they are the only neutral fermions in the SM.

After spontaneous symmetry breaking, a Dirac mass term $m_D = hv$, is generated by the vacuum expectation value of the Higgs field, $v = 174$ GeV. Using the identity $\overline{\nu_L} N_R = \overline{(N_R)^c} (\nu_L)^c$, one can then rewrite the mass term in a more compact form:

$$\mathcal{L}_{\text{mass}} = -\frac{1}{2} \begin{pmatrix} \overline{\nu_L} & \overline{(N_R)^c} \end{pmatrix} \begin{pmatrix} 0 & m_D \\ m_D^T & M_M \end{pmatrix} \begin{pmatrix} (\nu_L)^c \\ N_R \end{pmatrix} + h.c. \quad (\text{B.3})$$

The see-saw mechanism then assumes that the entries of the Majorana mass matrix are much larger than all Dirac matrix elements, i.e. $M_M \gg m_D$. Under this assumption, the mass matrix in Eq. (B.3) can be block-diagonalized with a 6×6 unitary matrix V :

$$V \begin{pmatrix} 0 & m_D \\ m_D^T & M_M \end{pmatrix} V^T \simeq \begin{pmatrix} m_\nu & 0 \\ 0 & M \end{pmatrix} K, \quad (\text{B.4})$$

where

$$m_\nu = m_D \frac{1}{M_M} m_D^T, \quad (\text{B.5})$$

$$V = \begin{pmatrix} 1 & -m_D M_M^{-1} \\ M_M^{-1} m_D^T & 1 \end{pmatrix}, \quad (\text{B.6})$$

and

$$K = \begin{pmatrix} -1 & 0 \\ 0 & 1 \end{pmatrix}. \quad (\text{B.7})$$

The K matrix only makes sure that the mass eigenvalues are positive.

The matrix in Eq. (B.5) corresponds to the light neutrino mass matrix, which has naturally suppressed entries due to the heavy scale in the denominator. This is the reason why this mechanism is called the see-saw mechanism. As explained in Appendix A, the matrix that diagonalizes the mass matrix m_ν for the light neutrinos is the PMNS mixing matrix [cf. Eq. (A.5)], so that

$$U^\dagger m_\nu U^* = \text{diag}(m_1, m_2, m_3), \quad (\text{B.8})$$

which are the masses of the three light neutrinos. The corresponding mass eigenstates are given by

$$\nu_i \simeq \sum_\alpha (U^T)_{i\alpha} \{ [\nu_{L\alpha} - (\nu_{L\alpha})^c] - m_{D\alpha i} M_i^{-1} [(N_{Ri})^c - N_{Ri}] \}. \quad (\text{B.9})$$

It can be easily checked that $\nu_i = -\nu_i^c$, which means that the light neutrinos are Majorana particles.

On the other hand, the lower right block on the right-hand side of Eq. (B.4) was diagonal before the diagonalization and, to leading order, it remains diagonal, i.e. $M \simeq M_M$. The entries are $M_1 \leq M_2 \leq M_3$, corresponding to three heavy neutrinos. The corresponding mass eigenstates are given by

$$N_i \simeq \sum_{\alpha} M_i^{-1} (m_D^T)_{i\alpha} [\nu_{L\alpha} + (\nu_{L\alpha})^c] + [(N_{Ri})^c + N_{Ri}]. \quad (\text{B.10})$$

It can be checked again that $N_i^c = N_i$, which means that the heavy neutrinos are Majorana particles.

Finally, let us note that the extension of the SM in Eq. (B.1) introduces 18 new parameters: 6 masses, 6 mixing angles and 6 CP -violating phases. The number of parameters in principle accessible in low-energy neutrino experiments is 9: the masses of the 3 light neutrinos and the 6 parameters (3 mixing angles and 3 CP -violating phases) in the PMNS matrix [cf. Eq. (A.5)].

Bibliography

- [1] A. S. Beach *et. al.*, *Measurement of the cosmic-ray antiproton to proton abundance ratio between 4-GeV and 50-GeV*, *Phys. Rev. Lett.* **87** (2001) 271101, [[astro-ph/0111094](#)].
- [2] E. W. Kolb and M. S. Turner, *The Early Universe*. Westview Press, 1994.
- [3] B. Fields and S. Sarkar, *Big-bang nucleosynthesis (PDG mini-review)*, [astro-ph/0601514](#).
- [4] **WMAP** Collaboration, D. N. Spergel *et. al.*, *Wilkinson Microwave Anisotropy Probe (WMAP) three year results: Implications for cosmology*, *Astrophys. J. Suppl.* **170** (2007) 377, [[astro-ph/0603449](#)].
- [5] W.-M. Yao *et. al.*, *Review of Particle Physics*, *Journal of Physics G* **33** (2006) 1+.
- [6] A. Strumia, *Baryogenesis via leptogenesis*, [hep-ph/0608347](#).
- [7] A. D. Sakharov, *Violation of CP Invariance, c Asymmetry, and Baryon Asymmetry of the Universe*, *Pisma Zh. Eksp. Teor. Fiz.* **5** (1967) 32–35.
- [8] G. 't Hooft, *Symmetry breaking through Bell-Jackiw anomalies*, *Phys. Rev. Lett.* **37** (1976) 8–11.
- [9] V. A. Kuzmin, V. A. Rubakov, and M. E. Shaposhnikov, *On the Anomalous Electroweak Baryon Number Nonconservation in the Early Universe*, *Phys. Lett.* **B155** (1985) 36.
- [10] P. Arnold and L. D. McLerran, *Sphalerons, Small Fluctuations and Baryon Number Violation in Electroweak Theory*, *Phys. Rev.* **D36** (1987) 581.

- [11] N. S. Manton, *Topology in the Weinberg-Salam Theory*, *Phys. Rev.* **D28** (1983) 2019.
- [12] M. Kobayashi and T. Maskawa, *CP Violation in the Renormalizable Theory of Weak Interaction*, *Prog. Theor. Phys.* **49** (1973) 652–657.
- [13] W. Bernreuther, *CP violation and baryogenesis*, *Lect. Notes Phys.* **591** (2002) 237–293, [[hep-ph/0205279](#)].
- [14] K. Jansen, *Status of the Finite Temperature Electroweak Phase Transition on the Lattice*, *Nucl. Phys. Proc. Suppl.* **47** (1996) 196–211, [[hep-lat/9509018](#)].
- [15] M. E. Shaposhnikov, *Baryon Asymmetry of the Universe in Standard Electroweak Theory*, *Nucl. Phys.* **B287** (1987) 757–775.
- [16] M. B. Gavela, P. Hernandez, J. Orloff, and O. Pene, *Standard model CP violation and baryon asymmetry*, *Mod. Phys. Lett.* **A9** (1994) 795–810, [[hep-ph/9312215](#)].
- [17] B. Pontecorvo, *Inverse beta processes and nonconservation of lepton charge*, *Sov. Phys. JETP* **7** (1958) 172–173.
- [18] B. Pontecorvo, *Mesonium and antimesonium*, *Sov. Phys. JETP* **6** (1957) 429.
- [19] Z. Maki, M. Nakagawa, and S. Sakata, *Remarks on the unified model of elementary particles*, *Prog. Theor. Phys.* **28** (1962) 870.
- [20] **Super-Kamiokande** Collaboration, Y. Fukuda *et. al.*, *Evidence for oscillation of atmospheric neutrinos*, *Phys. Rev. Lett.* **81** (1998) 1562–1567, [[hep-ex/9807003](#)].
- [21] **K2K** Collaboration, M. H. Ahn *et. al.*, *Measurement of neutrino oscillation by the K2K experiment*, *Phys. Rev.* **D74** (2006) 072003, [[hep-ex/0606032](#)].
- [22] **MINOS** Collaboration, D. G. Michael *et. al.*, *Observation of muon neutrino disappearance with the MINOS detectors and the NuMI neutrino beam*, *Phys. Rev. Lett.* **97** (2006) 191801, [[hep-ex/0607088](#)].
- [23] A. Strumia and F. Vissani, *Neutrino masses and mixings and.*, [[hep-ph/0606054](#)].

- [24] R. Davis, *Solar neutrinos. II: Experimental*, *Phys. Rev. Lett.* **12** (1964) 303–305.
- [25] J. N. Bahcall, M. H. Pinsonneault, and S. Basu, *Solar models: Current epoch and time dependences, neutrinos, and helioseismological properties*, *Astrophys. J.* **555** (2001) 990–1012, [astro-ph/0010346].
- [26] **Kamiokande** Collaboration, Y. Fukuda *et. al.*, *Solar neutrino data covering solar cycle 22*, *Phys. Rev. Lett.* **77** (1996) 1683–1686.
- [27] **Super-Kamiokande** Collaboration, J. Hosaka *et. al.*, *Solar neutrino measurements in Super-Kamiokande-I*, *Phys. Rev.* **D73** (2006) 112001, [hep-ex/0508053].
- [28] **SAGE** Collaboration, J. N. Abdurashitov *et. al.*, *Measurement of the solar neutrino capture rate by the Russian-American gallium solar neutrino experiment during one half of the 22-year cycle of solar activity*, *J. Exp. Theor. Phys.* **95** (2002) 181–193, [astro-ph/0204245].
- [29] **GALLEX** Collaboration, W. Hampel *et. al.*, *GALLEX solar neutrino observations: Results for GALLEX IV*, *Phys. Lett.* **B447** (1999) 127–133.
- [30] **GNO** Collaboration, M. Altmann *et. al.*, *Complete results for five years of GNO solar neutrino observations*, *Phys. Lett.* **B616** (2005) 174–190, [hep-ex/0504037].
- [31] **SNO** Collaboration, Q. R. Ahmad *et. al.*, *Measurement of the charged current interactions produced by B-8 solar neutrinos at the Sudbury Neutrino Observatory*, *Phys. Rev. Lett.* **87** (2001) 071301, [nucl-ex/0106015].
- [32] **SNO** Collaboration, Q. R. Ahmad *et. al.*, *Measurement of day and night neutrino energy spectra at SNO and constraints on neutrino mixing parameters*, *Phys. Rev. Lett.* **89** (2002) 011302, [nucl-ex/0204009].
- [33] **B.** Collaboration, *First real time detection of Be7 solar neutrinos by Borexino*, *Phys. Lett.* **B658** (2008) 101–108, [0708.2251].
- [34] L. B. Okun, M. B. Voloshin, and M. I. Vysotsky, *Neutrino electrodynamics and possible consequences for solar neutrinos*, *Sov. Phys. JETP* **64** (1986) 446–452.

- [35] L. B. Okun, M. B. Voloshin, and M. I. Vysotsky, *Electromagnetic Properties of Neutrino and Possible Semiannual Variation Cycle of the Solar Neutrino Flux*, *Sov. J. Nucl. Phys.* **44** (1986) 440.
- [36] **KamLAND** Collaboration, K. Eguchi *et. al.*, *First results from KamLAND: Evidence for reactor anti- neutrino disappearance*, *Phys. Rev. Lett.* **90** (2003) 021802, [[hep-ex/0212021](#)].
- [37] **KamLAND** Collaboration, T. Araki *et. al.*, *Measurement of neutrino oscillation with KamLAND: Evidence of spectral distortion*, *Phys. Rev. Lett.* **94** (2005) 081801, [[hep-ex/0406035](#)].
- [38] **CHOOZ** Collaboration, M. Apollonio *et. al.*, *Search for neutrino oscillations on a long base-line at the CHOOZ nuclear power station*, *Eur. Phys. J.* **C27** (2003) 331–374, [[hep-ex/0301017](#)].
- [39] C. Kraus *et. al.*, *Final results from phase II of the Mainz neutrino mass search in tritium beta decay*, *Eur. Phys. J.* **C40** (2005) 447–468, [[hep-ex/0412056](#)].
- [40] V. M. Lobashev *et. al.*, *Direct search for mass of neutrino and anomaly in the tritium beta-spectrum*, *Phys. Lett.* **B460** (1999) 227–235.
- [41] **KATRIN** Collaboration, A. Osipowicz *et. al.*, *KATRIN: A next generation tritium beta decay experiment with sub-eV sensitivity for the electron neutrino mass*, [hep-ex/0109033](#).
- [42] S. M. Bilenky and S. T. Petcov, *Massive Neutrinos and Neutrino Oscillations*, *Rev. Mod. Phys.* **59** (1987) 671.
- [43] H. V. Klapdor-Kleingrothaus, I. V. Krivosheina, A. Dietz, and O. Chkvorets, *Search for neutrinoless double beta decay with enriched Ge-76 in Gran Sasso 1990-2003*, *Phys. Lett.* **B586** (2004) 198–212, [[hep-ph/0404088](#)].
- [44] H. V. Klapdor-Kleingrothaus, A. Dietz, H. L. Harney, and I. V. Krivosheina, *Evidence for neutrinoless double beta decay*, *Mod. Phys. Lett.* **A16** (2001) 2409–2420, [[hep-ph/0201231](#)].
- [45] C. Arnaboldi *et. al.*, *Results from the CUORICINO neutrinoless double beta decay experiment*, 0802.3439.

-
- [46] H. V. Klapdor-Kleingrothaus *et. al.*, *Latest results from the Heidelberg-Moscow double-beta- decay experiment*, *Eur. Phys. J.* **A12** (2001) 147–154, [[hep-ph/0103062](#)].
- [47] **IGEX** Collaboration, C. E. Aalseth *et. al.*, *Neutrinoless double-beta decay of Ge-76: First results from the International Germanium Experiment (IGEX) with six isotopically enriched detectors*, *Phys. Rev.* **C59** (1999) 2108–2113.
- [48] **IGEX** Collaboration, C. E. Aalseth *et. al.*, *The IGEX Ge-76 neutrinoless double-beta decay experiment: Prospects for next generation experiments*, *Phys. Rev.* **D65** (2002) 092007, [[hep-ex/0202026](#)].
- [49] I. Abt *et. al.*, *A new Ge-76 double beta decay experiment at LNGS*, [hep-ex/0404039](#).
- [50] **Majorana** Collaboration, C. E. Aalseth *et. al.*, *The Majorana neutrinoless double-beta decay experiment*, *Phys. Atom. Nucl.* **67** (2004) 2002–2010, [[hep-ex/0405008](#)].
- [51] R. Ardito *et. al.*, *CUORE: A cryogenic underground observatory for rare events*, [hep-ex/0501010](#).
- [52] S. Hannestad and G. G. Raffelt, *Neutrino masses and cosmic radiation density: Combined analysis*, *JCAP* **0611** (2006) 016, [[astro-ph/0607101](#)].
- [53] P. Minkowski, *$\mu \rightarrow e \gamma$ at a Rate of One Out of 1-Billion Muon Decays?*, *Phys. Lett.* **B67** (1977) 421.
- [54] T. Yanagida in *Workshop on Unified Theories*, *KEK Report 79-18*, p. 95, 1979.
- [55] M. Gell-Mann, P. Ramond, and R. Slansky, *Supergravity*, p. 315. Amsterdam: North Holland, 1979.
- [56] S. L. Glashow, *1979 Cargese Summer Institute on Quarks and Leptons*, p. 687. New York: Plenum, 1980.
- [57] R. Barbieri, D. V. Nanopoulos, G. Morchio, and F. Strocchi, *Neutrino Masses in Grand Unified Theories*, *Phys. Lett.* **B90** (1980) 91.

- [58] R. N. Mohapatra and G. Senjanovic, *Neutrino Masses and Mixings in Gauge Models with Spontaneous Parity Violation*, *Phys. Rev.* **D23** (1981) 165.
- [59] M. Magg and C. Wetterich, *Neutrino mass problem and gauge hierarchy*, *Phys. Lett.* **B94** (1980) 61.
- [60] G. Lazarides, Q. Shafi, and C. Wetterich, *Proton Lifetime and Fermion Masses in an $SO(10)$ Model*, *Nucl. Phys.* **B181** (1981) 287.
- [61] R. Foot, H. Lew, X. G. He, and G. C. Joshi, *Seesaw neutrino masses induced by a triplet of leptons*, *Z. Phys.* **C44** (1989) 441.
- [62] E. Ma, *Pathways to naturally small neutrino masses*, *Phys. Rev. Lett.* **81** (1998) 1171–1174, [[hep-ph/9805219](#)].
- [63] M. Fukugita and T. Yanagida, *Baryogenesis Without Grand Unification*, *Phys. Lett.* **B174** (1986) 45.
- [64] D. Bodeker, G. D. Moore, and K. Rummukainen, *Chern-Simons number diffusion and hard thermal loops on the lattice*, *Phys. Rev.* **D61** (2000) 056003, [[hep-ph/9907545](#)].
- [65] P. Arnold, D. Son, and L. G. Yaffe, *The hot baryon violation rate is $O(\alpha(w)^{5/4} T^4)$* , *Phys. Rev.* **D55** (1997) 6264–6273, [[hep-ph/9609481](#)].
- [66] G. D. Moore, *Sphaleron rate in the symmetric electroweak phase*, *Phys. Rev.* **D62** (2000) 085011, [[hep-ph/0001216](#)].
- [67] M. Plumacher, *Baryogenesis and lepton number violation*, *Z. Phys.* **C74** (1997) 549–559, [[hep-ph/9604229](#)].
- [68] I. Affleck and M. Dine, *A New Mechanism for Baryogenesis*, *Nucl. Phys.* **B249** (1985) 361.
- [69] M. Dine, L. Randall, and S. D. Thomas, *Baryogenesis from flat directions of the supersymmetric standard model*, *Nucl. Phys.* **B458** (1996) 291–326, [[hep-ph/9507453](#)].
- [70] K. Hamaguchi, *Cosmological baryon asymmetry and neutrinos: Baryogenesis via leptogenesis in supersymmetric theories*, [hep-ph/0212305](#).

- [71] E. K. Akhmedov, V. A. Rubakov, and A. Y. Smirnov, *Baryogenesis via neutrino oscillations*, *Phys. Rev. Lett.* **81** (1998) 1359–1362, [[hep-ph/9803255](#)].
- [72] T. Asaka and M. Shaposhnikov, *The nuMSM, dark matter and baryon asymmetry of the universe*, *Phys. Lett.* **B620** (2005) 17–26, [[hep-ph/0505013](#)].
- [73] H. Fritzsch and P. Minkowski, *Unified Interactions of Leptons and Hadrons*, *Ann. Phys.* **93** (1975) 193–266.
- [74] M. A. Luty, *Baryogenesis via leptogenesis*, *Phys. Rev.* **D45** (1992) 455–465.
- [75] G. F. Giudice, A. Notari, M. Raidal, A. Riotto, and A. Strumia, *Towards a complete theory of thermal leptogenesis in the SM and MSSM*, *Nucl. Phys.* **B685** (2004) 89–149, [[hep-ph/0310123](#)].
- [76] A. Pilaftsis and T. E. J. Underwood, *Resonant leptogenesis*, *Nucl. Phys.* **B692** (2004) 303–345, [[hep-ph/0309342](#)].
- [77] W. Buchmuller and M. Plumacher, *Spectator processes and baryogenesis*, *Phys. Lett.* **B511** (2001) 74–76, [[hep-ph/0104189](#)].
- [78] E. Nardi, Y. Nir, J. Racker, and E. Roulet, *On Higgs and sphaleron effects during the leptogenesis era*, *JHEP* **01** (2006) 068, [[hep-ph/0512052](#)].
- [79] G. C. Branco *et al.*, *Minimal scenarios for leptogenesis and CP violation*, *Phys. Rev.* **D67** (2003) 073025, [[hep-ph/0211001](#)].
- [80] W. Buchmuller, P. Di Bari, and M. Plumacher, *Leptogenesis for pedestrians*, *Ann. Phys.* **315** (2005) 305–351, [[hep-ph/0401240](#)].
- [81] W. Buchmuller, P. Di Bari, and M. Plumacher, *Cosmic microwave background, matter-antimatter asymmetry and neutrino masses*, *Nucl. Phys.* **B643** (2002) 367–390, [[hep-ph/0205349](#)].
- [82] E. W. Kolb and S. Wolfram, *Baryon Number Generation in the Early Universe*, *Nucl. Phys.* **B172** (1980) 224.
- [83] J. A. Harvey and M. S. Turner, *Cosmological baryon and lepton number in the presence of electroweak fermion number violation*, *Phys. Rev.* **D42** (1990) 3344–3349.

- [84] M. Laine and M. E. Shaposhnikov, *A remark on sphaleron erasure of baryon asymmetry*, *Phys. Rev.* **D61** (2000) 117302, [[hep-ph/9911473](#)].
- [85] A. Anisimov, A. Broncano, and M. Plumacher, *The CP-asymmetry in resonant leptogenesis*, *Nucl. Phys.* **B737** (2006) 176–189, [[hep-ph/0511248](#)].
- [86] M. Flanz, E. A. Paschos, and U. Sarkar, *Baryogenesis from a lepton asymmetric universe*, *Phys. Lett.* **B345** (1995) 248–252, [[hep-ph/9411366](#)].
- [87] L. Covi, E. Roulet, and F. Vissani, *CP violating decays in leptogenesis scenarios*, *Phys. Lett.* **B384** (1996) 169–174, [[hep-ph/9605319](#)].
- [88] W. Buchmuller, P. Di Bari, and M. Plumacher, *The neutrino mass window for baryogenesis*, *Nucl. Phys.* **B665** (2003) 445–468, [[hep-ph/0302092](#)].
- [89] J. A. Casas and A. Ibarra, *Oscillating neutrinos and $\mu \rightarrow e, \gamma$* , *Nucl. Phys.* **B618** (2001) 171–204, [[hep-ph/0103065](#)].
- [90] K. S. Babu, C. N. Leung, and J. T. Pantaleone, *Renormalization of the neutrino mass operator*, *Phys. Lett.* **B319** (1993) 191–198, [[hep-ph/9309223](#)].
- [91] S. Antusch, J. Kersten, M. Lindner, and M. Ratz, *Running neutrino masses, mixings and CP phases: Analytical results and phenomenological consequences*, *Nucl. Phys.* **B674** (2003) 401–433, [[hep-ph/0305273](#)].
- [92] M. Fujii, K. Hamaguchi, and T. Yanagida, *Leptogenesis with almost degenerate Majorana neutrinos*, *Phys. Rev.* **D65** (2002) 115012, [[hep-ph/0202210](#)].
- [93] P. Di Bari, *Seesaw geometry and leptogenesis*, *Nucl. Phys.* **B727** (2005) 318–354, [[hep-ph/0502082](#)].
- [94] S. Blanchet and P. Di Bari, *Leptogenesis beyond the limit of hierarchical heavy neutrino masses*, *JCAP* **0606** (2006) 023, [[hep-ph/0603107](#)].
- [95] P. Di Bari, *Leptogenesis, neutrino mixing data and the absolute neutrino mass scale*, [hep-ph/0406115](#).

- [96] S. Davidson and A. Ibarra, *A lower bound on the right-handed neutrino mass from leptogenesis*, *Phys. Lett.* **B535** (2002) 25–32, [hep-ph/0202239].
- [97] T. Asaka, K. Hamaguchi, M. Kawasaki, and T. Yanagida, *Leptogenesis in inflationary universe*, *Phys. Rev.* **D61** (2000) 083512, [hep-ph/9907559].
- [98] T. Hambye, Y. Lin, A. Notari, M. Papucci, and A. Strumia, *Constraints on neutrino masses from leptogenesis models*, *Nucl. Phys.* **B695** (2004) 169–191, [hep-ph/0312203].
- [99] W. Buchmuller, P. Di Bari, and M. Plumacher, *A bound on neutrino masses from baryogenesis*, *Phys. Lett.* **B547** (2002) 128–132, [hep-ph/0209301].
- [100] H. Pagels and J. R. Primack, *Supersymmetry, Cosmology and New TeV Physics*, *Phys. Rev. Lett.* **48** (1982) 223.
- [101] S. Weinberg, *Does Gravitation Resolve the Ambiguity Among Supersymmetry Vacua?*, *Phys. Rev. Lett.* **48** (1982) 1776–1779.
- [102] M. Y. Khlopov and A. D. Linde, *Is It Easy to Save the Gravitino?*, *Phys. Lett.* **B138** (1984) 265–268.
- [103] J. R. Ellis, J. E. Kim, and D. V. Nanopoulos, *Cosmological Gravitino Regeneration and Decay*, *Phys. Lett.* **B145** (1984) 181.
- [104] T. Moroi, H. Murayama, and M. Yamaguchi, *Cosmological constraints on the light stable gravitino*, *Phys. Lett.* **B303** (1993) 289–294.
- [105] M. Bolz, A. Brandenburg, and W. Buchmuller, *Thermal Production of Gravitinos*, *Nucl. Phys.* **B606** (2001) 518–544, [hep-ph/0012052].
- [106] J. Pradler and F. D. Steffen, *Thermal gravitino production and collider tests of leptogenesis*, *Phys. Rev.* **D75** (2007) 023509, [hep-ph/0608344].
- [107] J. Pradler and F. D. Steffen, *Constraints on the reheating temperature in gravitino dark matter scenarios*, *Phys. Lett.* **B648** (2007) 224–235, [hep-ph/0612291].
- [108] K. Kohri, T. Moroi, and A. Yotsuyanagi, *Big-bang nucleosynthesis with unstable gravitino and upper bound on the reheating temperature*, *Phys. Rev.* **D73** (2006) 123511, [hep-ph/0507245].

- [109] G. Lazarides and Q. Shafi, *Origin of matter in the inflationary cosmology*, *Phys. Lett.* **B258** (1991) 305–309.
- [110] H. Murayama, H. Suzuki, T. Yanagida, and J. Yokoyama, *Chaotic inflation and baryogenesis by right-handed sneutrinos*, *Phys. Rev. Lett.* **70** (1993) 1912–1915.
- [111] T. Asaka, K. Hamaguchi, M. Kawasaki, and T. Yanagida, *Leptogenesis in inflaton decay*, *Phys. Lett.* **B464** (1999) 12–18, [[hep-ph/9906366](#)].
- [112] R. Jeannerot, S. Khalil, and G. Lazarides, *Leptogenesis in smooth hybrid inflation*, *Phys. Lett.* **B506** (2001) 344–350, [[hep-ph/0103229](#)].
- [113] K. Hamaguchi, H. Murayama, and T. Yanagida, *Leptogenesis from sneutrino-dominated early universe*, *Phys. Rev.* **D65** (2002) 043512, [[hep-ph/0109030](#)].
- [114] F. Hahn-Woernle and M. Plumacher, *Effects of reheating on leptogenesis*, [0801.3972](#).
- [115] Y. Grossman, T. Kashti, Y. Nir, and E. Roulet, *Leptogenesis from supersymmetry breaking*, *Phys. Rev. Lett.* **91** (2003) 251801, [[hep-ph/0307081](#)].
- [116] G. D’Ambrosio, G. F. Giudice, and M. Raidal, *Soft leptogenesis*, *Phys. Lett.* **B575** (2003) 75–84, [[hep-ph/0308031](#)].
- [117] A. Pilaftsis, *CP violation and baryogenesis due to heavy Majorana neutrinos*, *Phys. Rev.* **D56** (1997) 5431–5451, [[hep-ph/9707235](#)].
- [118] A. Pilaftsis, *Heavy Majorana neutrinos and baryogenesis*, *Int. J. Mod. Phys.* **A14** (1999) 1811–1858, [[hep-ph/9812256](#)].
- [119] E. Nardi, Y. Nir, E. Roulet, and J. Racker, *The importance of flavor in leptogenesis*, *JHEP* **01** (2006) 164, [[hep-ph/0601084](#)].
- [120] A. Abada, S. Davidson, F.-X. Josse-Michaux, M. Losada, and A. Riotto, *Flavour issues in leptogenesis*, *JCAP* **0604** (2006) 004, [[hep-ph/0601083](#)].
- [121] J. M. Cline, K. Kainulainen, and K. A. Olive, *Protecting the primordial baryon asymmetry from erasure by sphalerons*, *Phys. Rev.* **D49** (1994) 6394–6409, [[hep-ph/9401208](#)].

- [122] S. Antusch and A. M. Teixeira, *Towards constraints on the SUSY seesaw from flavour- dependent leptogenesis*, *JCAP* **0702** (2007) 024, [[hep-ph/0611232](#)].
- [123] S. Blanchet and P. Di Bari, *Flavor effects on leptogenesis predictions*, *JCAP* **0703** (2007) 018, [[hep-ph/0607330](#)].
- [124] L. D. McLerran, E. Mottola, and M. E. Shaposhnikov, *Sphalerons and axion dynamics in high temperature QCD*, *Phys. Rev.* **D43** (1991) 2027–2035.
- [125] L. Bento, *Sphaleron relaxation temperatures*, *JCAP* **0311** (2003) 002, [[hep-ph/0304263](#)].
- [126] G. D. Moore, *Computing the strong sphaleron rate*, *Phys. Lett.* **B412** (1997) 359–370, [[hep-ph/9705248](#)].
- [127] R. Barbieri, P. Creminelli, A. Strumia, and N. Tetradis, *Baryogenesis through leptogenesis*, *Nucl. Phys.* **B575** (2000) 61–77, [[hep-ph/9911315](#)].
- [128] S. Blanchet and P. Di Bari, *New aspects of leptogenesis bounds*, [arXiv:0807.0743](#).
- [129] A. Abada *et. al.*, *Flavour matters in leptogenesis*, *JHEP* **09** (2006) 010, [[hep-ph/0605281](#)].
- [130] F. X. Josse-Michaux and A. Abada, *Study of flavour dependencies in leptogenesis*, *JCAP* **0710** (2007) 009, [[hep-ph/0703084](#)].
- [131] T. Endoh, T. Morozumi, and Z.-h. Xiong, *Primordial lepton family asymmetries in seesaw model*, *Prog. Theor. Phys.* **111** (2004) 123–149, [[hep-ph/0308276](#)].
- [132] A. Pilaftsis and T. E. J. Underwood, *Electroweak-scale resonant leptogenesis*, *Phys. Rev.* **D72** (2005) 113001, [[hep-ph/0506107](#)].
- [133] S. Blanchet, P. Di Bari, and G. G. Raffelt, *Quantum Zeno effect and the impact of flavor in leptogenesis*, *JCAP* **0703** (2007) 012, [[hep-ph/0611337](#)].
- [134] A. De Simone and A. Riotto, *On the impact of flavour oscillations in leptogenesis*, *JCAP* **0702** (2007) 005, [[hep-ph/0611357](#)].

- [135] G. Raffelt, G. Sigl, and L. Stodolsky, *NonAbelian Boltzmann equation for mixing and decoherence*, *Phys. Rev. Lett.* **70** (1993) 2363–2366, [[hep-ph/9209276](#)].
- [136] A. Basboll and S. Hannestad, *Decay of heavy Majorana neutrinos using the full Boltzmann equation including its implications for leptogenesis*, *JCAP* **0701** (2007) 003, [[hep-ph/0609025](#)].
- [137] H. A. Weldon, *Effective Fermion Masses of Order gT in High Temperature Gauge Theories with Exact Chiral Invariance*, *Phys. Rev.* **D26** (1982) 2789.
- [138] N. F. Bell, R. F. Sawyer, and R. R. Volkas, *Synchronisation and MSW sharpening of neutrinos propagating in a flavour blind medium*, *Phys. Lett.* **B500** (2001) 16–21, [[hep-ph/0011068](#)].
- [139] A. De Simone and A. Riotto, *Quantum Boltzmann Equations and Leptogenesis*, *JCAP* **0708** (2007) 002, [[hep-ph/0703175](#)].
- [140] A. De Simone and A. Riotto, *On Resonant Leptogenesis*, *JCAP* **0708** (2007) 013, [[0705.2183](#)].
- [141] G. C. Branco, W. Grimus, and L. Lavoura, *The seesaw mechanism in the presence of a conserved lepton number*, *Nucl. Phys.* **B312** (1989) 492.
- [142] M. Shaposhnikov, *A possible symmetry of the nuMSM*, *Nucl. Phys.* **B763** (2007) 49–59, [[hep-ph/0605047](#)].
- [143] J. Kersten and A. Y. Smirnov, *Right-Handed Neutrinos at LHC and the Mechanism of Neutrino Mass Generation*, *Phys. Rev.* **D76** (2007) 073005, [[0705.3221](#)].
- [144] R. Gonzalez Felipe, F. R. Joaquim, and B. M. Nobre, *Radiatively induced leptogenesis in a minimal seesaw model*, *Phys. Rev.* **D70** (2004) 085009, [[hep-ph/0311029](#)].
- [145] G. C. Branco, R. Gonzalez Felipe, F. R. Joaquim, and B. M. Nobre, *Enlarging the window for radiative leptogenesis*, *Phys. Lett.* **B633** (2006) 336–344, [[hep-ph/0507092](#)].
- [146] A. Pilaftsis, *Resonant tau leptogenesis with observable lepton number violation*, *Phys. Rev. Lett.* **95** (2005) 081602, [[hep-ph/0408103](#)].

- [147] F. del Aguila, J. A. Aguilar-Saavedra, and R. Pittau, *Heavy neutrino signals at large hadron colliders*, *JHEP* **10** (2007) 047, [[hep-ph/0703261](#)].
- [148] A. de Gouvea, *GeV Seesaw, Accidentally Small Neutrino Masses, and Higgs Decays to Neutrinos*, 0706.1732.
- [149] O. Vives, *Flavoured leptogenesis: A successful thermal leptogenesis with $N(1)$ mass below $10^{*}8\text{-GeV}$* , *Phys. Rev.* **D73** (2006) 073006, [[hep-ph/0512160](#)].
- [150] G. Engelhard, Y. Grossman, E. Nardi, and Y. Nir, *The importance of $N2$ leptogenesis*, *Phys. Rev. Lett.* **99** (2007) 081802, [[hep-ph/0612187](#)].
- [151] T. Shindou and T. Yamashita, *A novel washout effect in the flavored leptogenesis*, *JHEP* **09** (2007) 043, [[hep-ph/0703183](#)].
- [152] M. Raidal, A. Strumia, and K. Turzyski, *Low-scale standard supersymmetric leptogenesis*, *Phys. Lett.* **B609** (2005) 351–359, [[hep-ph/0408015](#)].
- [153] **Belle** Collaboration, K. Hayasaka *et. al.*, *New search for $\tau \rightarrow \mu$ gamma and $\tau \rightarrow e$ gamma decays at Belle*, 0705.0650.
- [154] **BABAR** Collaboration, B. Aubert *et. al.*, *Search for lepton flavor violating decays $\tau_{+-} \rightarrow l_{+-} \pi^0$, $l_{+-} \eta$, $l_{+-} \eta'$* , *Phys. Rev. Lett.* **98** (2007) 061803, [[hep-ex/0610067](#)].
- [155] G. C. Branco, T. Morozumi, B. M. Nobre, and M. N. Rebelo, *A bridge between CP violation at low energies and leptogenesis*, *Nucl. Phys.* **B617** (2001) 475–492, [[hep-ph/0107164](#)].
- [156] G. C. Branco, R. Gonzalez Felipe, F. R. Joaquim, and M. N. Rebelo, *Leptogenesis, CP violation and neutrino data: What can we learn?*, *Nucl. Phys.* **B640** (2002) 202–232, [[hep-ph/0202030](#)].
- [157] S. Davidson and A. Ibarra, *Leptogenesis and low energy phases*, *J. Phys.* **G29** (2003) 1881–1883.
- [158] M. N. Rebelo, *Leptogenesis without CP violation at low energies*, *Phys. Rev.* **D67** (2003) 013008, [[hep-ph/0207236](#)].

- [159] T. Endoh, S. Kaneko, S. K. Kang, T. Morozumi, and M. Tanimoto, *CP violation in neutrino oscillation and leptogenesis*, *Phys. Rev. Lett.* **89** (2002) 231601, [[hep-ph/0209020](#)].
- [160] P. H. Frampton, S. L. Glashow, and T. Yanagida, *Cosmological sign of neutrino CP violation*, *Phys. Lett.* **B548** (2002) 119–121, [[hep-ph/0208157](#)].
- [161] S. Pascoli, S. T. Petcov, and A. Riotto, *Connecting low energy leptonic CP-violation to leptogenesis*, *Phys. Rev.* **D75** (2007) 083511, [[hep-ph/0609125](#)].
- [162] G. C. Branco, R. Gonzalez Felipe, and F. R. Joaquim, *A new bridge between leptonic CP violation and leptogenesis*, *Phys. Lett.* **B645** (2007) 432–436, [[hep-ph/0609297](#)].
- [163] S. Pascoli, S. T. Petcov, and A. Riotto, *Leptogenesis and low energy CP violation in neutrino physics*, *Nucl. Phys.* **B774** (2007) 1–52, [[hep-ph/0611338](#)].
- [164] A. Anisimov, S. Blanchet, and P. Di Bari, *Viability of Dirac phase leptogenesis*, *JCAP* **0804** (2008) 033, [[arXiv:0707.3024](#)].
- [165] S. Uhlig, *Leptogenesis with exclusively low-energy CP Violation in the Context of Minimal Lepton Flavour Violation*, [0709.4624](#).
- [166] E. Molinaro, S. T. Petcov, T. Shindou, and Y. Takanishi, *Effects of Lightest Neutrino Mass in Leptogenesis*, [0709.0413](#).
- [167] N. Cabibbo, *Time Reversal Violation in Neutrino Oscillation*, *Phys. Lett.* **B72** (1978) 333.
- [168] S. M. Bilenky, J. Hosek, and S. T. Petcov, *On Oscillations of Neutrinos with Dirac and Majorana Masses*, *Phys. Lett.* **B94** (1980) 495.
- [169] V. D. Barger, K. Whisnant, and R. J. N. Phillips, *CP Violation in Three Neutrino Oscillations*, *Phys. Rev. Lett.* **45** (1980) 2084.
- [170] P. I. Krastev and S. T. Petcov, *Resonance Amplification and t Violation Effects in Three Neutrino Oscillations in the Earth*, *Phys. Lett.* **B205** (1988) 84–92.

-
- [171] C. Jarlskog, *Commutator of the Quark Mass Matrices in the Standard Electroweak Model and a Measure of Maximal CP Violation*, *Phys. Rev. Lett.* **55** (1985) 1039.
- [172] S. T. Petcov, *Dirac and Majorana CP-violation*, *Nucl. Phys. Proc. Suppl.* **145** (2005) 148–153.
- [173] **The T2K Collaboration**, Y. Itow *et. al.*, *The JHF-Kamioka neutrino project*, [hep-ex/0106019](#).
- [174] **NOvA Collaboration**, D. S. Ayres *et. al.*, *NOvA proposal to build a 30-kiloton off-axis detector to study neutrino oscillations in the Fermilab NuMI beamline*, [hep-ex/0503053](#).
- [175] **Neutrino Factory/Muon Collider Collaboration**, C. H. Albright *et. al.*, *The neutrino factory and beta beam experiments and development*, [physics/0411123](#).
- [176] C. Aalseth *et. al.*, *Neutrinoless double beta decay and direct searches for neutrino mass*, [hep-ph/0412300](#).
- [177] A. Morales and J. Morales, *The neutrinoless double beta decay: The case for germanium detectors*, *Nucl. Phys. Proc. Suppl.* **114** (2003) 141–157, [[hep-ph/0211332](#)].
- [178] P. Langacker, S. T. Petcov, G. Steigman, and S. Toshev, *On the Mikheev-Smirnov-Wolfenstein (MSW) Mechanism of Amplification of Neutrino Oscillations in Matter*, *Nucl. Phys.* **B282** (1987) 589.
- [179] S. Pascoli, S. T. Petcov, and C. E. Yaguna, *Quasi-degenerate neutrino mass spectrum, $\mu \rightarrow e + \gamma$ decay and leptogenesis*, *Phys. Lett.* **B564** (2003) 241–254, [[hep-ph/0301095](#)].
- [180] S. T. Petcov, T. Shindou, and Y. Takanishi, *Majorana CP-violating phases, RG running of neutrino mixing parameters and charged lepton flavour violating decays*, *Nucl. Phys.* **B738** (2006) 219–242, [[hep-ph/0508243](#)].
- [181] S. T. Petcov and T. Shindou, *Charged lepton decays $l(i) \rightarrow l(j) + \gamma$, leptogenesis CP-violating parameters and Majorana phases*, *Phys. Rev.* **D74** (2006) 073006, [[hep-ph/0605151](#)].
- [182] J. F. Nieves and P. B. Pal, *Minimal rephasing invariant CP violating parameters with Dirac and Majorana fermions*, *Phys. Rev.* **D36** (1987) 315.

-
- [183] L. Wolfenstein, *CP Properties of Majorana Neutrinos and Double beta Decay*, *Phys. Lett.* **B107** (1981) 77.
- [184] S. F. King, *Invariant see-saw models and sequential dominance*, *Nucl. Phys.* **B786** (2007) 52–83, [[hep-ph/0610239](#)].
- [185] A. Ibarra and G. G. Ross, *Neutrino properties from Yukawa structure*, *Phys. Lett.* **B575** (2003) 279–289, [[hep-ph/0307051](#)].
- [186] P. H. Chankowski and K. Turzyski, *Limits on $T(\text{reh})$ for thermal leptogenesis with hierarchical neutrino masses*, *Phys. Lett.* **B570** (2003) 198–204, [[hep-ph/0306059](#)].
- [187] P. Huber, M. Lindner, and W. Winter, *Superbeams versus neutrino factories*, *Nucl. Phys.* **B645** (2002) 3–48, [[hep-ph/0204352](#)].
- [188] S. F. King, *Large mixing angle MSW and atmospheric neutrinos from single right-handed neutrino dominance and $U(1)$ family symmetry*, *Nucl. Phys.* **B576** (2000) 85–105, [[hep-ph/9912492](#)].
- [189] S. F. King, *Neutrino mass models*, *Rept. Prog. Phys.* **67** (2004) 107–158, [[hep-ph/0310204](#)].
- [190] V. Cirigliano, B. Grinstein, G. Isidori, and M. B. Wise, *Minimal flavor violation in the lepton sector*, *Nucl. Phys.* **B728** (2005) 121–134, [[hep-ph/0507001](#)].
- [191] V. Cirigliano, G. Isidori, and V. Porretti, *CP violation and leptogenesis in models with minimal lepton flavour violation*, *Nucl. Phys.* **B763** (2007) 228–246, [[hep-ph/0607068](#)].
- [192] G. C. Branco, A. J. Buras, S. Jager, S. Uhlig, and A. Weiler, *Another look at minimal lepton flavour violation, $l(i) \rightarrow l(j)$ gamma, leptogenesis, and the ratio $M(\nu)/\Lambda(\text{LFV})$* , *JHEP* **09** (2007) 004, [[hep-ph/0609067](#)].
- [193] S. Davidson, J. Garayoa, F. Palorini, and N. Rius, *Insensitivity of flavoured leptogenesis to low energy CP violation*, *Phys. Rev. Lett.* **99** (2007) 161801, [[0705.1503](#)].
- [194] A. G. Cocco, G. Mangano, and M. Messina, *Capturing Relic Neutrinos with beta-decaying nuclei*, [0711.1762](#).

-
- [195] R. Lazauskas, P. Vogel, and C. Volpe, *Charged current cross section for massive cosmological neutrinos impinging on radioactive nuclei*, *J. Phys.* **G35** (2008) 025001, [0710.5312].
- [196] M. Blennow, *Prospects for cosmic neutrino detection in tritium experiments in the case of hierarchical neutrino masses*, 0803.3762.
- [197] K. Hagiwara, N. Okamura, and K.-i. Senda, *Solving the neutrino parameter degeneracy by measuring the T2K off-axis beam in Korea*, *Phys. Lett.* **B637** (2006) 266–273, [hep-ph/0504061].
- [198] O. Mena, S. Palomares-Ruiz, and S. Pascoli, *Determining the neutrino mass hierarchy and CP violation in NO ν A with a second off-axis detector*, *Phys. Rev.* **D73** (2006) 073007, [hep-ph/0510182].
- [199] C. Balazs, M. S. Carena, A. Menon, D. E. Morrissey, and C. E. M. Wagner, *The supersymmetric origin of matter*, *Phys. Rev.* **D71** (2005) 075002, [hep-ph/0412264].
- [200] A. Menon, D. E. Morrissey, and C. E. M. Wagner, *Electroweak baryogenesis and dark matter in the nMSSM*, *Phys. Rev.* **D70** (2004) 035005, [hep-ph/0404184].